PhD Thesis

The Interplay of Unitary and Permutation Symmetries in Composite Quantum Systems

Author:
Dávid Jakab

Supervisors:
Dr. Zoltán Zimborás
Dr. Gergely Szirmai

University of Pécs

Physics Doctoral School
Quantum Optics and Quantum Information Program

Wigner Research Centre for Physics

2022

"*But man is not made for defeat. A man can be destroyed but not defeated.*"

Ernest Hemingway

Abstract

The Interplay of Unitary and Permutation Symmetries in Composite Quantum Systems

by Dávid Jakab

We study three different topics linked together by an interplay of SU(d) and permutation symmetries.

First, we study the spin-1 bilinear-biquadratic model on the complete graph of N sites. Due to the complete permutation invariance, this Hamiltonian can be re-expressed as a linear combination of SU(2) and SU(3) quadratic Casimir operators. Using group representation theory, we explicitly diagonalize the Hamiltonian and map out the ground-state phase diagram of the model. Furthermore, the complete energy spectrum, with degeneracies, is obtained analytically for any number of sites.

In the second topic, we slightly relax the permutation symmetry, and study a bipartite collective spin-1 model with an exchange interaction that has different strength between and within the two subsystems. Such a setup is inspired by recent experiments with ultracold atoms. Using the SU(3) symmetry of the exchange interaction and the permutation symmetry within the subsystems, we can employ representation theoretic methods to diagonalize the Hamiltonian of the system in the entire parameter space of the two coupling strengths. These techniques then allow us to explicitly construct and explore the ground-state phase diagram.

The third topic breaks with the investigation of spin models. Instead, we solve a version of the quantum marginal problem that is characterized by the same bipartite permutation symmetry as the previous spin model. This is the shareability, a.k.a. symmetric extendability problem. The question posed is, when can a given bipartite quantum state consistently arise as the reduced state of a larger composite system? The composite system is split into two parts, and we are only interested in the bipartite reduced states that overlap with both. We restrict the problem to Werner and isotropic states, the unitary symmetry of which allow us to use the same representation theoretic tools that we use during the study of our bipartite spin model. For both classes of states, we present necessary and sufficient conditions for shareability.

Acknowledgements

I thank, Zoltán Zimborás and Gergely Szirmai for all the time and effort they have dedicated to advising my research over the years, Karló Penc, for the many helpful discussions about interacting spin systems, and Adrián Solymos for his cooperation in the research of quantum shareability, and also for his crucial help in pointing out mistakes during the writing of this thesis. This work has been supported by Ministry of Innovation and Technology and the National Research, Development and Innovation Office (NKFIH) within the Quantum Information National Laboratory of Hungary and through OTKA Grants FK 135220

Contents

Chapter 1

Introduction

The central theme of this thesis is the interplay between permutation and SU(d) symmetries in various physical problems. We undertake three different projects. In the first two, we investigate highly symmetric magnetic systems, and in the third one, we solve of the quantum shareability problem for two different classes of bipartite quantum states.

Our approach for magnetic systems is from a theorist's point of view, as we look for setups that are simple enough that the ground states can be derived exactly, yet still general enough that the results may prove useful. The way we bestow this simplicity is through various degrees of permutation symmetry, which we interpret as applying a mean-field approximation to a lattice model. This permutation symmetry, along with the innate SU(d) symmetries of the interactions we study, allows us to apply the representation theory of Lie groups to the problems and calculate the ground state phase diagrams exactly.

The spin models we study interact with different three-level generalizations of the Heisenberg interaction. The first one is the bilinear-biquadratic interaction, which is the most general SU(2) symmetric two-particle interaction for three-level systems. We apply this interaction to the complete graph, i.e., all spins are connected to all other spins. In this way, the properties of the ground state are determined by a competition between the SU(2) and SU(3) symmetric parts of the Hamiltonian governing the interaction; moreover, the solution the ground state problem requires studying the way the representations of SU(2) are embedded into the representations of SU(3).

The second spin model we study features a three-level exchange interaction. Here, instead of breaking the global SU(3) symmetry of the model as in the previous case, we break the complete permutation symmetry by introducing a bipartite structure in the connectivity of the spins. This way, the ground state phases are determined by the interaction strengths within and between the two subsystems, and the model may accommodate bipartite symmetry breaking ground states normally associated with antiferromagnetism. We construct and explore the ground-state

phase diagram, and as it turns out, one of the five phases does indeed feature a strong bipartite symmetry breaking, meaning that the ground states are in different SU(3) representations. We have released two papers in international journals about the investigation of these permutation symmetric spin models [1, 2].

As the final research topic, we present a general solution to the shareability problem of SU(d) Werner and isotropic states. Sometimes also referred to as symmetric extendability, the essence of the shareability problem is the following: Alice and Bob are each given a composite quantum system. Is it possible that each bipartite subsystem in which one part is owned by Alice, and the other by Bob, is simultaneously in the state ρ? The maximal sizes of the two composite systems in which a given bipartite state ρ can be shared in such a way, serve as a measure of the entanglement of ρ. The global SU(d), and bipartite permutation symmetries that are inherent to this problem make it closely related to the second spin model we investigate. We derive our solution by generalizing to arbitrary dimension the same representation theoretic method that we use to obtain the phase diagram of our bipartite spin model. There preprint available about this topic [3].

We dedicate the first part of this thesis to the introduction of certain topics that give a context to, or are required to the understanding of the results. This includes a brief description of quantum magnetism, the introductions of the shareability problem, Werner and isotropic states, and a summary of the representation theory of the SU(d) group. This last topic, we introduce through the viewpoint of the Schur-Weyl duality relating SU(d) with the group of permutations, since permutation symmetry plays such a central role in this work. In the three chapters of the second part, we present the results related to the three research topics.

Part I

Motivation and background

Chapter 2

Quantum magnetism through toy models

In this chapter, we present a brief overview on some basic concepts in quantum magnetism, mainly through the lens of the Heisenberg model. We focus on the emergence, and possible lack of long range order, and its connection to quantum fluctuations; moreover, the methods by which one usually studies interacting spin systems. The purpose is to provide some context for our results regarding permutation symmetric spin systems in Chapters 5 and 6.

2.1 Magnetism in solid state systems

The magnetic structure of solid state materials originates from the electronic magnetic moments. More accurately, the magnetic moments of those electrons which are in isolation would be part of the open shells of the molecules constituting the material. Not all solid state matter has a magnetic structure however; many materials in nature are "dull" in the sense that the functions describing the state of electrons inside them are invariant w.r.t. time reversal. The magnetic structure is determined by the time averaged current density function which changes sign under time reversal, therefore in these materials it is identically 0.

There is direct magnetic interaction between the magnetic moments of the electrons, and between the magnetic moments and the lattice field. However, these are both weak relativistic effects, due to the $1/c^2$ factor in the interaction. They cannot explain the characteristic energy scales of the magnetic structure, like the Curie and Néel temperatures. The relevant interaction between the magnetic moments is something inherently quantum mechanical called the exchange effect. In broad terms it can be described as follows: Different spatial symmetries of the multi-particle electronic wave function generally correspond to different energies. Due to the fermionic nature of the electron and the indistinguishability of the particles, the possible values of the total spin are influenced by the spatial symmetry

of the wave function. In turn, the energy of the interacting electrons depends on the value of their total spin.

When the total spin of an electron-pair prefers to be maximized, we talk about ferromagnetic coupling. With maximal total spin, the spinor part of the electronic wave function is symmetric w.r.t. the exchange of particles, therefore, the spatial part must be antisymmetric. An antisymmetric spatial wave function vanishes when the particles are at the same location, and this is precisely where the Coulomb interaction is the strongest. Therefore, the maximal total spin state minimizes the contribution of the Coulomb interaction to the energy. When electrons are ferromagnetically coupled, generally their orbitals are orthogonal, but spatially close to each other, so their Coulomb interaction is relevant. Some examples where this happens are Fe Ni and Co.

When the energy of the interaction favors minimal total spin, the electrons are coupled antiferromagnetically. To give an intuitive picture of how this can happen in crystalline materials, we use the second quantized formalism. In this, the kinetic energy of the electrons on neighboring lattice sites, is described by a hopping term in the Hamiltonian:

$$H_{hop} = -t \sum_{s} (c_{1s}^{\dagger} c_{2s}^{\dagger} + c_{2s}^{\dagger} c_{1s}), \tag{2.1}$$

where $c_{is}^{\dagger}$ creates an electron on lattice site i with spin s. In materials, for example like Mott-insulators, where the electrons are more or less localized, and their kinetic energy is small compared to the various on-site energy terms in the Hamiltonian describing the system, the hopping term can be treated perturbatively. Using second order perturbation, the hopping term gives rise to processes in which an electron hops to a neighboring lattice site, then goes back to the original site, these often give a negative contribution to the energy. However, if the electrons in the neighboring sites are in the same spin-state, the exclusion principle forbids these processes, which makes the spins prefer antiparallel alignment. This type of interaction generally happens when the orbits of the interacting electron are not orthogonal, but spatially well separated. In some materials the magnetically active ions are separated by magnetically neutral ones. In this situation, the hopping term gives rise to similar processes, called superexchange, in higher order perturbation. This is the case for example, in transition metal oxides, where the magnetically neutral oxygen ions serve as a "bridge" for the electrons.

2.2 The Heisenberg model

In the general case, it is too cumbersome to work with the microscopic Hamiltonian consisting of the kinetic energies, and the various interactions of the electrons with each other, and the lattice. The exchange interaction can be described with mathematically less complicated effective Hamiltonian, which considers only the magnetic degrees of freedom, and reproduces the low energy part of the spectrum correctly. It is possible to derive this Hamiltonian solely from symmetry considerations. We only demand the interaction to be isotropic [1], and search for two-particle interactions between identical spin-1/2 particles that are invariant to the global rotations of the Hilbert spaces of the interacting particles. The subspace of global rotation invariant, bounded, linear operators on the two-particle Hilbert space is spanned by the square of the total spin operator $(\mathbf{S_i} + \mathbf{S_j})^2 = 2\mathbf{S_i}\mathbf{S_j} + 3/2\mathbb{1}$, or in other words, the quadratic Casimir operator of SU(2), and the identity operator [2]. $\mathbf{S}_i$ denotes the spin operator at site i. Consequently, in the case of spin-1/2, any power, and by extension, any analytical function of $\mathbf{S}_i\mathbf{S}_j$, can be expressed as a linear combination of $\mathbf{S}_i\mathbf{S}_j$, and the identity operator. Therefore, apart for a constant energy shift, the most general form of the Hamiltonian we are looking for is:

$$H = \sum_{ij} J(r_{ij})\mathbf{S}_i\mathbf{S}_j, \tag{2.2}$$

which is called the Heisenberg Hamiltonian. The parameter $J(r_{ij})$ is the exchange integral, and it is determined from the microscopic model. For $J(r_{ij}) < 0$, the coupling between the two spins is ferromagnetic, for $J(r_{ij}) > 0$, it is antiferromagnetic.

The Heisenberg model describes the most general rotation invariant interaction between magnetic moments, only in the case of spin-1/2. Despite this, it is often used to model interactions in higher spin systems, for example, the interactions between the atomic spins of trapped alkaline earth atoms. In order to retain the generality, one can either extend the SU(2) symmetry to SU(2S+1), and get a similar exchange type interaction, or introduce additional terms to the Hamiltonian, e.g., the bilinear-biquadratic model for spin-1 discussed further in Chapter 5.

[1] In the simple examples we gave for magnetic interaction in Section 2.1, the interaction really is isotropic. However, anisotropic exchange interactions also exist, for example the Dzyaloshinskii-Moriya interaction in which the breaking of the isotropy is the result of the spin-orbit coupling.

[2] This is explained more deeply in Chapter 3, which deals with the theory of Lie groups.

2.3 Long range order and quantum fluctuations in the Heisenberg model

When the temperature is much larger than the characteristic energies J of Eq. (2.2), the thermal fluctuations destroy all magnetic order. The system then becomes a paramagnet that that does not break any physical symmetries. On the other hand, at temperatures on, or under the scale of J, there is a diverse zoo of magnetic orders that may emerge. Symmetry-breaking long-range order is a possibility, but in many circumstances, frustration and quantum fluctuations prevent it from forming. The quantum paramagnets that arise this way are more varied compared to their thermal counterparts, because on sufficiently small temperatures, the system may be phase coherent and thus, possess "internal" symmetries that are not possible for a thermal paramagnet. In this section we give some well-known results about the ground state of Heisenberg-type models, and try to give an impression about why this breaking down of long-range order happens.

In order get an understanding of long-range order in the Heisenberg model, we examine its ground state and low energy excitations. For ferromagnetic coupling, $J(r_{ij}) < 0$, the energy of a single pair of interacting magnetic moments is minimal, when the total spin is maximal. This stays true even when the size of the system is increased. The ground state subspace of a ferromagnetic Heisenberg model is the subspace of the many-body Hilbert space with maximal total spin. Therefore, the energy of each pair of spins is simultaneously minimized, there is no competition between the interactions. Such a ferromagnetic ground state corresponds directly to the ground state of a classical Heisenberg ferromagnet, where $\mathbf{S_i}$ are treated as vectors.

The low energy excitations above a ferromagnetic ground state are described accurately by ferromagnetic spin-wave theory. This theory treats the quasiclassical ground state as a vacuum state, and the low-energy collective excitations of spins are described as bosonic quasiparticles called magnons. The zero-point oscillation of these magnons gives a correction to the magnetization of the ground state.

The correspondence with the ground state of a classical Heisenberg model breaks when the spins are coupled antiferromagnetically, $J(r_{ij}) > 0$. In the classical case, on a bipartite lattice, the ground state is the quintessential up-down Néel state. In a two-particle Hamiltonian for spin-S,

$$H_{ij} = J(r_{ij})(S_i^z S_j^z + 1/2(S_i^+ S_j^- + S_i^- S_j^+)) = J(r_{ij}) \left(\frac{1}{2}(\mathbf{S_i} + \mathbf{S_j})^2 - S(S+1)\mathbb{1} \right), \tag{2.3}$$

only the term proportional to $S_i^z S_j^z$ gives an energy contribution in the Néel state. The step operators S^+ and S^- introduce quantum fluctuations in the z component of the spin which destabilize the classical ground state. In fact, there is no isotropic microscopic Hamiltonian for which the Néel state is an eigenstate. Isotropic theories that exhibit this kind of classical antiferromagnetic long-range order are macroscopic, where one associates a magnetic moment with each sublattice [5, 6]. However, in certain cases, antiferromagnetic Heisenberg models can still feature spontaneous symmetry breaking order that resembles classical long-range order. For example, using the Hartree-Fock method on the $3d$ simple cubic lattice, it is possible to identify magnetic "sublattices", where the spins principally point up and down[3]. The thermal properties and neutron diffraction experiment on such materials suggest the validity of this result.

The ground state of the spin-1/2 two-particle Hamiltonian, Eq. (2.3), is the SU(2) singlet state $1/\sqrt{2}(|\uparrow\downarrow\rangle - |\downarrow\uparrow\rangle)$. Contrary to ferromagnetism, the energy of multiple Heisenberg bounds sharing a given spin cannot be optimized this way. It is not at all obvious that this singlet property of the ground state would remain true for larger system sizes, yet, it is the case for a large class antiferromagnetic models. The famous Marshall-Lieb-Mattis theorem [8, 9] states that: For an SU(2) symmetric antiferromagnetic Hamiltonian, on a finite bipartite lattice, with equal size bipartite sublattices, the ground state is in the SU(2) singlet subspace of the total many-body Hilbert space. States in the SU(2) singlet subspace are rotation invariant; therefore, a consequence of the Marshall-Lieb-Mattis theorem is, that there can be no spontaneous symmetry breaking and true long-range order in the ground state of systems where the theorem applies. Symmetry breaking can only occur in the thermodynamic limit. In the case when it happens, the symmetry breaking wave function can be constructed out of low energy eigenstates with a total spin larger than 0, and in the limit, its energy becomes asymptotically degenerate with the ground state energy.

We attain a rough estimate for the strength of the quantum fluctuations in the ground state of the Heisenberg model, by comparing the energy of a singlet bound, $-J(r_{ij})S(S+1)$, with the energy of the quasiclassical Néel state, $-J(r_{ij})S^2$, for the two-particle Hamiltonian Eq. (2.3). One can think of the difference of these two energies, as the energy contribution of the quantum fluctuations of S^z. The ratio of the contribution of the fluctuations to the classical ground state energy is $1/S$. If we assume that the energy of all bounds can be minimized simultaneously, the ratio for a larger system is $1/(zS)$, where z is the coordination number of the lattice. This assumption is obviously unsound, nevertheless, the general picture

[3]However, no proof exists for real magnetic sublattices in the ground state [7]

its result provides is correct: The effect of the quantum fluctuations on the ground state is larger for low spin and coordination number (and consequently, lattice dimension).

One consequence of the large quantum fluctuations in 1 and $2d$ antiferromagnetic systems is, that it is easier to for thermal fluctuations to destroy long range order, than it is on lattices with higher dimension. In 1 and $2d$, long-range thermal fluctuations can be created with little energy cost. Since these increase the entropy of the system more than short-range fluctuations, the free energy favors them, and symmetry-breaking long-range correlations are destroyed on finite temperatures. The Mermin-Wagner theorem [10] states that: There can be no spontaneous breaking of a continuous symmetry on finite temperature in 1 and $2d$ systems with sufficiently short-ranged interactions. The result of antiferromagnetic spin-wave theory done on 1 and $1d$ Heisenberg models suggests that true long-range order may not occur even in the ground state of such models: The magnon correction to the magnetization diverges in $1d$, and is comparable to the ground state magnetization in $2d$. This leads one to the conclusion, that the quasiclassical long-range ordered ground state the theory assumes is incorrect.

There is another consequence of large quantum fluctuations in $1d$: A fundamental difference between integer spin and half-integer spin irreducible representations (irreps) of SU(2) creates a profound difference in the ground state of such systems. The main effect of this difference is, that the wave-function of half-integer spin particles obtain a -1 factor when rotated by 2π, while the wave function of integer spin particles remains unchanged. In the continuum limit of the antiferromagnetic Heisenberg chain, one can treat the slowly varying part of the staggered magnetization as a field, and describe the low-momentum excitations with an effective field theory. Haldane showed, that in the integer spin case, the O(3) non-linear sigma model is the correct field theory to use. This model does not have a mass explicitly, however, a mass is dynamically generated by quantum fluctuations. This is the basis of the famous Haldane's conjecture, stating that integer spin antiferromagnetic chains are gapped. When there is a gap, the Goldstone theorem forbids spontaneous symmetry breaking in the ground state. The ground state of such systems is therefore truly disordered, with an exponentially decaying two-point correlation function.

In the half-integer spin case, the O(3) non-linear sigma model is no longer a good effective field theory. This is because due to the rotation property of half-integer spins, the long-wavelength fluctuations make additional terms relevant in the action integral of the model. On the contrary, there is an important result for half-integer spin systems, which states the opposite of Haldane's conjecture: Lieb,

Schultz, Mattis and Afflect showed [11], that on an even-length, antiferromagnetic, half-integer spin chain, given a particular ground-state wave function, one can construct on other wave function by rotations of spins, with an upper bound to its energy, that becomes asymptotically degenerate with the ground state-energy in the thermodynamic limit. The consequence of this is, that either there are gapless excitations in the thermodynamic limit, or the wave function constructed is also a ground state, and therefore the ground state is degenerate. The Bethe ansatz solution for the 1/2-spin Heisenberg chain [12] is an example for the former case. In general, the Heisenberg chains that fall in the former case do not have true long-range order. Instead, they exhibit quasi-order, where the two-point correlation function decays only algebraically. In these systems there are gapless Goldstone-like excitations that "perceive" the system as ordered in their sufficiently large environment.

Frustration, or in other words, the situation where interactions between different pairs of particles cannot be optimized simultaneously, is yet another mechanism that acts against the forming of long-range order in magnetic systems. This can result both from multiple types of competing interactions, e.g. in a J1-J2 Heisenberg model, or from lattice geometry. The result is a macroscopic scale degeneracy of the ground-state even in classical models. In certain cases however, quantum fluctuations counteract the effect of frustration by selecting a certain preferred ground state from the degenerate manifold with their contribution to the free energy. This phenomenon is named "order by disorder", and in a broad sense, it happens because the ground state degeneracy caused by frustration is "accidental", and not a result of some symmetry of the system. For example, order by disorder in an antiferromagnetic Heisenberg model succeeds on the kagome lattice [13], but fails on the pyrochlore lattice [14, 15].

2.4 Quantum paramagnets

In a thermal paramagnet, all magnetic order is destroyed by the thermal fluctuations, and no continuous physical symmetry is broken. It is not possible to categorize these paramagnets further if one takes only the magnetic degrees of freedom into account. However, the situation is different in macroscopically phase coherent quantum paramagnets, where long-range order is broken down by quantum fluctuations. These systems can exhibit internal orders, and non-trivial excitations, that cannot be described by Landau's theories of phase transitions and Fermi liquids respectively. The general theory of these magnetically disordered insulators started forming only around two decades ago.

In non phase-coherent matter, the mathematical object that describes the physical state of the system is a positive definite classical spatial probability distribution function. For example, in solid state materials, this is the time averaged microscopic charge density function. The conventional phases that appear in such systems are characterized by the spatial symmetries of this classical probability distribution. These symmetry transformations form a group, that is identical to one of the 230 space groups describing crystallographic structures.

When matter becomes phase-coherent, the relevant mathematical object that describes its state, is a complex wave function. Spatial symmetries alone are insufficient to characterize the phases arising in this situation. Such systems may have different phases, that have the same set of spatial symmetries. Landau's idea of characterizing the phases by their symmetries still works to an extent, but one has to extend spatial symmetries with the possible "internal" symmetries of a wave function, and this can give rise to non-physical order parameters. This categorization of paramagnetic phases by an extended set of symmetries is the main idea behind the projective symmetry group approach pioneered by Wen [16]. Beyond the wider range of possible symmetries, phase-coherent systems can also give rise to topological order. These phases cannot be categorized by symmetries alone, for that purpose, one needs to introduce topological concepts.

The appropriate language to describe quantum paramagnets, is the language of valence bonds. By Marshall's theorem, the ground state of most quantum antiferromagnets is in the total singlet subspace. This subspace is spanned by wave functions in which all electrons are paired into singlets, or valence bonds. Thus, the ground state can be expressed as a superposition of singlet coverings. This description was first introduced by Anderson, who coined the term resonating valence bond states for it [17, 18]. He also proposed, that there might be a link between these states, and high temperature superconductivity, since electrons are paired up [19, 20].

The two most qualitatively distinguishable types of quantum paramagnets are valence bond crystals (VBC), and spin liquids. The long-distance two-point correlation function vanishes in both, but in VBC states, there might be higher order correlations, e.g. dimer-dimer. These VBC states contain only nearest neighbor valence bonds, therefore, they break lattice translation symmetry with various unit cells. Contrarily, spin liquids contain valence bonds of varying lengths. As the name suggests, they do not break lattice translation symmetry, and all higher order correlations vanish at long distances. Spin liquids can be further classified by the lengths of the valence bonds that appear in them. There are short range, or gapped Z_2 spin liquids, and long-range algebraic spin liquids.

One peculiarity of quantum spin liquids, is that in many cases, they exhibit fractionalization even above 1d. A fractional excitation carries quantum numbers which are fractions of the local degrees of freedom, therefore, it cannot be associated with collective modes in the Landau sense. When true fractionalization occurs, the fractional excitations are deconfined, meaning that they can be moved infinitely apart, by expanding only finite energy. In 1d antiferromagnetic systems, fractional spin-1/2 spinon excitations, or in other words, spin-charge separation is rather common. These excitations are usually associated with kinks, domain walls and solitons. Contrarily, above 1d, spin-1 collective magnon excitations are much more prevalent. Not all spin liquids have fractionalization, for example fractional excitations are confined in algebraic spin liquids, but it might occur in Z_2 spin liquids. In the phases where it does occur, generally, there is topological order. Anderson proposed that fractionalization might play a role in high temperature superconductivity [19].

2.5 Methods for studying models of quantum magnetism

One can employ a number of methods for studying interacting spin systems. Each of these has its respective advantages and shortcomings.

In certain special cases, it is possible to find the exact ground state, and even the entire spectrum of the system with analytical methods only. This is usually done by finding some clever transformation that decouples the many coupled degrees of freedom. For example, the XY-chain can be solved by means of a Jordan-Wigner transformation, and the 2d Ising model by Bethe ansatz. Contrarily to these, some other exactly solvable models were born by searching for a parent Hamiltonian that has a given ground state. Such is the case with the AKLT state and its Haldane gapped parent Hamiltonian on a spin-1 chain [21, 22]. Although these systems might sometimes feel artificial, they do provide valuable insight into the nature of quantum magnetism.

When analytical solution is not a possibility, perhaps the most obvious method one can use is the exact diagonalization of the Hamiltonian for some finite lattice size. This is the most universally applicable numerical method, since it works for all parameter values and lattice configurations. Unfortunately, it is also the most resource intensive method. Due to the size of the Hilbert space scaling exponentially with the number of particles, the spectrum can only be calculated for at most a few 10s of spins this way. In the case of SU(n) symmetric antiferromagnets, the

efficiency of exact diagonalization can be improved somewhat, by restricting the calculation to the singlet sector. The method for achieving this, is a relatively recent development [23, 24].

For studying a larger number of spins, one has to give up on exact solutions, and use approximate methods. The quasiclassical Spin-wave theory and its generalizations are able to treat very large lattices, however, they are applicable only when the ground state is close to classical, and the quantum fluctuations can be neglected; spin-wave theory is therefore unfit for the study of quantum paramagnets.

Large quantum fluctuations usually necessitate numerical methods. Quantum Monte Carlo methods work for moderate system sizes, but they suffer from the infamous sign problem: When calculating a highly oscillatory sum with a quantum Monte Carlo method, the cancellations that arise greatly decrease the accuracy of the result. Such cancellations are present, due to the Pauli principle, when summing over many configurations in fermionic systems. This makes quantum Monte Carlo unsuitable for half-integer spins. Even in the case of integer spin systems, the sign problem usually limits the applicability of Quantum Monte Carlo methods to a small set of parameter values [25–27].

Tensor network algorithms are a powerful alternative to Monte Carlo. A tensor network, sometimes also referred to as a matrix product state, is a type of variational ansatz, that is really successful in describing frustrated magnetic systems, provided that the energy gap is large enough. It is applicable to large systems sizes, even for the thermodynamic limit in $1d$ [28–30], and can be generalized to higher dimensions [31–33]. The way entanglement is distributed in the ansatz states is governed by an auxiliary dimension d. For a large enough d, every state has a matrix product state representation, however the computation time scales with d^{12}, thus only smaller values of it are feasible. Nevertheless, many of the states arising in physics can be approximated well with a small value of d.

In spite of all the progress made with classical simulations, physical theories must ultimately be judged by experiment. Unfortunately, experiments on solid state systems have a number of inconveniences: It is usually difficult to find materials that realize magnetically interesting Hamiltonians; in the rare cases where this is possible, these materials are described by rather complicated chemical formulas, and fabricating them is a science on its own. Furthermore, the Hamiltonians that can be implemented this way, are often plagued by undesirable residual interactions, that cannot be entirely neglected, and their parameters are not tuneable. Finally, due to the size of inter-atomic distances, the measurements one can make on such a solid state sample, for example by neutron scattering, are restricted to

observables that are averaged over many sites.

A possible solution to the problems of solid state experiments is, following the suggestion of Feynman [34] to simulate quantum magnetic materials with different quantum systems. There is no insurmountable theoretical barrier against building a universal quantum computer [35]. Such a machine could simulate any local quantum system efficiently using a set of universal quantum gates. This approach to simulation is usually referred to as a digital quantum simulator, and its realization is still in the early stages. A much less ambitious enterprise is abandoning the universal requirement, and constructing an easily controllable and measurable quantum system, that can simulate a small class of different quantum systems. The chief condition for this to be possible, is the existence of an isomorphic mapping between the observable algebras of the two systems. This approach is called an analog quantum simulator, and it has already been realized with several experimental platforms. Some examples are: ultracold quantum gases, polar molecules, trapped ions, photonic systems, quantum dots and superconducting circuits [36].

A particular analog quantum simulator, that suits perfectly to the simulation of solid state systems, can be implemented with ultracold atoms trapped in an optical lattice. In this type of arrangement, neutral atoms are held at the nodes of an interference pattern between laser beams, as a result of their polarization induced by the laser light [37]. Perhaps the largest advantage of ultracold atomic systems compared to other analog quantum simulators, is the scalability neutral atoms provide. Many thousands of atoms can be trapped simultaneously. It is possible to trap exactly one atom at each node, and the lattice geometry, dimensionality, disorder and depth can all be controlled. Even lattices with artificial gauge fields can be engineered [38]. These fields can be stronger than what is available in solid state experiments, which enables the investigation of new topological quantum phases. Quantum gas microscopes provide a way observe, and manipulate the system on the level of individual atoms [39–41].

The simulation of quantum magnetism requires two or more local quantum states, that can act as the elementary magnetic moments. These states can be encoded in various ways, for example, the Ising model can be realized by representing the two spin states with the difference of the occupation numbers between neighboring sites [42]. However, the most common approach is to use internal atomic Zeeman levels. Alkaline earth atoms are a good candidate for the simulation of SU(2), or even SU(N) symmetric magnetic models [43]. The two valence electrons give them a rich atomic structure to be exploited. In particular, the $g = {}^1S_0$ and $e = {}^3P_0$ electronic clock states of these atoms both have zero electronic angular momentum J. This means, that in these states J is almost perfectly decoupled

from the nuclear spin I. The charge neutral atoms interact in short range s-wave scattering; since this interaction is governed by the electronic structure of the atoms, the s-wave scattering lengths involving only the g and e states are going to be independent of the nuclear spin to a very good approximation. This implies, that by trapping the $2I + 1$ hyperfine sublevels of these states, one can simulate SU$(2I + 1)$ symmetric magnetic interactions. The scattering lengths of these interactions can be tuned in a wide range using external magnetic fields, by utilizing various scattering resonances.

An additional perk quantum simulators provide, is experimental access to systems with long-range interaction. This can be achieved, for example, with Rydberg atoms [44], or ion traps [45]. With the use of trapped atoms, even the infinite range SU(N) symmetric interaction, which is a subject of this thesis, is achievable experimentally: In the proposal [46], instead of an optical lattice, many thermal atoms are loaded into the same highly anharmonic trap, and the lattice sites are encoded into the occupied orbitals of the trap potential. Experiments like these open up a way to realize scenarios that were previously thought as being only of theoretical interest, e.g., Curie-Weiss-type transverse-field Ising models (i.e., the Lipkin-Meshkov-Glick model) [47–50], or the Haldane-Shastry model [51, 52]. This allows the many-body community to study phenomena that do not exist in short-range models, for example, the breaking of continuous symmetries in one-dimensional models.

2.6 Mean field theories and permutation symmetry

Of the many techniques used to investigate quantum spin systems, we give special attention to perhaps the simplest one, mean-field theories. These use variational wave functions of product form to characterize the ground state properties of certain problems. The use of this method excludes all effects of quantum correlations from one's analysis, thus the validity of the results depends heavily on the level of entanglement of the ground state of the particular problem. In mathematical physics literature, permutation symmetric models in the thermodynamic limit are also often referred to as mean field models. The connection between the two interpretations of the word is formalized by the quantum de Finetti theorem. Several versions of this theorem have been developed in recent times [53–56]. Its fundamental statement is, that for an N-partite, permutation symmetric quantum state ρ, the state of any k-partite subsystem can be efficiently approximated by a convex

combination of independent, identically distributed product states,

$$\mathrm{Tr}_{N-k}(\rho) \approx \sum_i p_i \sigma_i^{\otimes k}, \quad \text{where } p_i \geq 0 \text{ and } \sum_i p_i = 1. \tag{2.4}$$

The different versions of the theorem use different types of distances, e.g., trace distance, but the error of the approximation is always proportional to k/N. Note that the permutation symmetry of ρ implies that the reduced state is independent of which $N-k$ subsystems one chooses to trace out.

The ground state of a permutation symmetric system is not necessarily permutation symmetric itself; however, one can always create a permutation symmetric mixture of ground states. Let P_{GS} denote the orthogonal projector to the ground state subspace of the permutation symmetric Hamiltonian H of an N-partite quantum system, and d_{GS} the dimension of this subspace. Consider the "twirl" with the permutation group of the subsystems, S_N,

$$\overline{\rho}_{GS} = \frac{1}{d_{GS} N!} \sum_{\pi_i \in S_N} \pi_i^{-1} P_{GS} \pi_i. \tag{2.5}$$

With this, we have

$$\mathrm{Tr}(\overline{\rho}_{GS} H) = \frac{1}{d_{GS} N!} \sum_{\pi_i \in S_N} \mathrm{Tr}(P_{GS} \pi_i H \pi_i^{-1}) = \frac{1}{d_{GS}} \mathrm{Tr}(P_{GS} H) = E_{GS}; \tag{2.6}$$

therefore, $\overline{\rho}_{GS}$ itself must be a statistical mixture of pure ground states.

Now assume that H contains at most k-particle interactions. This means that the expected value of the energy depends only on the k-particle reduced states of $\overline{\rho}_{GS}$; therefore, in the thermodynamic limit by the quantum de Finetti theorem,

$$E_{GS} = \mathrm{Tr}(\overline{\rho}_{GS} H) = \mathrm{Tr}\left(\sum_i p_i \sigma_i^{\otimes N} H \right). \tag{2.7}$$

Since E_{GS} is the lowest eigenvalue of H, this means that the non-entangled state, $\sum_i p_i \sigma_i^{\otimes N}$, must also be a statistical mixture of ground states. In this way, mean field approximation yields an exact ground state for permutation symmetric spin models in the thermodynamic limit.

Chapter 3

The Schur-Weyl duality and the representation theory of $\mathrm{SU}(d)$

The purpose of this chapter is to introduce the classification of the irreducible representations, and the fusion rules of the special unitary group $\mathrm{SU}(d)$. The usual way to present these concepts is through the highest weights of representations, see e.g. [57]. However, considering how significant permutation symmetry is for this work, we take a path less traversed and answer our questions through the relationship of $\mathrm{SU}(d)$ and the group of permutations of N element sets, S_N. At the heart of this connection lies the Schur-Weyl duality, which we use to trace back the classification, and fusion rules of $\mathrm{SU}(d)$ irreps to the representation theory of S_N. This chapter assumes a basic understanding of the theory of Lie groups, for a thorough introduction of this subject see [58]. We provide somewhat more than the minimum amount of necessary facts; our reasoning is that this topic is usually swept under the rug in the physical literature, while discussed in much more abstract terms in the mathematical one. We hope that a good summary might be useful to some even outside the context of this thesis.

3.1 The Schur-Weyl duality

In its most general form, the Schur-Weyl duality relates the finite dimensional irreducible representations of the group of complex, invertible $d \times d$ matrices, the general linear group $\mathrm{GL}(d)$, and S_N. It is an archetypal situation in representation theory, where two different kinds of symmetries determine each other.

Consider the N-partite composite Hilbert space $\mathcal{H} = (\mathbb{C}^d)^{\otimes N}$, where the symbols $\otimes N$ in the exponent denote the N-th tensor power. The permutations in S_N act naturally on $\mathcal{H}$ by permuting the components of the tensor product; we call this the *natural representation*, $D_N^{S_N}$. The natural representation, $D_N^{\mathrm{GL}(d)}$, of

$g \in \mathrm{GL}(d)$ on $\mathcal{H}$, acts globally with g:

$$D_N^{\mathrm{GL}(d)}(g) = g^{\otimes N}. \tag{3.1}$$

The natural actions of these two groups commute with each other. The fundamental statement of the Schur-Weyl duality is proved by using the double centralizer theorem. It states that the connection goes further than mere commutation. We denote the complex subalgebra generated by the $A \subseteq \mathcal{A}$ subset of a complex algebra $\mathcal{A}$ with $\mathbb{C}[A]$; the centralizer of A, i.e., the set of those elements of $\mathcal{A}$ that commute with all elements of A, is denoted by A'.

Theorem 1 (Schur-Weyl duality)**.** $\mathbb{C}[D_N^{S_N}[S_N]]$*, and* $\mathbb{C}[D_N^{\mathrm{GL}(d)}[\mathrm{GL}(d)]]$ *are the full centralizers of each other in the algebra of endomorphisms* $\mathrm{End}(\mathcal{H})$*. That is,*

$$\begin{aligned} &\mathbb{C}[D_N^{S_N}[S_N]]' = \mathbb{C}[D_N^{\mathrm{GL}(d)}[\mathrm{GL}(d)]] \quad \textit{and} \\ &\mathbb{C}[D_N^{\mathrm{GL}(d)}[\mathrm{GL}(d)]]' = \mathbb{C}[D_N^{S_N}[S_N]]. \end{aligned} \tag{3.2}$$

In other words, every permutation invariant linear operator on $\mathcal{H}$ can be expressed as a complex linear combination of operators in $D_N^{\mathrm{GL}(d)}[\mathrm{GL}(d)]$; vice versa, every linear operator on $\mathcal{H}$ invariant to global $\mathrm{GL}(d)$ transformations can be expressed as a complex linear combination of permutations in $D_N^{S_N}[S_N]$.

By using Schur's lemma, one can rephrase the Schur-Weyl duality in terms of irreducible representations. Let

$$D_N^{S_N} \cong \bigoplus_\lambda \left[(D_\lambda^{S_N})^{\oplus m_\lambda^{S_N}} \right] \tag{3.3}$$

be the decomposition of $D_N^{S_N}$ into irreducible representations $D_\lambda^{S_N}$ of S_N with multiplicities $m_\lambda^{S_N}$, where by $\cong$ we denote unitary equivalence. Accordingly, the Hilbert space decomposes as

$$\mathcal{H} = \bigoplus_\lambda (\mathcal{H}_\lambda \otimes \mathcal{K}_\lambda), \tag{3.4}$$

where the permutations in $D_N^{S_N}$ act irreducibly on $\mathcal{K}_\lambda$, and as identity on $\mathcal{H}_\lambda$; or to put it in another way:

$$D_N^{S_N}(\pi) = \bigoplus_\lambda \mathbb{1}_{\mathcal{H}_\lambda} \otimes D_\lambda^{S_N}(\pi) \qquad \forall \pi \in S_N. \tag{3.5}$$

Furthermore, $\dim(\mathcal{K}_\lambda) = \dim(D_\lambda^{S_N})$ and $\dim(\mathcal{H}_\lambda) = m_\lambda^{S_N}$. The terms $\mathcal{H}_\lambda \otimes \mathcal{K}_\lambda$ of Eq. (3.4) are the irreducible sectors of S_N, which contain all instances of the irrep

λ on $\mathcal{H}$.

The following is a simple corollary of Schur's lemma:

Lemma 2. *Let V and W be complex, finite dimensional vector spaces, G a group, and D_V^G a complex linear representation of G on V. D_V^G is irreducible iff,*

$$\{D_V^G(g) \otimes \mathbb{1}_W : g \in G\}' = \{\mathbb{1}_V \otimes A : A \in \mathrm{End}(W)\}. \tag{3.6}$$

Proposition 1. *The irreducible sectors of* GL(d) *and S_N on $\mathcal{H}$ coincide. That is, the natural representation of* GL(d) *decomposes to irreducibles as:*

$$D_N^{\mathrm{GL}(d)}(g) \cong \bigoplus_\lambda D_\lambda^{\mathrm{GL}(d)}(g) \otimes \mathbb{1}_{\mathcal{K}_\lambda} \qquad \forall g \in \mathrm{GL}(d), \tag{3.7}$$

where $D_\lambda^{\mathrm{GL}(d)}$ is an irreducible representation acting on the $\mathcal{H}_\lambda$ tensor factors of the Hilbert space decomposition Eq. (3.4).

Proof. According to Lemma 2, every element in the centralizer $D_N^{S_N}[S_N]'$ acts as identity on the $\mathcal{K}_\lambda$ tensor factors, i.e.,

$$\forall X \in D_N^{S_N}[S_N]' \quad \exists A_\lambda^X \in \mathrm{End}(\mathcal{H}_\lambda) : \quad X = \bigoplus_\lambda A_\lambda^X \otimes \mathbb{1}_{\mathcal{K}_\lambda}. \tag{3.8}$$

By the Schur-Weyl duality, this must also be a property of $D_N^{\mathrm{GL}(d)}[\mathrm{GL}(d)]$. Therefore, there must exist a linear representation $D_\lambda^{\mathrm{GL}(d)}$ of GL(d) on each $\mathcal{H}_\lambda$, for which

$$D_N^{\mathrm{GL}(d)}(g) \cong \bigoplus_\lambda D_\lambda^{\mathrm{GL}}(g) \otimes \mathbb{1}_{\mathcal{K}_\lambda} \qquad \forall g \in \mathrm{GL}(d). \tag{3.9}$$

It is not yet clear if D_λ^{GL} is irreducible. For this reason, we use the Schur-Weyl duality again in the other direction. The commutant $D_N^{\mathrm{GL}(d)}[\mathrm{GL}(d)]'$ must be compatible with the irrep decomposition of $D_N^{S_N}$ in Eq. (3.5), therefore,

$$\forall X \in D_N^{\mathrm{GL}(d)}[\mathrm{GL}(d)]' \quad \exists B_\lambda^X \in \mathrm{End}(\mathcal{K}_\lambda) : \quad X = \bigoplus_\lambda \mathbb{1}_{\mathcal{H}_\lambda} \otimes B_\lambda^X, \tag{3.10}$$

and according to Lemma 2, each $D_\lambda^{\mathrm{GL}(d)}$ must be irreducible. □

Proposition 1 implies that, for fixed values of N and d, the decomposition Eq. (3.4) of $\mathcal{H}$ into irreducible sectors provides a bijection between the GL(d) and S_N irreps that appear in it.

3.2 The Schur-Weyl duality for $\mathrm{U}(d)$ and $\mathrm{SU}(d)$

The notion of compactness is in a sense, a way to generalize certain fundamental properties of finite sets to infinite sets. Compact Lie groups are better understood, and are easier to work with than non-compact Lie groups, because many properties of finite groups carry over to them. $\mathrm{GL}(d)$ is not compact, however, in a qualitative way, its representation theory is controlled by its maximal compact subgroup, the group of unitary transformations $\mathrm{U}(d)$. Here, we show that the Schur-Weyl duality is true when $\mathrm{GL}(d)$ is replaced by $\mathrm{U}(d)$ or $\mathrm{SU}(d)$.

Let $\mathfrak{gl}(d)$ denote the (complex) Lie algebra of $\mathrm{GL}(d)$, or in other words, the set of $d \times d$ complex matrices. Let $\mathfrak{u}(d)$, denote the (real) Lie algebra of $\mathrm{U}(d)$, or the set of $d \times d$ skew-hermitian matrices. The natural representation of $m \in \mathfrak{gl}(d)$ on $\mathcal{H}$ that corresponds to Eq. (3.1) is:

$$D_N^{\mathfrak{gl}(d)}(m) = m \otimes \mathbb{1} \otimes \cdots \otimes \mathbb{1} + \mathbb{1} \otimes m \otimes \cdots \otimes \mathbb{1} + \cdots + \mathbb{1} \otimes \cdots \otimes \mathbb{1} \otimes m. \quad (3.11)$$

Proposition 2.

$$\mathfrak{gl}(d) = \mathbb{C}[\mathfrak{u}(d)]. \quad (3.12)$$

Proof. For all $m \in \mathfrak{gl}(d)$ we define the skew-hermitian matrices $u^{(m)}$ and $v^{(m)}$ with,

$$v^{(m)} = \frac{i}{2}(m + m^\dagger), \quad u^{(m)} = \frac{1}{2}(m - m^\dagger). \quad (3.13)$$

Then,

$$m = u - iv. \quad (3.14)$$

□

Corollary. *The Schur-Weyl duality is true with* $\mathrm{GL}(d)$ *replaced by* $\mathrm{U}(d)$.

Proof. A matrix commutes with all elements of a connected Lie group of matrices if and only if it commutes with all elements of its Lie algebra; therefore we have:

$$\begin{aligned}\mathbb{C}[D_N^{\mathrm{GL}(d)}[\mathrm{GL}(d)]]' = \mathbb{C}[D_N^{\mathrm{GL}(d)}[\mathfrak{gl}(d)]]' = \\ \mathbb{C}[D_N^{\mathrm{GL}(d)}[\mathfrak{u}(d)]]' = \mathbb{C}[D_N^{\mathrm{GL}(d)}[\mathrm{U}(d)]]'.\end{aligned} \quad (3.15)$$

□

The Lie algebra of $\mathrm{SU}(d)$, $\mathfrak{su}(d)$ is the set of $d \times d$ traceless skew-hermitian matrices. This tracelessness calls for an additional step compared to the $\mathrm{U}(d)$ case.

Proposition 3. *The Schur-Weyl duality is true with* $\mathrm{GL}(d)$ *replaced by* $\mathrm{SU}(d)$.

Proof. For all $m \in \mathfrak{gl}(d)$ we define the traceless skew-hermitian matrices $u^{(m)}$ and $v^{(m)}$ with:

$$\begin{aligned} v^{(m)} &= i\left(\frac{1}{2}(m+m^\dagger) - \frac{\Re(\mathrm{Tr}(m))}{d}\mathbb{1}\right), \\ u^{(m)} &= \frac{1}{2}(m-m^\dagger) - \frac{\Im(\mathrm{Tr}(m))}{d}\mathbb{1}, \end{aligned} \tag{3.16}$$

and we have,

$$m = u^{(m)} - iv^{(m)} + \frac{\mathrm{Tr}(m)}{d}\mathbb{1}, \tag{3.17}$$

therefore,

$$\mathfrak{gl}(d) = \mathbb{C}[\mathfrak{su}(d) \cup \{\mathbb{1}\}], \tag{3.18}$$

but,

$$\mathbb{C}[\mathfrak{su}(d) \cup \{\mathbb{1}\}]' = \mathbb{C}[\mathfrak{su}(d)]', \tag{3.19}$$

because the additional identity matrix does not influence the commutant. □

From here on we will use the notations $D_\lambda^{\mathrm{U}(d)}, D_\lambda^{\mathrm{SU}(d)}$, for a representation of $GL(d)$ restricted to the corresponding subgroup. A consequence of propositions 2 and 3 is that the Schur-Weyl duality allows one to label the U(d) and SU(d) irreps appearing in the irrep decompositions of $D_N^{\mathrm{U}(d)}$ and D_N^{SU} with the corresponding irreps of S_N.

3.3 Young diagrams, and the group of permutations

We are tracing back most problems concerning the irreps of SU(d) to the same problems for S_N, therefore, a few words about the group of permutations is in order. The representation theory of S_N was constructed by Frobenius, Schur, and Young, and its distinctive feature is a close connection to combinatorics. This connection can be ascribed to the fact that the irreducible representations of S_N are in a natural one-one correspondence with the integer partitions of N. In the following, we elaborate on this classification.

An integer partition of a positive integer N, is a weakly decreasing sequence of positive integers $\lambda = (\lambda_1, \lambda_2, \ldots, \lambda_l)$ satisfying $\sum_{i=1}^{l} \lambda_i = N$. For example, the partitions of 4 are,

$$(4),\ (3,1),\ (2,2),\ (2,1,1),\ (1,1,1,1). \tag{3.20}$$

We denote λ being an integer partition of N by $\lambda \vdash N$. For integer partitions with repeating numbers, we will sometimes use the power notation, e.g., $(2,2,2,1,1) \cong$

$(2^3, 1^2)$. An integer partition $\lambda = (\lambda_1, \lambda_2, \ldots, \lambda_l)$ is often visualized with a Young diagram: A collection of N boxes arranged in left justified rows, where the i-th row contains λ_i boxes. For example,

$$(3,2,1) \cong \ydiagram{3,2,1}\,, \quad (4,2) \cong \ydiagram{4,2}\,. \tag{3.21}$$

We will refer to the integer partition corresponding to a diagram as the shape of the diagram. The irreducible representations of S_N are labeled by integer partitions, or Young diagrams. Here, we give an intuitive understanding for why this happens. Every permutation $\pi \in S_N$ can be uniquely decomposed into disjoint cycles, i.e., each number in $\{1, 2, \ldots, N\}$ appears in exactly one cycle. For example, $(1,2)(3,4,5) \in S_5$ is the permutation that swaps 1 and 2, and sends $3 \to 4 \to 5 \to 3$. In this way, the lengths of the cycles of any given permutation in S_N, make up a partition of N when arranged in a weakly decreasing order. We call this partition the cycle type of the permutation, e.g., the cycle type of the permutation in the last example is $(3,2)$. One can think of the conjugation of a permutation π with another one σ, as relabeling the elements in the cycle notation of π with σ. For example, if σ maps x to x' and

$$\pi = (abc)(de), \quad \text{then} \quad \sigma\pi\sigma^{-1} = (a'b'c')(d'e'). \tag{3.22}$$

It follows, that π and $\sigma\pi\sigma^{-1}$ have the same cycle types, and also that two permutations are the conjugates of each other if and only if they have the same cycle type. Therefore, the conjugacy classes of S_N are characterized by the cycle types, or in other words, the integer partitions of N. Elementary group theory tells us, that the number of irreps of a finite group is equal to the number of conjugacy classes. There is in fact an elaborate scheme which constructs an irrep of S_N corresponding to each integer partition of N. This is described in detail, for example in [59].

There is a different convention for labeling integer partitions, commonly used in particle physics, that stems from the highest weight classification of irreps. These are the so called *Dynkin labels*, which use the differences of the subsequent elements of the integer partitions. We denote the use of Dynkin labels by square brackets:

$$(\lambda_1, \lambda_2, \ldots, \lambda_l) \cong [\lambda_1 - \lambda_2, \lambda_2 - \lambda_3, \ldots, \lambda_{l-1} - \lambda_l, \lambda_l]. \tag{3.23}$$

An advantage of this convention, is that the partitions are labeled uniquely by *unordered* sequences of non-negative integers, which sometimes removes cumbersome constrains in calculations.

3.4 The irrep decomposition of the composite Hilbert space

Now that we established that the irreps of S_N can be labeled uniquely by partitions of N, or Young diagrams, the next important question to answer is: Which S_N irreps appear in the decomposition of the natural representation, $D_N^{S_N}$, and what are their dimensions and multiplicities? In this work, we do not plan to go too deeply into the representation theory of S_N, thus we merely state the results without proof here. The reader can consult the classical works written by Littlewood [60], Murnaghan [61], G. de B. Robinson [62] or a more recent summary by Sagan [59] for further details on the representation theory of S_N.

First, look at the case of $d \geq N$. Let $\{|v_i\rangle\}_{i=1}^N$ be an orthonormal set of vectors on $\mathbb{C}^d$. Now consider the subspace of $\mathcal{H} = (\mathbb{C}^d)^{\otimes N}$ spanned by the product vectors:

$$V_R = \mathrm{Span}\{|v_{\sigma(1)}\rangle \otimes |v_{\sigma(2)}\rangle \otimes \cdots \otimes |v_{\sigma(N)}\rangle \ : \ \sigma \in S_N\}. \tag{3.24}$$

It is clear that V_R is invariant to the natural action of S_N on $\mathcal{H}$. Moreover, the basis vectors of V_R can be identified with the elements of S_N itself. In fact, the S_N representation we obtain by restricting $D_N^{S_N}$ to V_R is equivalent to the regular representation of S_N, i.e., the representation of S_N on its own group algebra. The regular representation of a compact group contains all of its irreducible representations, therefore $D_N^{S_N}$ as well must contain all irreps of S_N with some non-zero multiplicities.

The case of $d \leq N$ is somewhat more complicated. Let λ be a Young diagram that has at least one column of height k. A peculiarity of the irreps of S_N, is that for the irrep corresponding to λ, one can find a set of basis vectors $\{e_i^\lambda\}$ spanning the irrep, and for each basis vector, a permutation subgroup

$$H_i \subseteq S_N, \ H_i \cong S_k, \quad \text{for which} \quad \pi e_i^\lambda = \mathrm{Sgn}(\pi) e_i^\lambda \quad \forall\ \pi \in H_i; \tag{3.25}$$

I.e., the basis vector e_i^λ is antisymmetric for all odd permutations in H_i. In the case of our natural representation on the composite Hilbert space $\mathcal{H}$, this means that e_i^λ should be antisymmetric to the swapping of any pair out of k given one-particle Hilbert spaces. It is not possible to construct such a vector when $k > d$, thus, $D_N^{S_N}$ cannot contain irreps corresponding to Young diagrams that have more that d rows.

Now, we give the full irrep decomposition of $D_N^{S_N}$. First, we need some new definitions: A *semistandard Young tableau* of shape λ and dimension d, is the Young diagram with shape λ, filled with numbers ranging from 1 to d, in such a way

that the numbers are non-decreasing in the rows, and increasing in the columns. For example, the semistandard Young tableaux of shape $(3,1)$ and dimension 2 are:

$$\begin{array}{|c|c|c|}\hline 1&1&1\\\hline 2\\\cline{1-1}\end{array}\,,\quad \begin{array}{|c|c|c|}\hline 1&1&2\\\hline 2\\\cline{1-1}\end{array}\,,\quad \begin{array}{|c|c|c|}\hline 1&2&2\\\hline 2\\\cline{1-1}\end{array}\,. \tag{3.26}$$

We denote that λ is an integer partition of N with at most d parts, i.e., a Young diagram with at most d rows, by $\lambda \vdash_d N$.

Proposition 4. *The irrep decomposition of $D_N^{S_N}$ is given by,*

$$D_N^{S_N} \cong \bigoplus_{\lambda \vdash_d N} m_\lambda^{(d)} D_\lambda^{S_N}, \tag{3.27}$$

where the multiplicity $m_\lambda^{(d)}$ is given by the number of semistandard Young tab-leaux with shape λ and dimension d.

The value of $m_\lambda^{(d)}$ can be expressed in a closed form by a so called *Hook length formula* [57],

$$m_\lambda^{(d)} = \prod_{(i,j)\in\lambda} \frac{d-i+j}{h_\lambda(i,j)}, \tag{3.28}$$

where $h_\lambda(i,j)$ is the "hook length" of the box at the i-th row and j-th column of the diagram λ, meaning the number of boxes at positions (k,l), such that $i=k$ and $l \geq j$, or $i \geq k$ and $l = j$. As an example, we write the corresponding hook length inside every box in the diagram $\lambda = (3,2,1)$:

$$\begin{array}{|c|c|c|}\hline 5&3&1\\\hline 3&1\\\cline{1-2} 1\\\cline{1-1}\end{array}\,,\quad m_{(3,2,1)}^{(3)} = 8. \tag{3.29}$$

For the cases of $d=2$ and $d=3$, it is relatively straightforward to express the hook lengths with the Dynkin labels of the diagram, and calculate the product:

$$m_{[p,q]}^{(2)} = (p+1) \quad \text{and} \quad m_{[p,q,l]}^{(3)} = (p+1)(q+1)(p+q+2)/2. \tag{3.30}$$

The dimension of the irrep $D_\lambda^{S_N}$ can also be expressed in a combinatorial way, it is given by the number of standard Young tableaux with shape λ. A standard Young tableau, is a Young diagram filled with numbers ranging from 1 to N, in such a way that the numbers are strictly increasing in both the rows and the columns. For example, the standard Young tableaux of shape $(3,1)$ are:

$$\begin{array}{|c|c|c|}\hline 1&2&3\\\hline 4\\\cline{1-1}\end{array}\,,\quad \begin{array}{|c|c|c|}\hline 1&2&4\\\hline 3\\\cline{1-1}\end{array}\,,\quad \begin{array}{|c|c|c|}\hline 1&3&4\\\hline 2\\\cline{1-1}\end{array}\,. \tag{3.31}$$

It is possible to express the number of standard Young tableaux with shape λ by an other hook-length formula:

$$\dim(D_\lambda^{S_N}) = \frac{N!}{\prod_{i,j} h_\lambda(i,j)}. \tag{3.32}$$

In terms of the irrep decomposition Eq. (3.4) of the composite Hilbert space, $m_\lambda^{(d)}$ is the dimension of $\mathcal{H}_\lambda$, and $\dim(D_\lambda^{S_N})$ is the dimension of $\mathcal{K}_\lambda$. According to the Schur-Weyl duality, this means that $m_\lambda^{(d)}$ is the dimension, and $\dim(D_\lambda^{S_N})$ is the multiplicity of the SU(d) irrep corresponding to the partition λ in the irrep decomposition of $D_N^{\mathrm{SU}(d)}$. Indeed, $m_{[p,q]}^{(2)}$ is equal to the dimension of the spin-$p/2$ irreducible representation of SU(2). We will expand on this connection later on.

3.5 Classifying the irreps of U(d)

The Schur-Weyl duality allows one to uniquely label the U(d) irreps that appear in the irreducible decomposition of an N-partite composite Hilbert space, with the S_N irreps, or Young diagrams, that correspond to them in Eq. (3.4). From this, a new question arises: Can this method be extended to label the U(d) irreps independently of any particular composite Hilbert space? That is, is it possible to find for every U(d) irrep, a number $N \in \mathbb{N}$ and an irrep of S_N which uniquely determines it with the Schur-Weyl duality? This would be possible if for each irrep of U(d), there exists exactly one $N \in \mathbb{N}$ for which the irrep appears in the irreducible decomposition of $D_N^{\mathrm{U}(d)} = (D_{(1)}^{\mathrm{U}(d)})^{\otimes N}$, where $D_{(1)}^{\mathrm{U}(d)}$ denotes the defining representation of U(d). It turns out that for the group U(d), this statement is only half-true. We are going to start with the true part.

Proposition 5. *If $D_\lambda^{\mathrm{U}(d)}$ is an irrep of* U(d)*, then $D_\lambda^{\mathrm{U}(d)}$ cannot appear in the irreducible decomposition of $D_N^{\mathrm{U}(d)}$ for more than one value of N.*

Proof. We can express any $u \in \mathrm{U}(d)$ as a product of a complex unit, and an element of SU(d),

$$\begin{aligned} u &= (\det u)^{1/d} \frac{u}{(\det u)^{1/d}} \quad \text{and therefore,} \\ D_N^{\mathrm{U}(d)}(u) &= (\det u)^{N/d} D_N^{\mathrm{U}(d)} \left(\frac{u}{(\det u)^{1/d}} \right). \end{aligned} \tag{3.33}$$

It also follows, that if the irrep $D_\lambda^{\mathrm{U}(d)}$ is present in the irrep decomposition of $D_N^{\mathrm{U}(d)}$, then

$$D_\lambda^{\mathrm{U}(d)}(u) = (\det u)^{N/d} D_\lambda^{\mathrm{U}(d)}\left(\frac{u}{(\det u)^{1/d}}\right). \tag{3.34}$$

If $D_\lambda^{\mathrm{U}(d)}$ were to appear in the irrep decomposition both $D_N^{\mathrm{U}(d)}$ and $D_{N'}^{\mathrm{U}(d)}$ for some $N' \neq N$, then for any fixed $u \in \mathrm{U}(d)$ we must have,

$$(\det u)^{N'/d} D_\lambda^{\mathrm{U}(d)}\left(\frac{u}{(\det u)^{1/d}}\right) \cong (\det u)^{N/d} D_\lambda^{\mathrm{U}(d)}\left(\frac{u}{(\det u)^{1/d}}\right), \tag{3.35}$$

w.r.t. unitary equivalence. This is a contradiction that one can see e.g., by comparing the determinants of the two sides.

□

The false part of our statement at the beginning is, that every irrep of $\mathrm{U}(d)$ appears in the irrep decomposition of $D_N^{\mathrm{U}(d)}$ for some $N \in \mathbb{N}$. An obvious counterexample would be the complex conjugate of the defining representation, or in other words, its dual representation $\overline{D_{(1)}^{\mathrm{U}(d)}}$. In this representation, we have,

$$\overline{D_{(1)}^{\mathrm{U}(d)}}(u) = (\det u)^{-1/d} \overline{D_{(1)}^{\mathrm{U}(d)}}\left(\frac{u}{(\det u)^{1/d}}\right), \tag{3.36}$$

which is incompatible with Eq. (3.34) for any $N \in \mathbb{N}$. Thus, according to Proposition 5, we can only uniquely label by a single Young diagram those irreps of $\mathrm{U}(d)$ which appear in the decomposition of $D_N^{\mathrm{U}(d)}$ for some $N \in \mathbb{N}$.

3.6 Classifying the irreps of $\mathrm{SU}(d)$

In this section we show that unlike in the case of $\mathrm{U}(d)$, it is truly possible to label all irreps of $\mathrm{SU}(d)$ with Young diagrams. This endeavor is going to involve some additional difficulties, because Proposition 5 does not apply for $\mathrm{SU}(d)$. Let us start with showing that all the irreps of $\mathrm{SU}(d)$ appear in the tensor powers of the defining representation.

We established with $\mathrm{U}(d)$, that for a compact group in general, the tensor powers of the defining representation do not necessarily contain all irreps. This changes if we add the dual of the defining representation to the mixture.

Proposition 6. *For a compact group G, and a faithful, unitary, finite dimensional representation D, every G-irrep appears in the irreducible decomposition of $D^{\otimes N} \otimes \overline{D}^{\otimes M}$ for some $N, M \in \mathbb{N}$.*

This Proposition is a corollary of a Galois correspondence between the closed normal subgroups of G, and the representation subrings of the representation ring of G. For a more through explanation see Appendix A.

Proposition 7. *All irreps of* SU(d) *appear in the irreducible decomposition of* $D_N^{\mathrm{SU}(d)} = \left(D_{(1)}^{\mathrm{SU}(d)}\right)^{\otimes N}$*, for some* $N \in \mathbb{N}$.

Proof. In Proposition 6, we can set $D = D_{(1)}^{\mathrm{SU}(d)}$, therefore, we only have to show that for SU(d), the dual of the defining representation appears in the irrep decomposition of some tensor power of the defining representation.

Now consider the composite Hilbert space $\mathcal{H} = (\mathbb{C}^d)^{\otimes d}$ and its antisymmetric subspace $(\mathbb{C}^d)^{\wedge d}$. This subspace is one-dimensional and spanned by the wedge-product vector,

$$|v_a\rangle = |v_1\rangle \wedge |v_2\rangle \wedge \cdots \wedge |v_d\rangle = \sum_{i_1,i_2,\ldots,i_d} \epsilon_{i_1,i_2,\ldots,i_d} |v\rangle_{i_1} \otimes |v\rangle_{i_2} \otimes \ldots \otimes |v\rangle_{i_d}, \quad (3.37)$$

where $\{|v_i\rangle\}_{i=1}^d$ is an orthonormal basis of $\mathbb{C}^d$. Projecting $D_d^{\mathrm{SU}(d)}$ to the antisymmetric subspace gives us,

$$\begin{aligned} &(|v_a\rangle\langle v_a|) D_d^{\mathrm{SU}(d)}(g) (|v_a\rangle\langle v_a|) = \\ &\qquad \det(D_{(1)}^{\mathrm{SU}(d)}(g)) |v_a\rangle\langle v_a| = |v_a\rangle\langle v_a| \qquad \forall g \in \mathrm{SU}(d), \end{aligned} \quad (3.38)$$

or in other words, the trivial representation. Since the irrep decomposition of $\left(D_{(1)}^{\mathrm{SU}(d)}\right)^{\otimes d}$ contains the trivial representation, the decomposition of $\left(D_{(1)}^{\mathrm{SU}(d)}\right)^{\otimes d-1}$ has to contain $\overline{D_{(1)}^{\mathrm{SU}(d)}}$. □

Now, we have to somehow deal with the fact that Proposition 5 does not work for SU(d), and the same irrep can appear in the decomposition of $D_N^{\mathrm{SU}(d)}$ for multiple values of N. An easy example for this is the case of SU(2). The well-known spin addition rule is,

$$D_{s_1}^{\mathrm{SU}(2)} \otimes D_{s_2}^{\mathrm{SU}(2)} \cong \bigoplus_{s=|s_1-s_2|}^{s_1+s_2} D_s^{\mathrm{SU}(2)}, \quad (3.39)$$

where we momentarily broke our previous convention and labeled irreps with their spins. According to Eq. (3.39), the trivial representation, $s = 0$, appears in the N-fold tensor powers of the defining representation, $s = 1/2$, for every even N. A way to avoid this problem is to look at irreps of SU(d), as irreps of U(d) that are restricted to the SU(d) $\subset$ U(d) subgroup. An U(d) irrep, when restricted to SU(d) stays irreducible. Indeed, assume that it contains a nontrivial SU(d)

invariant subspace, then the subspace would also have to be U(d) invariant, since U(d) transformations differ from SU(d) only by rotations of the complex plane. According to Proposition 7, one can obtain all irreps of SU(d) as restrictions of some U(d) irreps appearing in the decomposition of $D_N^{\mathrm{U}(d)}$ for some $N \in \mathbb{N}$; i.e., the restrictions of U(d) irreps that can be uniquely labeled by a Young diagrams.

It is not true however, that restricting different irreps of U(d) always results in different SU(d) irreps.

Proposition 8. *By restricting the $U(d)$ irreps corresponding to the Young-diagrams with Dynkin labels $[\lambda_1, \lambda_2, \ldots, \lambda_d]$ and $[\mu_1, \mu_2, \ldots, \mu_d]$ to the* SU(d) $\subset$ U(d) *subgroup, unitary equivalent $SU(d)$ irreps are obtained if and only if: $\lambda_i = \mu_i$ for all $1 \leq i \leq d-1$.*

The proof for this proposition can be found in [63]. Irreps of SU(d) are therefore labeled uniquely by equivalence classes of Young diagrams. The diagrams in the same equivalence class differ from each other only by columns of height d on their left side. E.g., for SU(3)

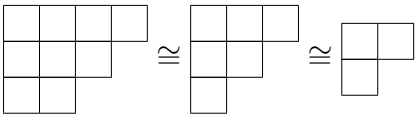

(3.40)

Furthermore, every equivalence class has exactly one diagram with $d-1$ rows in it; thus, $d-1$ row diagrams also uniquely label SU(d) irreps. We will use the latter method by default, and drop the d-th number of the partitions corresponding to SU(d) diagrams unless for some reason it is convenient to choose a different representant.

The equivalence classes are consistent with the Schur-Weyl duality in the sense that no two diagrams in an equivalence class have the same number of boxes, therefore, by Proposition 4, no pair of Young diagrams can be from the same equivalence class in the irrep decomposition of the Hilbert space $\mathcal{H} = (\mathbb{C}^d)^{\otimes N}$ in Eq. (3.4).

3.7 The fusion rules of SU(d)

The fusion rules of a group describe how a tensor product of irreps decomposes into a direct sum of other irreps, i.e., it gives the coefficients $m_\lambda^{\mu,\nu}$ in,

$$D_\mu \otimes D_\nu \cong \bigoplus_\lambda m_\lambda^{\mu,\nu} D_\lambda, \tag{3.41}$$

where D_μ, D_ν and D_λ denote irreps. Attempting to determine the SU(d) fusion rules through the link given by the Schur-Weyl duality, leads one further away from the representation theory of S_N, into the land of combinatorics. We shall refrain from going too much into details about this topic, and give only a brief summary.

The first thing to notice, is that we cannot simply trace back the SU(d) fusion rules to the S_N ones. Since the natural representations on composite Hilbert spaces obey $D_N^{\mathrm{SU}(d)} \otimes D_M^{\mathrm{SU}(d)} = D_{N+M}^{\mathrm{SU}(d)}$, the Schur-Weyl duality maps the tensor product of SU(d) irreps into an operation between irreps of various permutation groups, that maps a pair of S_N and S_M irreps into an S_{N+M} irrep. The way to solve this problem is to introduce a certain "outer product". That is, to go from the representation, or character ring of a single permutation group, $\mathcal{R}(S_N)$, to $\oplus_N \mathcal{R}(S_N)$, and introduce a ring product on it that maps a pair of elements from $\mathcal{R}(S_N)$ and $\mathcal{R}(S_M)$ into an element of $\mathcal{R}(S_{N+M})$; this is sometimes referred to as a graded ring structure. To obtain the desired ring product, we view $S_N \times S_M$ as a subgroup of S_{N+M}, and for the characters $\chi_\mu \in \mathcal{R}(S_N)$, $\chi_\nu \in \mathcal{R}(S_M)$, define the product $\chi_\mu \cdot \chi_\nu$ to be the character of S_{N+M} induced from the character $\chi_\mu \chi_\nu$ of the group $\chi_\mu \times \chi_\nu$,

$$\chi_\mu \cdot \chi_\nu = (\chi_\mu \chi_\nu) \uparrow^{S_{N+M}}, \tag{3.42}$$

and extend this definition bilinearly to the entirety of $\oplus_N \mathcal{R}(S_N)$. The mapping from the irreps of SU(d) to those of the permutation group provided by the Schur-Weyl duality, maps the tensor product of SU(d) irreps to the product defined with (3.42).

Determining the irrep decomposition of the product in (3.42) involves following the thread of yet another mapping between different areas of mathematics. This time, it is the additive isomorphism between the character ring of all permutation groups, $\oplus_N \mathcal{R}(S_N)$, and the ring of symmetric polynomials as described e.g., in [59]. The most important property of this isomorphism, is that it maps the product in (3.42) to the product of polynomials, and the elements of $\mathcal{R}(S_N)$, into symmetric polynomials of degree N, thereby preserving the graded ring structure. In particular, the isomorphism maps irreducible characters into *Schur functions*, a specific class of symmetric polynomials that constitutes a basis of symmetric polynomials. A unique Schur function can be constructed for each Young diagram. The question of the SU(d) fusion rules is thus transformed into the question of expanding the product of two Schur functions on the basis of Schur functions.

3.7.1 The Littlewood-Richardson rule

A combinatorial algorithm for decomposing the product of Schur functions was found by Littlewood and Richardson in 1934 [64], however they only proved its validity for certain simple cases. Their conjecture resisted rigorous proving attempts for over 40 years, by which time the necessary combinatorial framework was developed by Robinson, Schensted, Schützenberger and Knuth. The first rigorous proof for the general case was eventually achieved by Thomas [65].

In this section, we present the Littlewood-Richardson algorithm applied to the SU(d) and U(d) fusion rules. This algorithm involves attaching the boxes of one diagram in the product to the other. In order to be able to describe this process in detail, we first introduce some new concepts regarding Young diagrams.

Let (λ, μ) be a pair of Young diagrams for which λ contains μ, i.e., $\lambda_i \geq \mu_i \ \forall i$. The *skew diagram* λ/μ is the formal difference of the two diagrams: The set of boxes of λ that are not contained in μ. E.g.,

$(4,3,2)/(2,1) \cong$ 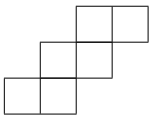 , $(5,4,3)/(3,2,1) \cong$ 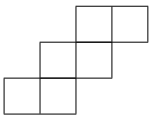 . (3.43)

As the above example shows, the shape of λ/μ does not determine λ and μ uniquely. The concepts of standard and semistandard tableaux are extended to skew shapes in the obvious way.

The *content* of a Young tableau is the sequence of frequencies of the numbers $1, 2, \ldots$ inside the boxes of the tableau. E.g.,

$$\mathrm{cont}\left(\begin{array}{|c|c|c|c|}\hline 1&1&1&2\\\hline 2&2&3\\\cline{1-3}\end{array}\right) = (3,3,1). \tag{3.44}$$

Sorted in decreasing order, the content is an integer partition corresponding to the same number as the shape of the tableau.

A *ballot sequence* is a sequence of positive integers, $\pi = i_1 i_2 \ldots i_n$, such that for any prefix subsequence, $\pi_k = i_1 i_2 \ldots i_k$, and any positive integer l, the frequency of the number l in π_k is at least as large as the frequency of $l+1$. E.g.,

$$\pi = 1\ 1\ 1\ 2\ 2\ 2\ 3, \tag{3.45}$$

is a ballot sequence, but

$$\pi = 1\ 2\ 3\ 1\ 2\ 2\ 1, \tag{3.46}$$

is not, as the 6th element breaks the rule. To make sense of the naming, think of an election in which candidate l has a weak lead over candidate $l+1$ during the

entire process of counting the ballots.

Now, we are finally ready to state the Littlewood-Richardson rule.

Theorem 3 (Littlewood-Richardson rule)**.** *The multiplicity, $m_\lambda^{\mu,\nu}$, of the irrep $D_\lambda^{\mathrm{SU}(d)}$ in the irreducible decomposition of tensor product of irreps, $D_\mu^{\mathrm{SU}(d)} \otimes D_\nu^{\mathrm{SU}(d)}$, is equal to the number of semistandard skew-tableaux with shape λ/μ and content ν, for which the sequence of numbers in the tableau read from right to left, top to bottom is a ballot sequence.*

One can visualize the rule by filling row i of the diagram ν with the number i, and attaching the boxes of the tableau thus created to the diagram μ in all possible ways such that the result has at most d rows, and the requirements of Theorem 3 are fulfilled. E.g, for the product of SU(4) representations,

$D_{(2,1)} \otimes D_{(2,1,1)} \cong$ 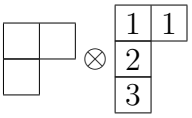 $\cong$ 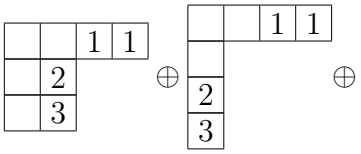 $\oplus$ $\oplus$

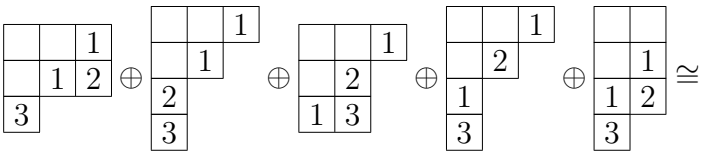

(3.47)

$$D_{(4,2,2)} \oplus D_{(4,1,1,1)} \oplus D_{(3,3,1)} \oplus 2D_{(3,2,1,1)} \oplus D_{(3,2,2)} \oplus D_{(2,2,2,1)} \cong$$
$$D_{(4,2,2)} \oplus D_{(3)} \oplus D_{(3,3,1)} \oplus 2D_{(3,2,1,1)} \oplus D_{(3,2,2)} \oplus D_{(1,1,1)}$$

While it is not entirely apparent from Theorem 3, but in accordance with the commutativity of the tensor product, the diagrams resulting from the algorithm are independent of the order of λ and μ in the product. We will now show some simple applications of the Littlewood-Richardson rules.

First, we confirm our statement in Section 3.4, about the dimension of $D_\lambda^{S_N}$ being equal to the number of standard Young tableaux with shape λ. According to the Schur-Weyl duality, the dimension of $D_\lambda^{S_N}$ is equal to multiplicity of $D_\lambda^{\mathrm{SU}(d)}$ in $(D_{(1)}^{\mathrm{SU}})^{\otimes N}$. Now write the number i to the i-th single-box Young diagram in this tensor power, and start expanding the tensor products, left to right, using the fusion rule. At the end of the process we get all the standard Young tableaux of all shapes $\mu \vdash_d N$; thus, the number of results with shape λ, i.e., the multiplicity of $D_\lambda^{\mathrm{SU}(d)}$, is equal to the number of standard Young tableaux with shape λ.

Armed with the knowledge of the fusion rules, we can now explain why SU(d) irreps labeled with diagrams differing only in height d columns are equivalent, as stated in Proposition 8. Let us take a step back and look at the irreps of U(d): As Eq. (3.38) shows, the partition (1^d) corresponds to the irrep mapping

each $u \in \mathrm{U}(d)$ to its determinant. Applying the Littlewood-Richardson algorithm yields,

$$\det(u) D^{\mathrm{U}(d)}_{(\mu_1,\mu_2,\dots\mu_d)}(u) = D^{\mathrm{U}(d)}_{(\mu_1,\mu_2,\dots\mu_d)}(u) \otimes D^{\mathrm{U}(d)}_{(1^d)}(u) \cong D^{\mathrm{U}(d)}_{(\mu_1+1,\mu_2+1,\dots\mu_d+1)}(u) \qquad \forall u \in \mathrm{U}(d). \tag{3.48}$$

Thus, U(d) representations labeled with Young diagrams $\mu_1 + k, \mu_2 + k, \dots, \mu_d + k$ differ only in a $\det^k$ factor.

Lastly, we introduce the relationship between the Young diagrams of an SU(d) irrep and its dual. The decomposition of the tensor product $D^{\mathrm{SU}(d)}_{\mu} \otimes D^{\mathrm{SU}(d)}_{\nu}$ contains the trivial representation iff $D^{\mathrm{SU}(d)}_{\nu} \cong \overline{D^{\mathrm{SU}(d)}_{\mu}}$. Since in the case of SU(d), the trivial representation is labeled by any height d rectangle diagram, let us look at the skew shape $(\mu_1^d)/\mu$ that complements μ to such a rectangle. This shape does not, in general, describe a normal Young diagram; however, after rotation by π, one gets the Young diagram $\overline{\mu} = (\mu_1 - \mu_d, \mu_1 - \mu_{d-1}, \dots, \mu_1 - \mu_2, 0)$.

Proposition 9. *The product $D^{\mathrm{SU}(d)}_{\mu} \otimes D^{\mathrm{SU}(d)}_{\overline{\mu}}$ contains the trivial representation.*

Proof. We must show that we can reshuffle the boxes of $\overline{\mu}$ into shape $(\mu_1^d)/\mu$ in a way that meets the criteria of the Littlewood-Richardson rules. One can decompose any skew diagram into a sequence of *horizontal strips*: The i-th horizontal strip $h_i(\lambda/\mu)$ of a skew diagram λ/μ, is the skew-diagram composed of the i-th box in every column of λ/μ counted from top to bottom. We denote the length of $h_i(\lambda/\mu)$ with $|h_i(\lambda/\mu)|$. Clearly, for a normal Young diagram λ, $|h_i(\lambda)| = \lambda_i$. Rotating a Young diagram by π does not change the number of columns with any given length, therefore, the length of the horizontal strips are invariant to such a rotation. Thus, $|h_i(\mu_1^d/\mu)| = \overline{\mu}_i$. In order to get a skew tableau with shape $(\mu_1^d)/\mu$, content $\overline{\mu}$, and box labels that constitute a ballot sequence, simply fill $h_i\left((\mu_1^d)/\mu\right)$ with the number i, such as in Fig. 3.1. □

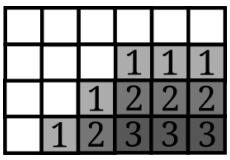

FIGURE 3.1: The Littlewood-Richardson skew tableau with shape $(6^4)/(6,3,2,1)$ and content $\overline{(6,3,2,1)}$.

Motivated by this result, we define the dual of an integer partition μ as $\overline{\mu}_i := \mu_1 - \mu_{d-i+1}$, and as a generalization of the concept, the M-dual for any positive integer $M \geq \mu_1$ as $\overline{\mu}_i^M := M - \mu_{d-i+1}$.

3.7.2 A closed formula for the fusion rules

There is a less-known result by H. Schlosser [66], that expresses the outcome of the Littlewood-Richardson algorithm with a closed formula. As we make use of it in our work in Chapter 6, in this section, we present the formula without proof.

Using the equivalence relation defined by Proposition 8, we can assume without loss of generality, that the SU(d) irreps in the tensor product have at most $d-1$ rows. Additionally, since all the semistandard skew tableaux constructed in the algorithm have ballot sequence fillings, boxes with label j can only appear in the j-th row or below. Let $k_{d-j,h}$, where $1 \leq j \leq d-1$ and $1 \leq h \leq d-j+1$, denote the number of boxes with label j in the $d-h+1$-th row of a λ/ν shaped skew tableau constructed in the Littlewood-Richardson algorithm applied to the product $D_\nu^{\mathrm{SU}(d)} \otimes D_\mu^{\mathrm{SU}(d)}$. Since the number of boxes with label j must be equal to the length of the j-th row of μ, we eliminate $d-1$ variables by setting: $k_{d-j,d-j+1} = \mu_j - \sum_{i=1}^{d-j} k_{d-j,i}$. With this notation, the length of the r-th line of a diagram λ in the product $D_\nu^{\mathrm{SU}(d)} \otimes D_\mu^{\mathrm{SU}}$ is expressed as,

$$\lambda_r = \nu_r + \mu_r - \sum_{i=1}^{d-r} k_{d-r,i} + \sum_{i=1}^{r-1} k_{d-i,d-r+1}, \tag{3.49}$$

where we define $\sum_{i=1}^{0} \cdots = 0$. The construction of the product diagrams using the $k_{d-j,h}$ indices is illustrated in Fig. 3.2.

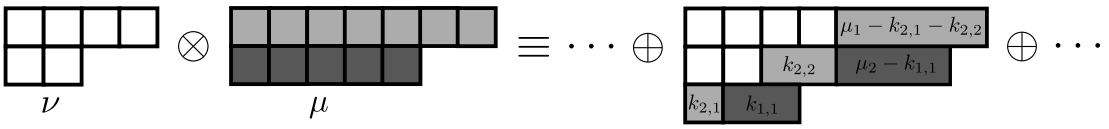

FIGURE 3.2: An illustration of the distribution of boxes corresponding the $k_{d-j,h}$ indices in the product of the SU(3) diagrams ν and μ.

We can express the irrep decomposition of the product by summing over the $k_{d-j,h}$ indices,

$$D_\nu^{\mathrm{SU}(d)} \otimes D_\mu^{\mathrm{SU}(d)} \cong \bigoplus_{\substack{k_{d-1,1}= \\ l(1,1)}}^{u(1,1)} \cdots \bigoplus_{\substack{k_{d-1,d-1}= \\ l(1,d-1)}}^{u(1,d-1)} \bigoplus_{\substack{k_{d-2,1}= \\ l(2,1)}}^{u(2,1)} \cdots \bigoplus_{\substack{k_{d-2,d-2}= \\ l(2,d-2)}}^{u(2,d-2)} \cdots \bigoplus_{\substack{k_{1,1}= \\ l(d-1,1)}}^{u(d-1,1)} D_\lambda^{\mathrm{SU}(d)}. \tag{3.50}$$

In order to obtain a semistandard tableau when attaching the boxes of μ to ν during the process of the algorithm, one has to start by attaching all the boxes with label 1, then attach all boxes with label 2 etc. In this way, the possible distributions of

the boxes with label j in the resulting skew tableau depend only on the distribution of the already attached boxes with labels $j' \leq j$. Additionally, we choose to step through all the possibilities of attaching the boxes with label j, by starting with row d and then going upward. The order of the direct sums in Eq. (3.50) read from the outside going inwards reflects this process, i.e., the lower and upper limits of each $k_{d-j,h}$ index, are functions of the indices deeper in the expression. The essence of Schlosser's result is in determining these upper, and lower, limits. A product diagram described by a set of $k_{d-j,h}$ indices stays consistent with all the restrictions of Littlewood-Richardson algorithm iff the indices are within the corresponding limits.

$$\begin{aligned}
&l(1,h) = 0, \\
&l(j,h) = \max\left\{0, \sum_{i=1}^{h+1} k_{d-j+1,i} - \sum_{i=1}^{h-1} k_{d-j,i} - \mu_{j-1} + \mu_j\right\} \quad \text{for } j > 1, \\
&u(j,h) = \min\left\{\nu_{d-h} - \nu_{d-h+1} + \sum_{i=1}^{j-1}(k_{d-i,h+1} - k_{d-i,h}) \,, \right. \\
&\qquad\qquad \left. \sum_{i=0}^{h-1}(\mu_{j+i} - \mu_{j+1+1} - k_{d-j,i})\right\},
\end{aligned} \tag{3.51}$$

where we define $k_{d-j,0} = 0$. Note that in the cases when the multiplicity of a diagram in the product is more than one, it will appear in Eq. (3.50) for multiple sets of indices.

As an example, we apply Eq. (3.50) to SU(2),

$$D^{\mathrm{SU}(2)}_{(\nu_1,0)} \otimes D^{\mathrm{SU}(2)}_{(\mu_1,0)} \cong \bigoplus_{k_{1,1}=0}^{\min\{\nu_1,\mu_1\}} D^{\mathrm{SU}(2)}_{(\nu_1+\mu_1-k_{1,1},k_{1,1})} \cong \bigoplus_{k_{1,1}=0}^{\min\{\nu_1,\mu_1\}} D^{\mathrm{SU}(2)}_{(\nu_1+\mu_1-2k_{1,1},0)}. \tag{3.52}$$

This recovers the spin addition formula, Eq. (3.39), that we expect, with the Young diagram $(\nu, 0)$ corresponding to the spin-$\nu/2$ irrep of SU(2). Another example, which we will make use of later, is the case of $d = 3$. We use Proposition 8, and dispose of the 3rd row of the resulting Young diagrams from the start,

$$\begin{aligned}
&D^{\mathrm{SU}(3)}_{(\nu_1,\nu_2)} \otimes D^{\mathrm{SU}(3)}_{(\mu_1,\mu_2)} \cong \\
&\bigoplus_{k_{2,1}=0}^{u(1,1)} \bigoplus_{k_{2,2}=0}^{u(1,2)} \bigoplus_{k_{1,1}=l(2,1)}^{u(2,1)} D^{\mathrm{SU}(3)}_{(\nu_1+\mu_1-2k_{2,1}-k_{2,2}-k_{1,1},\nu_2+\mu_2-k_{2,1}+k_{2,2}-2k_{1,1})} \quad \text{where,} \\
&\quad u(1,1){=}\min\{\mu_1-\mu_2,\nu_2\}, \quad u(1,2){=}\min\{\nu_1-\nu_2,\mu_1{-}k_{2,1}\}, \\
&u(2,1){=}\min\{\nu_2{+}k_{2,2}{-}k_{2,1},\mu_2\}, \quad l(1,1){=}\max\{0,k_{2,2}{+}k_{2,1}{-}\mu_1+\mu_2\}.
\end{aligned} \tag{3.53}$$

3.8 The quadratic Casimir operator of $\mathrm{SU}(d)$

The universal enveloping algebra of the Lie algebra $\mathfrak{g}$, is the largest associative algebra generated by $\mathfrak{g}$, in which the Lie bracket $\{x, y\}$ corresponds to the commutator $xy - yx$. The Casimir operators of $\mathfrak{g}$, are a set of symmetric, homogeneous polynomials of elements of $\mathfrak{g}$, that form a basis of the center of the universal enveloping algebra. The eigenvalues of these operators are often used to characterize the irreducible representations of $\mathfrak{g}$. $\mathfrak{su}(d)$ has $d-1$ independent Casimir operators. Out of these, only the quadratic one will be relevant in this work; this section is dedicated to its definition.

First, we have to specify a basis on $\mathfrak{su}(d)$. The real Lie algebra $\mathfrak{su}(d)$ consists of traceless skew-hermitian matrices. Constructing a basis on this algebra for arbitrary dimension d is a convoluted problem; however, if we use the basis elements only for the purpose of defining Casimir operators, we can introduce a major simplification: We use the complexified algebra $\mathbb{C}[\mathfrak{su}(d)]$ in place of $\mathfrak{su}(d)$; this changes the resulting Casimir operators by at most a complex factor.

$\mathbb{C}[\mathfrak{su}(d)]$ consists of traceless, complex $d \times d$ matrices. It is easy to specify a basis on this algebra for arbitrary dimensions. As explained in Section 3.2, $\mathbb{C}[\mathfrak{u}(d)] = \mathfrak{gl}(d)$. The matrix units $\{|\alpha\rangle\langle\beta|\}_{\alpha,\beta=1}^{d}$, where $\{|\alpha\rangle\}_{\alpha=1}^{d}$ is an orthonormal basis of $\mathbb{C}^d$, form a basis on $\mathfrak{gl}(d)$. In order to obtain a set of elements that span $\mathbb{C}[\mathfrak{su}(d)]$, we only have to impose the tracelessness condition. We define,

$$E^{\alpha\beta} = |\alpha\rangle\langle\beta| - \frac{1}{d}\delta_{\alpha\beta}\mathbb{1}. \tag{3.54}$$

This can be interpreted as projecting the matrix units $|\alpha\rangle\langle\beta|$ to the subspace of traceless matrices using the Hilbert-Schmidt inner product. Since we have $\sum_\alpha E^{\alpha\alpha} = 0$, only $d-1$ of the d diagonal elements are linearly independent; in order to get a proper basis of $\mathbb{C}[\mathfrak{su}(d)]$, we discard E^{dd}. From the commutator of the basis elements, we get the structure constants $c^{\mu\nu}_{\alpha\beta,\gamma\delta}$ of the algebra.

$$\left[E^{\alpha\beta}, E^{\gamma\delta}\right] = \sum_{\mu,\nu=1}^{d} c^{\mu\nu}_{\alpha\beta,\gamma\delta} E^{\mu\nu} \quad \text{where} \quad c^{\mu\nu}_{\alpha\beta,\gamma\delta} = \delta_{\beta\gamma}\delta_{\mu\alpha}\delta_{\nu\beta} - \delta_{\alpha\delta}\delta_{\mu\gamma}\delta_{\nu\beta}. \tag{3.55}$$

Using the structure constants, the quadratic Casimir operator is expressed as,

$$\begin{aligned} C_2^{\mathrm{SU}(d)} &= \sum_{\alpha,\beta,\gamma,\delta=1}^{d} \left(g^{-1}\right)_{\alpha\beta,\gamma\delta} E^{\alpha\beta}E^{\gamma\delta} = \sum_{\alpha,\beta=1}^{d} E^{\alpha\beta}E^{\beta\alpha} \quad \text{where,} \\ g_{\alpha\beta,\gamma\delta} &= \sum_{\mu,\nu,\epsilon,\zeta=1}^{d} c^{\mu\nu}_{\alpha\beta,\epsilon\zeta} c^{\epsilon\zeta}_{\gamma\delta,\mu\nu} \quad \text{is the metric tensor.} \end{aligned} \tag{3.56}$$

The eigenvalues of the U(d) and SU(d) Casimir operators were worked out by Perelomov and Popov in the 1960s [67]. Their result for the eigenvalue of $C_2^{\mathrm{SU}(d)}$ corresponding to the irrep $\lambda = (\lambda_1, \lambda_2, \ldots, \lambda_d)$ is,

$$\begin{aligned} &D_\lambda^{\mathrm{SU}(d)}(C_2^{\mathrm{SU}(d)}) = c_2^{\mathrm{SU}(d)}(\lambda)\mathbb{1} \quad \text{where,} \\ &c_2^{\mathrm{SU}(d)}(\lambda) = \sum_{i=1}^{d} \left[(\tilde{\lambda}_i + d - i)^2 - (d-i)^2 \right], \text{and} \\ &\tilde{\lambda}_i = \lambda_i - \frac{1}{d}\sum_{j=1}^{d} \lambda_i. \end{aligned} \tag{3.57}$$

Here, we did not explicitly use the previously established convention of setting $\lambda_d = 0$ for SU(d) diagrams. It is apparent however, that the $\tilde{\lambda}_i$ values are identical for equivalent SU(d) diagrams, and thus, so are the $c_2^{\mathrm{SU}(d)}(\lambda)$ eigenvalues. In particular, the eigenvalue for SU(3), with the convention reintroduced, is

$$c_2^{\mathrm{SU}(3)}((\lambda_1, \lambda_2)) = \frac{2}{3}(\lambda_1^2 + \lambda_2^2 - \lambda_1\lambda_2 + 3\lambda_1). \tag{3.58}$$

From here on, we introduce another convention regarding the Casimir operators. Since only the quadratic ones will be important to us, we stop denoting the order in the lower index, and instead, use it to denote the number of sites in the tensor product representations of the quadratic Casimir operator, i.e., $C_N^{\mathrm{SU}(d)} = D_N(C_2^{\mathrm{SU}(d)})$.

Chapter 4

The shareability of Werner and isotropic states

Suppose we partition the subsystems of a composite quantum system into two groups of sizes n_{L} and n_{R}. A bipartite quantum state is n_{L}-n_{R} shareable if it can simultaneously arise as the reduced state of all subsystem-pairs in which the components are taken from different groups. In order to provide the necessary background knowledge for our results concerning shareability, in this chapter, we formally introduce the concept along with its most important properties. In particular, we explore the relationship of shareability and quantum entanglement. After this basic introduction, we restrict our investigation to two special classes of unitary invariant bipartite quantum states: Werner [68] and isotropic [69] states. This chapter assumes that the reader is familiar with the concept of quantum states, and their basic properties. For an introduction to this topic, see e.g. [70].

4.1 Shareability

Assume we have two experimenters, each with absolute control over his own local quantum system, but with no way to directly influence the other experimenter's system. If they cannot communicate at all, and their systems received no prior preparation, then the two systems must be uncorrelated, i.e., the joint quantum system is in a product state, $\rho = \rho_{\mathrm{L}} \otimes \rho_{\mathrm{R}}$. If the experimenters are allowed to exchange classical information, e.g., talk on the phone, they are able to realize a class of transformations known as local operations and classical communication or LOCC for short. Starting from uncorrelated states, with these transformations, they are able to achieve a certain degree of correlation, but they still cannot prepare any arbitrary state on their joint system. The joint states they are able to prepare are statistical mixtures, i.e., convex combinations of uncorrelated states; these are

called separable,

$$\rho = \sum_i p_i \rho_{\mathrm{L},i} \otimes \rho_{\mathrm{R},i}, \quad \text{where } \sum_i p_i = 1, \quad 0 \leq p_i \leq 1. \tag{4.1}$$

Preparing any other state in the composite quantum system requires the sending of some third, auxiliary quantum system from one experimenter to the other. The correlations that can be created in such a way are peculiar to quantum physics; we call the non-separable states that exhibit these correlations entangled. Understanding the nature of quantum correlations present in entangled states, and the ways in which they are different from classical correlations, is one of the central goals of quantum information science; an endeavor that has many practical consequences in quantum chemistry, many-body physics, statistical physics, etc.

Determining whether a pure state is entangled or not is a simple task. As a direct consequence of the Schmidt decomposition, $|\psi\rangle\langle\psi| \in \mathcal{S}(\mathcal{H}_L \otimes \mathcal{H}_R)$ can be written in the form of Eq. (4.1) iff $|\psi\rangle = |\psi_L\rangle \otimes |\psi_R\rangle$ is a product vector. This means that correlated pure states cannot be only classically correlated. Confirming or denying entanglement for a mixed state is significantly harder. The main source of difficulty is, that the decomposition of a mixed state into a convex combination of pure states is not unique. For example, a mixed state of a qubit can be mapped to a point inside the Bloch sphere. Each chord of the sphere that intersect this point, corresponds to a decomposition of the mixed state into a convex combination of the two pure states at the ends of the chord. The problem this lack of uniqueness brings about, is that even though a given decomposition might give the impression that the state is entangled, it is hard to rule out the existence of a different decomposition into a mixture of pure product states.

Many approaches have been developed for the confirmation, and characterization of entanglement. The one we will study here, hinges on the observation that entanglement cannot be arbitrarily shared between many parties. This is commonly known as the monogamy of entanglement [71–74]. In the most extreme case, pure entangled states cannot be shared at all, i.e., a bipartite system in a pure entangled state cannot be correlated with any third system. This result is used to guarantee the security of many quantum protocols. We give a proof here, as it is short and enlightening.

Proposition 10. *Let $|\psi_{\mathrm{AB}}\rangle\langle\psi_{\mathrm{AB}}| \in \mathcal{S}(\mathcal{H}_{\mathrm{A}} \otimes \mathcal{H}_{\mathrm{B}})$ be a pure, entangled state. If a state on a larger system $\rho_{\mathrm{ABC}} \in \mathcal{S}(\mathcal{H}_{\mathrm{A}} \otimes \mathcal{H}_{\mathrm{B}} \otimes \mathcal{H}_{\mathrm{C}})$ has reduced state $\mathrm{Tr}_{\mathrm{C}}(\rho_{\mathrm{ABC}}) = |\psi_{\mathrm{AB}}\rangle\langle\psi_{\mathrm{AB}}|$, then it must be of the form $\rho_{\mathrm{ABC}} = |\psi_{\mathrm{AB}}\rangle\langle\psi_{\mathrm{AB}}| \otimes \rho_{\mathrm{C}}$, for some $\rho_{\mathrm{C}} \in \mathcal{S}(\mathcal{H}_{\mathrm{C}})$.*

Proof. Consider first a simple corollary of the Schmidt decomposition: If a pure state, $|\psi_{\mathrm{AB}}\rangle\langle\psi_{\mathrm{AB}}| \in \mathcal{S}(\mathcal{H}_{\mathrm{A}} \otimes \mathcal{H}_{\mathrm{B}})$, has Schmidt rank r and Schmidt coefficients $\{\lambda_k\}_{k=1}^{r}$, then its marginals, $\mathrm{Tr}_{\mathrm{A}}|\psi_{\mathrm{AB}}\rangle\langle\psi_{\mathrm{AB}}|$ and $\mathrm{Tr}_{\mathrm{B}}|\psi_{\mathrm{AB}}\rangle\langle\psi_{\mathrm{AB}}|$, have rank r, and non-zero eigenvalues $\{\lambda_k^2\}_{k=1}^{r}$. An immediate consequence is that the marginals of pure entangled states must always be mixed.

The state ρ_{ABC}, can be either pure or mixed, let us start with the former case. Since $\mathrm{Tr}_{\mathrm{C}}\rho_{\mathrm{ABC}} = |\psi_{\mathrm{AB}}\rangle\langle\psi_{\mathrm{AB}}|$ is rank 1, ρ_{ABC} must have Schmidt rank 1; thus, its marginal on C must also be pure, i.e., $\rho_{\mathrm{ABC}} = |\psi_{\mathrm{AB}}\rangle\langle\psi_{\mathrm{AB}}| \otimes |\psi_{\mathrm{C}}\rangle\langle\psi_{\mathrm{C}}|$.

Now assume that ρ_{ABC} is mixed. In this case, it can be expressed as a convex combination of pure states: $\rho_{\mathrm{ABC}} = \sum_{i=1}^{n} p_i |\psi_{\mathrm{ABC}}^{(i)}\rangle\langle\psi_{\mathrm{ABC}}^{(i)}|$, where $p_i \in [0,1]$, and $\sum_{i=1}^{n} p_i = 1$. Therefore, for the marginal on AB, we have $|\psi_{\mathrm{AB}}\rangle\langle\psi_{\mathrm{AB}}| = \sum_{i=1}^{n} p_i \mathrm{Tr}_{\mathrm{C}}|\psi_{\mathrm{ABC}}^{(i)}\rangle\langle\psi_{\mathrm{ABC}}^{(i)}|$. Since pure states are the extremal points of the convex set $\mathcal{S}(\mathcal{H}_{\mathrm{A}} \otimes \mathcal{H}_{\mathrm{B}})$, $|\psi_{\mathrm{AB}}\rangle\langle\psi_{\mathrm{AB}}|$ can be expressed in the form of such a convex combination iff $\mathrm{Tr}_{\mathrm{C}}|\psi_{\mathrm{ABC}}^{(i)}\rangle\langle\psi_{\mathrm{ABC}}^{(i)}| = |\psi_{\mathrm{AB}}\rangle\langle\psi_{\mathrm{AB}}| \quad \forall i$. Now using the corollary of the Schmidt decomposition again yields $|\psi_{\mathrm{ABC}}^{(i)}\rangle\langle\psi_{\mathrm{ABC}}^{(i)}| = |\psi_{\mathrm{AB}}\rangle\langle\psi_{\mathrm{AB}}| \otimes |\psi_{\mathrm{C}}^{(i)}\rangle\langle\psi_{\mathrm{C}}^{(i)}|$. □

It is natural to ask: Does a similarly strict monogamy equation exist for mixed entangled states? The answer is no, and we demonstrate this with a counterexample. Suppose A sends one half of a Bell state, $|\psi^+\rangle = 1/\sqrt{2}(|01\rangle + |10\rangle)$, to B; however, C intercepts the message with 50% probability, and sends a blank (maximally mixed) state in its place. The resulting joint quantum state of A, B and C is:

$$\rho_{\mathrm{ABC}} = \frac{1}{2}\left(|\psi^+\rangle\langle\psi^+|_{\mathrm{AB}} \otimes \frac{\mathbb{1}_{\mathrm{C}}}{2} + |\psi^+\rangle\langle\psi^+|_{\mathrm{AC}} \otimes \frac{\mathbb{1}_{\mathrm{B}}}{2}\right). \tag{4.2}$$

This joint state shares the same correlations between AB and AC,

$$\mathrm{Tr}_{\mathrm{C}}\rho_{\mathrm{ABC}} = \mathrm{Tr}_{\mathrm{B}}\rho_{\mathrm{ABC}} = \frac{1}{2}\left(|\psi^+\rangle\langle\psi^+| + \frac{\mathbb{1}}{4}\right). \tag{4.3}$$

One can confirm that this reduced state is entangled, e.g., by verifying that its partial transpose is not positive. In general, it has been established that such explicit attempts at eavesdropping generate bipartite states that can be shared across multiple parties [72, 75].

As the last example demonstrates, the correlations described by some mixed entangled states can be shared simultaneously between multiple pairs. However, as we will show later, entangled states still have certain limits to how much they can be distributed across many systems. In order to explain this properly, we need a way to quantify how much a given quantum state can be shared.

Definition 1. A bipartite quantum state $\rho \in \mathcal{S}(\mathcal{H}_\mathrm{L} \otimes \mathcal{H}_\mathrm{R})$ is n_L-n_R shareable for some $n_\mathrm{L}, n_\mathrm{R} \in \mathbb{N}$ if there exists an $n_\mathrm{L} + n_\mathrm{R}$-partite "sharing" state, $\hat{\rho} \in \mathcal{S}(\mathcal{H}_\mathrm{L}^{\otimes n_\mathrm{L}} \otimes \mathcal{H}_\mathrm{R}^{\otimes n_\mathrm{R}})$, such that all left-right pairwise reduced states of $\hat{\rho}$ are equal to ρ. I.e.,

$$\mathrm{Tr}_{\overline{\mathrm{L}}_i\overline{\mathrm{R}}_j}\hat{\rho} = \rho, \quad \forall i = 1, 2, \ldots, n_\mathrm{L}; \quad j = 1, 2, \ldots, n_\mathrm{R}, \tag{4.4}$$

where $\overline{\mathrm{L}}_i\overline{\mathrm{R}}_j$ denotes the partial trace that restricts the composite Hilbert space to the i-th left and j-th right Hilbert space.

In this work, we deal only with the case where $\mathcal{H}_\mathrm{L} \cong \mathcal{H}_\mathrm{R} \cong \mathbb{C}^d$, but it is still useful to differentiate the left and right Hilbert spaces in the notation. With this definition, the bipartite state Eq. (4.3) in the eavesdropping example is at least 1-2 shareable, while pure entangled states are not, i.e. only 1-1 shareable. On the other end of the spectrum are the product states, which are clearly arbitrarily, or ∞-∞ shareable. In general, one can get the intuition that states get more shareable as they get less entangled, and thus, shareability can be used as a way to characterize the degree of entanglement; we will give further arguments for this later.

We can now finally clarify what "more shareable" means. A trivial consequence of Definition 1 is, that if a state is n_L-n_R shareable, then it must also be n'_L-n'_R shareable for all $n'_\mathrm{L} \leq n_\mathrm{L}$ and $n'_\mathrm{R} \leq n_\mathrm{R}$. This motivates the introduction of a partial order on shareabilities: $(n'_\mathrm{L}, n'_\mathrm{R}) \leq (n_\mathrm{L}, n_\mathrm{R})$ iff $n'_\mathrm{L} \leq n_\mathrm{L}$ and $n'_\mathrm{R} \leq n_\mathrm{R}$. Accordingly, each quantum state has a set of maximal shareabilities, that potentially gives information about its entanglement.

We note that a sharing state need not be unique. In fact, for a permutation $\pi \in S_{n_\mathrm{L}} \times S_{n_\mathrm{R}} \subset S_{n_\mathrm{L}+n_\mathrm{R}}$, that permutes only within the left and right sides, (A left-right permutation for short.) if $\hat{\rho}$ n_L-n_R shares ρ then,

$$\mathrm{Tr}_{\overline{\mathrm{L}}_i\overline{\mathrm{R}}_j}(D^{(S_{n_\mathrm{L}+n_\mathrm{R}})}_{n_\mathrm{L}+n_\mathrm{R}}(\pi^{-1})\hat{\rho}D^{(S_{n_\mathrm{L}+n_\mathrm{R}})}_{n_\mathrm{L}+n_\mathrm{R}}(\pi)) = \mathrm{Tr}_{\overline{\mathrm{L}_{\pi^{-1}(i)}}\,\overline{\mathrm{R}_{\pi^{-1}(j)}}}\hat{\rho} = \rho$$
$$\forall i = 1, 2, \ldots, n_\mathrm{L}; \quad j = 1, 2, \ldots, n_\mathrm{R}; \tag{4.5}$$

therefore $D^{(S_{n_\mathrm{L}+n_\mathrm{R}})}_{n_\mathrm{L}+n_\mathrm{R}}(\pi^{-1})\hat{\rho}D^{(S_{n_\mathrm{L}+n_\mathrm{R}})}_{n_\mathrm{L}+n_\mathrm{R}}(\pi)$ also n_L-n_R shares ρ. This permutation invariance of the sharing property is what essentially connects this topic to the other parts of this thesis. It allows us to apply the set of tools we use for dealing with Hamiltonians of high permutation symmetry to this problem. Beyond permutations, the convex combination of two sharing states that n_L-n_R share ρ is also an n_L-n_R sharing state for ρ; consequently, the sharing states of a given bipartite state form a convex set. In a similar fashion, the n_L-n_R shareable states also form a convex set. A sharing state for a convex combination of two n_L-n_R shareable

states, is just the convex combination of two corresponding sharing states with the same coefficients.

What we call a sharing state, is sometimes also referred to as a state extension. The relevance of state extension properties to entanglement was realized already in the late eighties by Werner [76, 77], after which the concept was further investigated. Some good summary papers of this are [78] and [79].

The problem of shareability can also be thought of as a special case of the quantum marginal, or local consistency problem. In this problem, we ask if some overlapping multipartite states, e.g. ρ_{AB} and ρ_{AC}, can be combined into a state of a larger system? I.e., does a state ρ_{ABC} exists, such that $\mathrm{Tr}_{\mathrm{C}}\rho_{\mathrm{ABC}} = \rho_{\mathrm{AB}}$ and $\mathrm{Tr}_{\mathrm{B}}\rho_{\mathrm{ABC}} = \rho_{\mathrm{AC}}$? This problem has been investigated extensively in both mathematical physics [80–82] and quantum chemistry [83]. In the shareability scenario, we instead want to know whether a given state is consistent with copies of itself, this simplifies the problem quite a bit. For example, the most obvious requirement of local consistency, that the single Hilbert space marginals should agree, i.e., $\mathrm{Tr}_B\rho_{AB} = \mathrm{Tr}_C\rho_{AC}$, is already built into shareability. Furthermore, in the case of the local consistency problem, it is possible even for classical probability distributions (with agreeing single party marginals) to not be consistent with each other due to certain convexity requirements [78]; while, as we are about to show, there are no restrictions for the shareability of classical probability distributions.

It is clear that uncorrelated, or product states are arbitrarily shareable. This brings about the next question: What are the shareability properties of the classically correlated, i.e., separable states? As it turns out, arbitrary shareability is a necessary and sufficient condition for separability. In fact, the concept of shareability itself was first introduced as a consequence of this result, which was born in the context of infinite quantum de Finetti theorems, and is credited to both [76] and [84]. We replicate it here, although most of the real work is offloaded to a theorem we will only refer to.

Proposition 11. *A bipartite quantum state $\rho \in \mathcal{S}(\mathcal{H}_{\mathrm{L}} \otimes \mathcal{H}_{\mathrm{R}})$ is separable iff it is arbitrarily shareable.*

Proof. We start with the easier direction of assuming ρ is separable. In this case, it can be expressed in the form $\rho = \sum_i p_i \rho_i^{(\mathrm{L})} \otimes \rho_i^{(\mathrm{R})}$, where $\sum_i p_i = 1$. Let n_{L} and n_{R} be arbitrary, then the state

$$\hat{\rho} = \sum_i p_i (\rho_i^{(\mathrm{L})})^{\otimes n_{\mathrm{L}}} \otimes (\rho_i^{(\mathrm{R})})^{\otimes n_{\mathrm{R}}}, \tag{4.6}$$

n_{L}-n_{R} shares ρ.

Now assume that ρ is arbitrarily shareable. In truth, we only need to consider the case in which $n_{\mathrm{L}} = 1$ and n_{R} is arbitrary. If we manage to show that 1-∞ shareable states are separable, then they must also be ∞-∞ shareable according to the previous part of the proof. Let $S_{n_{\mathrm{R}}} \subset S_{1+n_{\mathrm{R}}}$ be the subgroup of permutations of the elements $2, 3, \ldots, n_{\mathrm{R}}+1$, and $\hat{\rho}$ a 1-n_{R} sharing state for ρ. Consider the $S_{n_{\mathrm{R}}}$ symmetric sharing state,

$$\hat{\rho}' = \frac{1}{n_{\mathrm{R}}!} \sum_{\pi \in S_{n_{\mathrm{R}}}} D^{S_{1+n_{\mathrm{R}}}}_{n_{\mathrm{R}}+1}(\pi^{-1}) \hat{\rho} D^{S_{1+n_{\mathrm{R}}}}_{n_{\mathrm{R}}+1}(\pi). \tag{4.7}$$

If we let $n_{\mathrm{R}} \to \infty$, then Fannes' theorem [84] implies, that $\hat{\rho}'$ has a unique representation as a convex combination of $S_{n_{\mathrm{R}}}$ symmetric product states,

$$\hat{\rho}' = \sum_i p_i \rho_i^{(\mathrm{L})} \otimes \rho_i^{(\mathrm{R})} \otimes \rho_i^{(\mathrm{R})} \otimes \ldots \tag{4.8}$$

The bipartite reduced state of such a $\hat{\rho}'$ to any left-right pair of Hilbert spaces is separable. □

Now we have on one hand, separable states, which are the same as arbitrarily shareable states; and on the other hand, pure entangled states, which are not shareable at all. Next, we present some results about the entanglement of the shareable states that are in between. LOCC transformations play a central role in the ways entanglement is quantified, for an introduction into this topic see e.g. [85]. In general, the functions used to quantify entanglement are *entanglement monotones*. These are functions $f : \mathcal{S}(\mathcal{H}) \to \mathbb{R}^+$, that are monotonic under LOCC transformations. It is natural to ask, is the function that maps a given state to its set of maximal shareabilities an entanglement monotone in a generalized sense, w.r.t. the partial order of shareabilities? I.e., is it impossible for LOCC transformations to decrease the maximal shareabilities of a given state? The answer is conjectured to be yes, but as to the best of our knowledge, there are only partial proofs for it. As a basic example, consider the subset of LOCC transformations that can be expressed as a convex combination of local unitary operations $U_i^{(\mathrm{L})}, U_i^{(\mathrm{R})} \in \mathrm{U}(d)$,

$$\mathcal{M}(\rho) = \sum_i p_i U_i^{(\mathrm{L})} \otimes U_i^{(\mathrm{R})} \rho U_i^{(\mathrm{L})\dagger} \otimes U_i^{(\mathrm{R})\dagger}, \quad \text{where} \quad \sum_i p_i = 1. \tag{4.9}$$

It is easy to see that if $\hat{\rho}$ is an n_{L}-n_{R} sharing state for ρ, then $\left(U_i^{(\mathrm{L})}\right)^{\otimes n_{\mathrm{L}}} \otimes \left(U_i^{(\mathrm{R})}\right)^{\otimes n_{\mathrm{R}}} \hat{\rho} \left(U_i^{(\mathrm{L})\dagger}\right)^{\otimes n_{\mathrm{L}}} \otimes \left(U_i^{(\mathrm{R})\dagger}\right)^{\otimes n_{\mathrm{R}}}$ is an n_{L}-n_{R} sharing state for $U_i^{(\mathrm{L})} \otimes U_i^{(\mathrm{R})} \rho U_i^{(\mathrm{L})\dagger} \otimes U_i^{(\mathrm{R})\dagger}$. Since the set of n_{L}-n_{R} shareable states is convex, the $\mathcal{M}(\rho)$ must also be

n_{L}-n_{R} shareable. It is much less trivial to prove the conjecture when we incorporate local measurements, and local unitary transformations that depend on the measurement outcomes into the possible transformations. Nevertheless, in [86] it is proved that the set of 1-n_{R} shareable states, for arbitrary n_{R}, is closed under 1-LOCC transformations, i.e., local operations with only a single round of classical communications.

Besides LOCC transformations, an other way to connect the degree of shareability with that of entanglement, is to construct a bound for the distance from separable states in terms of shareability. We have established with Eq. (4.5), that when a sharing state exists, it can always be chosen to be symmetric to left-right permutations, i.e., to be a state on $\mathcal{H}_{\mathrm{L}}^{\vee n_{\mathrm{L}}} \otimes \mathcal{H}_{\mathrm{R}}^{\vee n_{\mathrm{R}}}$. In Section 2.6, we showed that finite quantum de Finetti theorems can be used to derive an upper bound on the distance between completely permutation symmetric, and i.i.d. separable states. The techniques used in the proofs of these theorems can be easily extended to the left-right symmetric sharing states that appear in the shareability problem. Here, we present a version of the trace norm bound for 1-n_{R} shareability from [79], that we extended to the n_{L}-n_{R} case.

Proposition 12. *Let $\rho \in \mathcal{S}(\mathcal{H}_{\mathrm{L}} \otimes \mathcal{H}_{\mathrm{R}})$ be n_{L}-n_{R} shareable. Then there exists a separable state, $\sigma \in \mathcal{S}(\mathcal{H}_{\mathrm{L}} \otimes \mathcal{H}_{\mathrm{R}})$ such that*

$$||\rho - \sigma||_1 \leq 2 - \frac{2n_{\mathrm{L}}n_{\mathrm{R}}}{(d+n_{\mathrm{L}})(d+n_{\mathrm{R}})}. \tag{4.10}$$

The proof is fairly straightforward, and also gives insight into how finite quantum de Finetti theorems work, we present it in Appendix B. The key idea is to take a left-right permutation symmetric sharing state, $\hat{\rho}$, and turn it into a separable state by coarse graining it with a left-right permutation symmetric projection valued measure (PVM) that corresponds to a set of pure product states; i.e, we prepare each $|\phi\rangle$ that we measure in, with the probability of measuring $|\phi\rangle$ in $\hat{\rho}$. If the PVM is chosen to be highly symmetric, then Schur's lemma can be used to do the heavy lifting in calculating the trace norm distance between $\hat{\rho}$ and the coarse grained state.

There is an operational interpretation of the trace norm bound in Eq. (4.10): Suppose we have an n_{L}-n_{R} shareable state ρ, and want to construct a two outcome positive operator valued measurement (POVM), that distinguishes ρ from some particular separable state σ. The outcome that our system is in state ρ, is described by the element $0 \leq M \leq \mathbb{1}$, while the outcome that the system is in state σ by $\mathbb{1} - M$. If we assume that our system is in state ρ or σ with equal probabilities, then it can be shown [70], that if we chose M optimally, the probability of our

measurement giving the correct result is:

$$\frac{1}{2}\mathrm{Tr}(M_{opt}\rho) + \frac{1}{2}\mathrm{Tr}((\mathbb{1} - M_{opt})\sigma) = \frac{1}{2} + \frac{||\rho - \sigma||_1}{4}. \tag{4.11}$$

When ρ is highly shareable, Eq. (4.10) implies that we can always find a separable state σ, for which the efficiency of our distinguishing measurement cannot be much higher than 1/2.

Proposition 12 has an interesting connection with many-body physics as well. Consider the quantum state of a lattice system with coordination number n_{L}; concentrating on the "star" formed by a central site, and its n_{L} nearest neighbors. The bipartite reduced states along the edges of this star must be at least 1-n_{L} shareable due to the lattice symmetries. According to Eq. (4.10), the higher the coordination number of the lattice, the closer its quantum state must be to a separable state. This explains the observation that mean field theories are more effective on lattices with high coordination numbers.

4.2 Werner states

Calculating the shareability properties of an arbitrary bipartite quantum state is a difficult task, that can only be done numerically. Finding an n_{L}-n_{R} sharing state for a given bipartite quantum state can be translated to a problem in semidefinite programming [87–89]. The time taken by state-of-the-art algorithms, e.g. [90], to solve such a problem scales polynomially in the dimension of the sharing state, which itself scales exponentially with n_{L} and n_{R}.

Our solution to this difficulty, is to restrict the types of states that we share to highly symmetric ones; this way, we are able to apply representation theory and derive exact results. For this endeavor, we choose two closely related sets of bipartite states. The first one is composed of all bipartite states invariant to global unitary transformations of the form $U \otimes U$, where $U \in \mathrm{U}(d)$; these states are also known as Werner states. The second one is the set of bipartite states invariant to transformations of the form $U \otimes U^*$, where $*$ denotes complex conjugation is some fixed basis, known as the set of isotropic states. We start our discussion with Werner states.

States invariant to $U \otimes U$ transformations were first introduced by Werner as an example for entangled states that can be described by a hidden variable model [68]. Since then, they found many uses in quantum information science; e.g., in the description of noisy quantum channels [91], in the study of deterministic purification [92], in the description of photonic qubits [93] where they may have

a role in combating decoherence [94, 95]. Additionally, they can also be prepared as the steady state of coherently driven atoms undergoing collective spontaneous decay [96].

$D_2^{\mathrm{U}(d)}$ decomposes to the two irreps, $(2,0,\ldots,0)$ and $(1,1,0,\ldots,0)$, supported on the symmetric and antisymmetric subspaces of $\mathbb{C}^d \otimes \mathbb{C}^d$ respectively. Accordingly, all operators invariant to $D_2^{\mathrm{U}(d)}$, can be expressed as linear combinations of two fixed, linearly independent, $D_2^{\mathrm{U}(d)}$ invariant operators. We choose these to be the identity, and the flip operator F, which exchanges the two parts of the tensor product. The additional condition, $\mathrm{Tr}(\rho) = 1$, further reduces the number of parameters to 1. We use the expected value of the flip operator, $\mathrm{Tr}(\rho F) = \phi$, as this single parameter to express an arbitrary Werner state as,

$$\rho^{\mathrm{W}}(\phi) = \frac{d}{d^2-1}\left[(d-\phi)\frac{\mathbb{1}}{d^2} + \left(\phi - \frac{1}{d}\right)\frac{F}{d}\right]. \tag{4.12}$$

The positivity of $\rho^{\mathrm{W}}(\phi)$ restricts the parameter space to $-1 \leq \phi \leq 1$.

Some insight can be gained by finding values of ϕ where Werner states take special forms. The most obvious of these is the completely mixed state, $\mathbb{1}/d^2$, that we get at $\phi = 1/d$. For additional special values, consider how the flip operator has eigenvalues 1 and -1, corresponding to the symmetric and antisymmetric subspaces. Thus, $\rho^{\mathrm{W}}(1)$ is proportional to the projector to the symmetric subspace, Π_2^+, and $\rho^{\mathrm{W}}(-1)$ is proportional to the projector to the antisymmetric subspace, Π_2^-. Assume that we make measurements in an orthonormal product basis, $\{|i\rangle \otimes |j\rangle\}_{i,j=1}^d$. The latter case of complete Fermi symmetry can be interpreted as a state in which these collective measurements cannot have agreeing outcomes, e.g, $|1\rangle \otimes |1\rangle$, etc. Since Werner states can be regarded as convex combinations of the states with complete Fermi, and complete Bose symmetries, we can think about the parameter ϕ as a number that characterizes the tendency of collective measurements to disagree.

We can immediately say something about the shareability properties at these special parameter values: As a start, the completely mixed state is clearly arbitrarily shareable, i.e. separable. Additionally, the projectors to the symmetric and antisymmetric parts of an N-partite Hilbert space, Π_N^+ and Π_N^-, have the special property $\mathrm{Tr}_n \Pi_N^{+/-} = \Pi_{N-n}^{+/-}$ independently of which $n < N$ Hilbert spaces we choose to trace out. This implies that $\rho^{\mathrm{W}}(1)$ is arbitrarily shareable, since the projection to the completely symmetric subspace is always a valid sharing state regardless of the number of Hilbert spaces on the left and right side. We conclude that, since convex combinations of separable states are also separable, Werner states with parameters $\phi \in [1/d, 1]$ must all be arbitrarily shareable. The previous reasoning

does not work for $\rho(-1)$, because depending on the dimension, a non-trivial, completely antisymmetric subspace might not exist. More precisely, iff $N > d$ then $\Pi_N^- = 0$, and iff $N = d$, Π_N^- is 1-dimensional. Consequently, in the case of $d = 2$, $\rho^{\mathrm{W}}(-1)$ is the pure singlet state, which is not shareable at all due to the monogamy of entanglement. For $d > 2$, $\rho^{\mathrm{W}}(-1)$ can be regarded as the partial trace of the pure, d-partite, antisymmetric state, $\frac{1}{\sqrt{d!}} \sum_{\pi \in S_d} \mathrm{sgn}(\pi) D_d^{S_d}(\pi) |1\rangle \otimes |2\rangle \otimes \ldots \otimes |d\rangle$; thus it is at least i-$(d-i)$ shareable for $i = 1, 2, \ldots, d-1$.

Now, we show that the parameter interval of separable Werner states is larger than $[1/d, 1]$. Consider the unitary "twirl", a completely positive, trace preserving (CPTP) superoperator, defined for some $A \in \mathcal{B}(\mathcal{H}_{\mathrm{L}} \otimes \mathcal{H}_{\mathrm{R}})$ with,

$$P_{U\otimes U}(A) = \int_{U(d)} \mathrm{d}U\, U \otimes U A U^\dagger \otimes U^\dagger, \tag{4.13}$$

where $\mathrm{d}U$ denotes the invariant Haar measure of $\mathrm{U}(d)$. It is easy to confirm, that this twirl is an orthogonal projection, w.r.t. the Hilbert-Schmidt inner product, from $\mathcal{B}(\mathcal{H}_{\mathrm{L}} \otimes \mathcal{H}_{\mathrm{R}})$, to the subspace of $D_2^{U(d)}$ invariant operators. In order to see which Werner state an arbitrary state, $\sigma \in \mathcal{S}(\mathcal{H}_{\mathrm{L}} \otimes \mathcal{H}_{\mathrm{R}})$, is mapped to by $P_{U\otimes U}$, it is not necessary to calculate the integral. Since Werner states are described by a single parameter, it is enough to check what happens to the expected value of the flip operator,

$$\mathrm{Tr}\left[P_{U\otimes U}(\sigma) F\right] = \int_{U(d)} \mathrm{d}U \mathrm{Tr}\left(\sigma (U^\dagger \otimes U^\dagger) F (U \otimes U)\right) = \mathrm{Tr}(\sigma F), \tag{4.14}$$

i.e., the expected value of the flip is invariant to the twirl; thus $P_{U\otimes U}(\sigma) = \rho^{\mathrm{W}}\left(\mathrm{Tr}(\sigma F)\right)$. Using this result, we show that:

Proposition 13. *A Werner state $\rho^{\mathrm{W}}(\phi)$ is separable iff $\phi \geq 0$.*

Proof. If $\sigma \in \mathcal{S}(\mathbb{C}^d \otimes \mathbb{C}^d)$ is separable then so must be $(U \otimes U)\sigma(U^\dagger \otimes U^\dagger)$. Expressing the integral with Riemann sums, $P_{U\otimes U}(\sigma)$ can be interpreted as the limit of a series of convex combinations of separable states, and therefore it is separable itself. Consequently, the set of separable Werner states is the image of the set of separable states under the twirl $P_{U\otimes U}$. In other words, it is enough to check what expected values can the flip operator have in separable states.

First, consider the product states $\sigma = \sigma_{\mathrm{L}} \otimes \sigma_{\mathrm{R}}$. We have $\mathrm{Tr}[(\sigma_{\mathrm{L}} \otimes \sigma_{\mathrm{R}})F] = \mathrm{Tr}(\sigma_{\mathrm{L}}\sigma_{\mathrm{R}}) \geq 0$, since the product of two positive operators is positive. The same inequality is also true for separable, i.e., convex combinations of product states. The equality is achieved, when the supports of σ_{L} and σ_{R} are orthogonal, and $\mathrm{Tr}[(\sigma_{\mathrm{L}} \otimes \sigma_{\mathrm{R}})F] = 1$ is achieved when σ_{L} and σ_{R} are identical pure states. Every

expected value of the flip operator in between can be realized by an appropriate convex combination of the previous two. □

Since the n_{L}-n_{R} shareable Werner states form a convex set, they must correspond to a closed interval in the parameter ϕ. Now that we also know which are the arbitrarily shareable Werner states, this statement can be refined: Werner states are n_{L}-n_{R} shareable in some interval $\phi \in [\phi_{n_{\mathrm{L}},n_{\mathrm{R}}}, 1]$, where $-1 \leq \phi_{n_{\mathrm{L}},n_{\mathrm{R}}} \leq 0$. Furthermore, According to the partial order of shareabilities described in Section 4.1, we can tell that if $n'_{\mathrm{L}} \leq n_{\mathrm{L}}$ and $n'_{\mathrm{R}} \leq n_{\mathrm{R}}$ then $\phi_{n'_{\mathrm{L}},n'_{\mathrm{R}}} \leq \phi_{n_{\mathrm{L}},n_{\mathrm{R}}}$. This leads us to expect that the entanglement of Werner states grows as ϕ decreases.

The suspicion is confirmed after looking at some standard measures of entanglement that are known for Werner states. Entanglement of formation is an entanglement measure, that can be interpreted as quantifying the resource cost of preparing ρ from maximally entangled states [85]. It is defined in a form that is easy to calculate only for pure states; for mixed states the definition is extended by a convex roof construction, that involves finding the minimum of a function over all decompositions of the mixed state into convex combinations of pure states. For this reason, there is no closed formula for the entanglement of formation of an arbitrary quantum state; however, for Werner states specifically, one was derived in [97]:

$$E_F(\rho^{\mathrm{W}}(\phi)) = \begin{cases} H_2\left(\frac{1}{2}\left[1-\sqrt{1-\phi^2}\right]\right) & \text{if } \phi < 0 \\ 0 \quad \text{if } \phi \geq 0 \end{cases}, \tag{4.15}$$

where H_2 is the binary entropy function. Concurrence is another entanglement measure, defined for pure states in a way that vanishes on product states:

$$\mathcal{C}(|\psi\rangle) = \sqrt{2\left(1 - \mathrm{Tr}[\mathrm{Tr}_L|\psi\rangle\langle\psi|]^2\right)}, \tag{4.16}$$

and extended to mixed states by a convex roof construction. Similarly to the case of E_F, there is no closed formula for an arbitrary quantum state, but one was developed for Werner states in [98]:

$$\mathcal{C}(\rho^{\mathrm{W}}(\phi)) = \begin{cases} -\phi & \text{if } \phi < 0 \\ 0 \quad \text{if } \phi \geq 0 \end{cases}. \tag{4.17}$$

This shows that we essentially parameterize our Werner states with their concurrence; which suggests that concurrence for Werner states could have some close connection with the flip operator. Both entanglement of formation, and concurrence are monotonously decreasing with ϕ, which confirms our intuitions about the entanglement of Werner states.

4.3 Isotorpic states

A parametrization of isotropic states follows straightforwardly from the parametrization of Werner states in Eq. (4.12). As a consequence of the identity,

$$\Big(U\otimes UA(U\otimes U)^\dagger\Big)^{t_R} = U\otimes U^* A^{t_R}(U\otimes U^*)^\dagger, \tag{4.18}$$

an operator $A\in\mathcal{B}(\mathcal{H}_\mathrm{L}\otimes\mathcal{H}_\mathrm{R})$ is invariant to $U\otimes U$ transformations iff its partial transpose is invariant to $U\otimes U^*$ transformations. It follows that like Werner states, isotropic states can also be described with a single parameter,

$$\rho^\mathrm{I}(\beta) = \frac{d}{d^2-1}\left[(d-\beta)\frac{\mathbb{1}}{d^2} + \left(\beta-\frac{1}{d}\right)\frac{F^{t_R}}{d}\right], \tag{4.19}$$

where $\beta = \mathrm{Tr}(\rho^\mathrm{I}(\beta)F^{t_R})$, and the positivity of $\rho^\mathrm{I}(\beta)$ requires that $0\leq\beta\leq d$.

It is perhaps more descriptive to interpret F^{t_R}/d as the maximally entangled state $|\psi^+\rangle = \sqrt{1/d}\sum_i|ii\rangle$. A result of this state appearing in our parametrization is, that the Choi–Jamiołkowski isomorphism between states and channels maps $\rho^\mathrm{I}(\beta)$ into the depolarization channel that completely randomizes a d-level system with probability $p=(d-\beta)/(d^2-1)$, and does nothing with probability $1-p$. As the sets of Werner and isotropic states are identical for qubits, this connection with the depolarization channel is often mistakenly ascribed to Werner states. We also note that the connection is not merely mathematical. Using an isotropic state as the shared resource in the standard teleportation protocol realizes the corresponding depolarizing channel physically [99].

We can derive the parameter range where isotropic states are separable with an argument similar to that in the proof of Proposition 13.

Proposition 14. *An isotropic state $\rho^\mathrm{I}(\beta)$ is separable iff $0\leq\beta\leq 1$.*

Proof. We start with showing that if $0\leq\beta\leq 1$, then $\rho^\mathrm{I}(\beta)$ is separable. The isotropic twirl superoperator $P_{U\otimes U^*}$ maps any separable state into a separable isotropic state; moreover, the expected value of F^{t_R} is invariant to $P_{U\otimes U^*}$, thus we need only to find separable states ρ with $0\leq\mathrm{Tr}(\rho F^{t_R})\leq 1$. Consider the family of states $\rho_x = |1\rangle\langle 1|\otimes|x\rangle\langle x|$, where $|x\rangle = x|1\rangle + \sqrt{1-|x|^2}|2\rangle$ and $0\leq|x|\leq 1$. With these explicitly separable product states, we get $\mathrm{Tr}(\rho_x F^{t_R}) = |x|^2$.

For the other direction, we use the reduction criterion for separability,

$$(\mathrm{Tr}_\mathrm{R}\rho)\otimes\mathbb{1} - \rho \geq 0. \tag{4.20}$$

Since $\rho^\mathrm{I}(\beta)$ violates Eq. (4.20) for $\beta>1$, these states must be entangled. □

As a consequence of violating the reduction criterion, entangled isotropic states can be distilled. In fact, this is the context in which isotropic states were first introduced in [69].

From the parameter range of arbitrary shareable isotropic states, it follows, that the parameter range corresponding to n_{L}-n_{R} shareability is $[0, \beta_{n_{\mathrm{L}},n_{\mathrm{R}}}]$, where $1 \leq \beta_{n_{\mathrm{L}},n_{\mathrm{R}}} \leq d$. Moreover, $\beta_{n_{\mathrm{L}},n_{\mathrm{R}}}$ must conform to the partial order of shareabilities, i.e., $\beta_{n_{\mathrm{L}}^{'},n_{\mathrm{R}}^{'}} \geq \beta_{n_{\mathrm{L}},n_{\mathrm{R}}}$ if $n_{\mathrm{L}}^{'} \leq n_{\mathrm{L}}$ and $n_{\mathrm{R}}^{'} \leq n_{\mathrm{R}}$. This suggests that the entanglement of isotropic states grows monotonously with β. Our intuition is supported by the concurrence,

$$\mathcal{C}(\rho^{\mathrm{I}}(\beta)) = \sqrt{\frac{2}{d(d-1)}}(\beta - 1), \tag{4.21}$$

which was derived in [100].

Part II

Results

From here on, we formulate the results of this thesis. In Chapters 5 and 6, we investigate two types of exactly solvable permutation symmetric models for three-component spin systems. In Chapter 5, the interaction we use can be interpreted as a generalization of the Heisenberg model to spin-1 particles, in the sense that it retains rotation invariance, while not admitting the more general SU(3) invariance. In solid state physics literature it, is referred to as the bilinear-biquadratic (BLBQ) interaction. We use a group theoretic approach to solve the eigenproblem of the Hamiltonian for an arbitrary number of sites. In Chapter 6, we use similar techniques on a different model. In this case, we use a highly symmetric SU(3) invariant exchange interaction. Instead of breaking the SU(3) symmetry with additional terms, like in Chapter 5, we break the complete permutation symmetry of the model and replace it with two permutation symmetric subsystems. In Chapter 7, we investigate a problem that is, at the first glance, completely different: The shareability problem of Werner and isotropic states; this is a permutation symmetric subproblem of the well-known quantum marginal problem. For the SU(d) symmetric Werner and isotropic states the shareability problem can be traced back to a ground state problem of a certain "Hamiltonian" that is similar to the one investigated in Chapter 6. We solve the problem extending the technique used to solve the ground state problem in Chapter 6 to arbitrary dimensions.

Chapter 5

The bilinear-biquadratic model on the complete graph

5.1 Introduction

A main theme of this thesis is approaching quantum spin systems in a very pragmatic manner, from the theorists point of view, by looking for systems that are simple enough to be exactly solvable, while still relevant enough, so that one can extract some more general wisdom from the results. Our key tool for bestowing this simplicity to our models is requiring permutation symmetry. This will allow us, through applying the theory of Lie groups, to calculate the spectrum of our models exactly for an arbitrary number of sites.

Permutation symmetry in a spin model with two-particle interaction implies that every pair of spins interacts with the same two-particle Hamiltonian; i.e., instead of a regular lattice, the interconnectedness of the spins is described by a complete graph. Classical spin models on complete graphs, such as the Curie-Weiss [101] or Sherrington-Kirpatrick [102] models, play an important role in statistical mechanics. The reason being that these can be treated relatively easily, yet still describe general features of the corresponding model on high-dimensional lattices. Due to recent results on quantum de Finetti theorems, see Section 2.6, these models can also be interpreted as mean-field approximations to regular lattice models. Inspired by this, several quantum spin boson and fermion models have been investigated on complete graphs [103–105]. The complete graph however, is the most frustrated layout of interactions possible; therefore, if there are competing interactions, e.g., antiferromagnetism, we expect the ground state to not resemble the classical mean-field analog at all.

The results obtained for fully connected systems are also potentially useful for types of cluster mean-field theories [106] where the "cluster" is chosen to be the complete graph. In such an approach one partitions the lattice into small

identical clusters, the interactions within a cluster are described exactly, while the interactions between cluster are treated in a mean-field way.

One of the effect of ultracold atom experiments on many-body physics, is a newfound interest in long-range systems. In some of these experiments, the interactions decay with an inverse power-law [45] or even of mean-field type [46]. This opens the way to experimentally realize long-range models and scenarios that were previously only thought of being of theoretical importance, e.g., Curie-Weiss type transverse-field Ising models (i.e., the Lipkin-Meshkov-Glick model) [47–50] or the Haldane-Shastry model [51, 52]; and to study phenomena that are not possible in short-range models, e.g., breaking of continuous symmetries in one-dimensional systems. Even complete graph models have a possible realization, and also a possible application in metrology, in such a fashion as was proposed for the SU(N) model in [46].

We chose the specific interaction that we put on the complete graph with the intent of getting something that is fairly general, while still remaining simple enough so that calculating the exact ground state is possible. To this end, we make use of the Schur-Weyl duality between the group of permutations and the general linear group, by imposing another symmetry condition on our interaction. This new symmetry should be described by some appropriate subgroup of the general linear group.

Since the beginning of quantum many-body physics, spin lattice system with rotational invariant, i.e., SU(2) symmetric, interaction terms have received a special attention. From a theoretical point of view, it was a natural generalization to also consider quantum spin models where SU(2) is enlarged to the symmetry group SU(N) with $N > 2$ [107–109]. A particular application was the case of materials described by spin models with orbital degeneracy yielding an SU(4) symmetric point [110–115], but the main motivation to study SU(N) spin systems remained mainly formal. In particular, one of the driving forces behind the theoretical studies was the realization that SU(N) symmetric spin models have very rich phase diagrams [108, 109, 116–120] [4]. Later these studies gained an unexpected experimental relevance with the advent of experiments with ultracold atomic systems.

As permutation symmetry would make two-level systems too simple to consider, we chose to focus on three-level systems. Our most symmetric, i.e., least general option is to impose SU(3) invariance. One way to achieve this is through generalizing the Heisenberg interaction to a three-level system, by substituting the spin operators with the generators of $\mathfrak{su}(3)$. This gives us an interaction Hamiltonian that is, analogously to the square of the total spin operator in the case of SU(2), proportional to the two-particle representation of the quadratic Casimir

operator $C_2^{\mathrm{SU}(3)}$. In fact, this is the most general SU(3) symmetric two-particle interaction: As explained in Section 3.4, under global SU(3) transformations, the two-particle Hilbert space, $\mathbb{C}^3 \otimes \mathbb{C}^3$, decomposes into two irreducible subspaces, labeled by $(2,0)$ and $(1,1)$. This means that any SU(3) invariant two-particle operators can be expressed as a linear combination of two, linearly independent operators of this nature, that is, in the form

$$H = \alpha C_2^{\mathrm{SU}(3)} + \beta \mathbb{1}. \tag{5.1}$$

A permutation symmetric system built with this two-particle interaction has a Hamiltonian that is proportional, not taking identity terms into account, to the N-site representation of the quadratic Casimir operator, $C_N^{\mathrm{SU}(3)}$. We deem this Hamiltonian too simple to be interesting. Indeed, the eigenspaces of $C_N^{\mathrm{SU}(3)}$ are the SU(3), and consequently S_N, irreducible sectors of the composite Hilbert space $\mathcal{H} = (\mathbb{C}^3)^{\otimes N}$ described in Section 3.4, and its eigenvalues are given in Eq. (3.58).

For this reason, we can relax our symmetry requirements, and chose a more general interaction. Hence, we pick the other popular way of generalizing the Heisenberg interaction, and search for the most general SU(2) symmetric[1] two-particle interaction for three-level systems. The naive approach of replacing the spin operators with their spin-1 representation, while yields an SU(2) symmetric interaction, does not satisfy our need for generality. The two-particle Hilbert space, $\mathbb{C}^3 \otimes \mathbb{C}^3$, decomposes into 3 irreducible subspaces under global SU(2) transformations, labeled by spin 0, 1 and 2; Thus, our desired interaction Hamiltonian can be constructed from the linear combination of $\mathbb{1}$ and two other SU(2) symmetric and linearly independent two-particle operators. We chose these to be the two-particle representations of the quadratic Casimir operators $C_2^{\mathrm{SU}(2)}$ and $C_2^{\mathrm{SU}(3)}$, and get the interaction Hamiltonian,

$$H_{ij} = \sin(\theta) C_{2\ ij}^{SU(3)} + \cos(\theta) C_{2\ ij}^{SU(2)}. \tag{5.2}$$

Here, we again discarded the term proportional to $\mathbb{1}$, and normalized the interaction strength so that only one parameter remains. The energy is measured in units for which the squared sum of the prefactors before the two terms gives unity. As a consequence of the permutation symmetry, this interaction yields a global

[1] Here, by SU(2) symmetric we mean that the interaction Hamiltonian is invariant to the tensor product of two spin-1 representations of SU(2). Accordingly, the two-particle Casimir operator, $C_2^{\mathrm{SU}(2)}$, also corresponds to this representation.

Hamiltonian containing the N-site representations of these Casimir operators,

$$H = \sum_{i<j} H_{ij} = \sin(\theta) C_N^{SU(3)} + \cos(\theta) C_N^{SU(2)}. \tag{5.3}$$

The competition between the SU(2) and SU(3) symmetric terms makes the investigation of this Hamiltonian far from trivial, and interesting from a theoretical perspective.

The same general SU(2) symmetric two particle interaction have been studied for a long time by solid state physicists; although, with different choice of the two SU(2) symmetric operators. It is called the bilinear-biquadratic (BLBQ) interaction, and its Hamiltonian is traditionally expressed as:

$$H_{ij} = \cos(\gamma) \mathbf{S}_i \mathbf{S}_j + \sin(\gamma) (\mathbf{S}_i \mathbf{S}_j)^2. \tag{5.4}$$

We show the equivalence of this interaction Hamiltonian with Eq. (5.2) in Appendix C. The conversion between the parameters γ and θ used in the two descriptions is given by

$$1 + \mathrm{ctg}(\theta) = \mathrm{ctg}(\gamma). \tag{5.5}$$

The first golden era of the BLBQ model was in the mid '80s, after Haldane's discovery that spin-1 Heisenberg chains can have a gapped excitation spectrum in contrary to spin-1/2 systems, where the spectrum is always gapless [121, 122]. This remarkable difference initiated an intensive study of the BLBQ chain, and its phase diagram, shown in Fig. 5.1, is mostly understood by now. Exact Bethe ansatz solutions exist for $\gamma = -\pi/4$ [123–125] and $\gamma = \pi/4$ [107, 126, 127]. When $\gamma = \arctan(1/3)$, Eq. (5.4) is just the parent Hamiltonian of the AKLT state [21, 22]. The AKLT state corresponds to a specific point inside the gapped Haldane phase [121, 122], located between $-\pi/4 < \gamma < \pi/4$, which is an example of symmetry protected topological phases [128]. The $\pi/4 < \gamma < \pi/2$ region is an extended critical phase with strong antiferroquadrupolar correlations. For $\pi/2 < \gamma < 5\pi/4$ ferromagnetic correlations dominate the ground state. Finally, if $5\pi/4 < \gamma < 7\pi/4$ the system is in a dimerized regime, which is again a gapped phase. There is another, conjectured, critical phase between the ferromagnetic and the dimerized phases, which was proposed by Chubukov [129, 130]. However, there is a still ongoing debate about its existence [28–30, 131, 132].

We know much less about the phases on two- and higher-dimensional lattices. Although in $d = 2$ and higher, especially on bipartite lattices, symmetry-breaking states start to be more frequent, and mean-field theories are performing better. On the two-dimensional square lattice, mean-field theory predicts a conventional

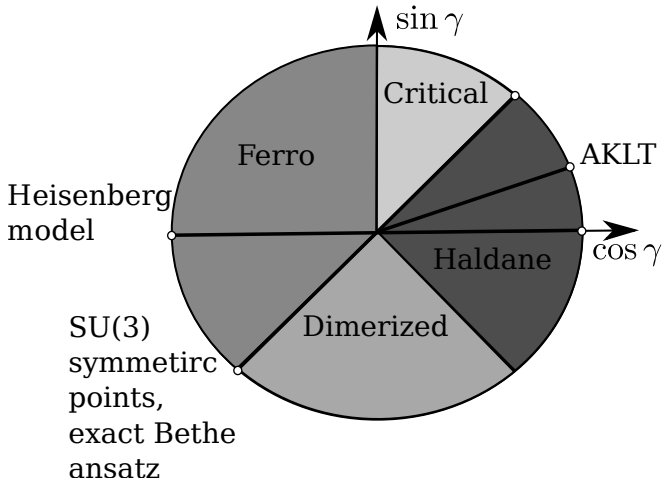

FIGURE 5.1: The phase diagram of the BLBQ chain.

ferromagnetic state for $\pi/2 < \gamma < 5\pi/4$, a ferroquadrupolar phase for $5\pi/4 < \gamma < 3\pi/2$, an antiferromagnetic (Néel ordered) phase between $-\pi/2 < \gamma < \pi/4$, and a semi-ordered phase for $\pi/4 < \gamma < \pi/2$ [133]. The ferroquadrupolar state is a symmetry-breaking state with non-vanishing quadrupole moment, however, with zero magnetization [134]. In the semi-ordered phase, the variational calculation gives a highly degenerate manifold of differently ordered states. Possibly, the inclusion of fluctuations selects one of these potential candidates, and in the end, the ground state becomes an ordered state. In the square lattice, Quantum Monte Carlo simulation is possible for $\pi < \gamma < 2\pi$, which confirms the mean-field results in this parameter range [26].

In spite of the apparent simplicity of the BLBQ model on a complete graph, the diagonalization of the Hamiltonian is far from trivial. The main tool used is the representation theory of Lie groups. In Sec. 5.2 we introduce the quantum numbers that uniquely label the eigenspaces of the Hamiltonian, then in Sec. 5.3 we provide the possible joint values of these quantum numbers. This allows us to determine the phase diagram and the spectrum of the model in Sec. 5.4 and Sec. 5.5, respectively. Finally, in Sec. 5.6 we give a brief summary and outlook.

5.2 The eigenspace decomposition of the Hamiltonian

Due to the permutation invariance of the Hamiltonian, its eigenspace decomposition can be obtained entirely through representation theoretic considerations. In this section, we provide the decomposition of the Hilbert space into the eigenspaces

of the Hamiltonian. The basic definitions and concepts are summarized in Chapter 3.

Let us first note, that from a representation theoretic point of view, $\mathfrak{su}(3)$ contains two non-equivalent classes of $\mathfrak{su}(2)$ subalgebras. The first one is composed of those $\mathfrak{su}(2)$ subalgebras, that are unitarily equivalent to the spin-1 representation of $\mathfrak{su}(2)$; while the subalgebras in the second class are unitarily equivalent to the direct sum of the spin-0 and the spin-$\frac{1}{2}$ representations. These are the only combinations of $\mathfrak{su}(2)$ irreps that yield a 3-dimensional representation. In the rest of the paper, the $\mathfrak{su}(2) \subset \mathfrak{su}(3)$ embedding will always refer to the $\mathfrak{su}(2)$ subalgebra of the first class, spanned by

$$S^1 = \begin{pmatrix} 0 & 0 & 0 \\ 0 & 0 & -i \\ 0 & i & 0 \end{pmatrix}, \quad S^2 = \begin{pmatrix} 0 & 0 & i \\ 0 & 0 & 0 \\ -i & 0 & 0 \end{pmatrix} \text{ and } \quad S^3 = \begin{pmatrix} 0 & -i & 0 \\ i & 0 & 0 \\ 0 & 0 & 0 \end{pmatrix}. \tag{5.6}$$

On the Hilbert space $\mathcal{H} = (\mathbb{C}^3)^{\otimes N}$ of the N-site model, the relevant representations of SU(2) and SU(3) are the N-fold direct products of the spin-1 SU(2) and the defining representation of SU(3), respectively. These N-fold direct products of representations can be decomposed into direct sums of irreps of the corresponding groups:

$$\left(D_1^{\mathrm{SU}(2)}\right)^{\otimes N} \cong \bigoplus_s m_s D_s^{\mathrm{SU}(2)}, \tag{5.7a}$$

$$\left(D_{(1,0)}^{\mathrm{SU}(3)}\right)^{\otimes N} \cong \bigoplus_\lambda m_\lambda D_\lambda^{\mathrm{SU}(3)}. \tag{5.7b}$$

In this decomposition, m_s and m_λ denote the multiplicities of the $D_s^{\mathrm{SU}(2)}$ and $D_\lambda^{\mathrm{SU}(3)}$ irreps. We label the SU(2) irreps with their spin value, which in our setup is always an integer. For the irreps of SU(3) we use the more general, Young diagram based labeling introduced in Chapter 3.

According to the decomposition of the composite Hilbert space $\mathcal{H}$ under permutations, as described in Section 3.4, the SU(3) irreps that appear in Eq. (5.7b) correspond to all $\lambda \vdash_3 N$ partitions. However, we adjust this labeling by the use of the equivalence relation between SU(3) diagrams, introduced in Section 3.6, and label the SU(3) irreps with two-row Young diagrams instead. In this new description, the symbol λ in Eq. (5.7b) labels Young diagrams of at most 2 rows and $N - 3i$ boxes, where $i = 0, 1, \ldots, \lfloor N/3 \rfloor$.

A different way of conveying Eq. (5.7), is that the Hilbert space has the following two decompositions into direct sums of SU(2) and SU(3) irreducible sectors,

$$\mathcal{H} = \bigoplus_s (\mathcal{K}_s \otimes \mathcal{H}_s) = \bigoplus_\lambda (\mathcal{K}_\lambda \otimes \mathcal{H}_\lambda)\,, \tag{5.8}$$

where global SU(2) and SU(3) transformations act irreducibly on $\mathcal{H}_s$ and $\mathcal{H}_\lambda$ respectively, and the dimensions of the multiplicity spaces $\mathcal{K}_s$ and $\mathcal{K}_\lambda$ are equal to m_s and m_λ. The value of m_s can be calculated with the usual spin addition, while m_λ is given by the hook length formula, Eq. (3.32).

As SU(2) $\subset$ SU(3), each SU(3) irreducible subspace in $\mathcal{H}$ is a direct sum of SU(2) irreducible subspaces:

$$D_\lambda^{\mathrm{SU}(3)}\Big|_{\mathrm{SU}(2)} \cong \bigoplus_s m_s^{(\lambda)} D_s^{\mathrm{SU}(2)}, \qquad \mathcal{H}_\lambda = \bigoplus_s \left(\mathcal{K}_s^{(\lambda)} \otimes \mathcal{H}_s^{(\lambda)}\right). \tag{5.9}$$

The left-hand side of the first equation denotes the restriction of the $D_\lambda^{\mathrm{SU}(3)}$ irrep to the SU(2) subgroup of SU(3). The corresponding multiplicity spaces and irreducible subspaces are $\mathcal{K}_s^{(\lambda)}$ and $\mathcal{H}_s^{(\lambda)}$ respectively, and the dimension of $\mathcal{K}_s^{(\lambda)}$ is $m_s^{(\lambda)}$. The compatibility between the two decompositions of the Hilbert space in Eq. (5.8) implies $\sum_\lambda m_s^{(\lambda)} = m_s$. Introducing the notation $s \prec \lambda$, which will mean that $D_s^{\mathrm{SU}(2)}$ appears in the irreducible decomposition of $D_\lambda^{\mathrm{SU}(3)}\Big|_{\mathrm{SU}(2)}$, (i.e. $m_s^{(\lambda)} \neq 0$) the complete N-particle Hilbert space can be written as the following direct sum of subspaces,

$$\mathcal{H} = \bigoplus_\lambda \bigoplus_{s \prec \lambda} \mathcal{K}_\lambda \otimes \mathcal{K}_s^{(\lambda)} \otimes \mathcal{H}_s^{(\lambda)}. \tag{5.10}$$

The BLBQ Hamiltonian on the complete graph, Eq. (5.3), is a linear combination of the SU(2) and SU(3) quadratic Casimir operators for N sites. This implies that the subspace $\mathcal{K}_\lambda \otimes \mathcal{K}_s^{(\lambda)} \otimes \mathcal{H}_s^{(\lambda)}$ is an eigenspace of H. Let $P_s^{(\lambda)}$ denote the projection to this subspace, i.e., to the spin-s subspace of $D_\lambda^{\mathrm{SU}(3)}\Big|_{\mathrm{SU}(2)}$. Now the Hamiltonian takes the form[2]

$$H = \sum_\lambda \sum_{s \prec \lambda} E_s^{(\lambda)}\, P_s^{(\lambda)}, \tag{5.11a}$$

$$E_s^{(\lambda)} = \frac{2}{3}\sin(\theta)(\lambda_1^2 + \lambda_2^2 - \lambda_1\lambda_2 + 3\lambda_1) + \cos(\theta)s(s+1), \tag{5.11b}$$

[2]The first term in the expression of the $E_s^{(\lambda)}$ eigenvalue we use here differs by an 1/2 factor compared to the same eigenvalue in our paper [1]. This is because for the shake of consistency with the other parts, in this thesis we defined the generators of SU(3) differently from [1], and this difference results in the operator $C_N^{\mathrm{SU}(3)}$ getting the extra 1/2 factor. As a consequence, the parameter θ in the Hamiltonian of Eq. (5.3) is not the same as parameter of the same name used in [1]. If we denote by θ' the parameter used in the paper, than the conversion between the two parameters is given by $\tan(\theta) = 2\tan(\theta')$.

where $E_s^{(\lambda)}$ is the eigenvalue corresponding to the subspace of $P_s^{(\lambda)}$. The first term is the eigenvalue of the quadratic Casimir of SU(3) in the (λ_1, λ_2) irrep, Eq. (3.58), while the second term is the usual total spin squared, i.e., the Casimir of SU(2).

Finding the ground state of H in Eq. (5.11a) means finding the quantum numbers λ_1, λ_2 and s, for which the energy in Eq. (5.11b) is minimal. However, the value of s cannot be chosen independently from those of λ_1 and λ_2, because not all spin-s representations appear in the SU(3) irrep characterized by λ_1 and λ_2. This is where the knowledge of $m_s^{(\lambda)}$ in Eq. (5.9) becomes important: only if m_λ and $m_s^{(\lambda)}$ are nonzero, does an eigenspace with quantum numbers λ_1, λ_2, and s appear in the decomposition Eq. (5.10), and consequently in Eq. (5.11a).

5.3 Restricting the representation of SU(3) to the SU(2) subgroup

In this section, we calculate the $m_s^{(\lambda)}$ multiplicities that appear in Eq. (5.9). Let us start with the two most straightforward cases: Restricting the trivial representation of SU(3) to SU(2) simply yields the spin-0 irrep, i.e., $m_0^{(0,0)} = 1$. Furthermore, as per our definition, the defining representation of SU(3) maps directly to the spin-1 irrep, which gives $m_1^{(1,0)} = 1$. For the rest, we start by giving a general rule for the SU(3) irreps characterized by the Young diagrams with only one row, i.e., we decompose $D^{\mathrm{SU}(3)}_{(\lambda_1,0)}\big|_{\mathrm{SU}(2)}$. Then, by recursion, we obtain the rule for the other irreps.

The SU(3) irrep corresponding to the single-row Young diagram $(N, 0)$ is supported on the completely symmetric part of the Hilbert space, $(\mathbb{C}^3)^{\vee N}$. $(\mathbb{C}^3)^{\vee N}$ can be decomposed into a direct sum of SU(2) irreducible subspaces, as shown in Eq. (5.9); each of these subspaces can in turn be decomposed into eigenspaces of the z-component of the total spin operator, $S^z = \sum_k S_k^z$. We denote the subspace corresponding to eigenvalue $\ell \in \{-s, \dots, s\}$ of the spin-s irrep by $V_\ell^{(s)}$, and the decomposition reads as

$$(\mathbb{C}^3)^{\vee N} = \bigoplus_s \left(\mathcal{K}_s^{(N,0)} \otimes \mathcal{H}_s^{(N,0)}\right) = \bigoplus_s \left(\mathcal{K}_s^{(N,0)} \otimes \bigoplus_{\ell=-s}^{s} V_\ell^{(s)}\right). \tag{5.12}$$

Let V_ℓ denote the S^z eigenspace with eigenvalue ℓ in $(\mathbb{C}^3)^{\vee N}$. The eigenvalue ℓ appears in spin-s representations iff $s \geq \ell$, thus

$$V_\ell = \bigoplus_{s \geq |\ell|} \left(\mathcal{K}_s^{(N,0)} \otimes V_\ell^{(s)}\right). \tag{5.13}$$

Furthermore, since every $V_\ell^{(s)}$ is one-dimensional, the dimension of V_ℓ is equal to the sum of multiplicities of spin-s irreps with $s \geq |\ell|$:

$$\dim(V_\ell) = \sum_{s \geq |\ell|} m_s^{(N,0)}. \tag{5.14}$$

We continue by figuring out these dimensions.

We use the $\{|1\rangle, |0\rangle, |-1\rangle\}$ eigenstates of S^z as our basis vectors on $\mathbb{C}^3$. The $\ell = N$ eigenvalue can only come from the $|1, 1, \ldots, 1\rangle$ vector, hence $m_N^{(N,0)} = 1$. A basis of the $\ell = N-1$ eigenspace in $(\mathbb{C}^3)^{\otimes N}$ can be constructed from the previous vector by lowering one of the spins to 0. This subspace is N-dimensional, but its intersection with $(\mathbb{C}^3)^{\vee N}$ is only 1-dimensional, spanned by the vector $|0, 1, 1, \ldots, 1\rangle + |1, 0, 1, \ldots, 1\rangle + \cdots + |1, 1, 1, \ldots, 0\rangle$. It follows that $\dim(V_{N-1}) = 1$ and $m_{N-1}^{(N,0)} = 0$.

We can get a basis of the $\ell = N-2$ eigenspace of $(\mathbb{C}^3)^{\otimes N}$ from the $|1, 1, \ldots, 1\rangle$ vector by either lowering two spins to 0, or by lowering one to -1. Any of the basis elements with 0 spin on two sites have the same projection to the symmetric subspace, and similarly only one symmetric vector can be generated from the basis elements with a single -1 spin. This gives us $\dim(V_{N-2}) = 2$ and $m_{N-2}^{(N,0)} = 1$.

Generalizing this procedure, we can see that for an arbitrary ℓ we can lower a spins to 0 and b spins to -1 such that $\ell = N - (a + 2b)$. Each different choice of a and b corresponds to one linearly independent element of V_ℓ; therefore, the number of integer solutions for $a, b \geq 0$ of the previous equation is the dimension of V_ℓ, resulting in

$$\dim(V_\ell) = \lfloor (N - |\ell|)/2 \rfloor + 1. \tag{5.15}$$

Here, $\lfloor . \rfloor$ denotes the floor function, i.e., $\lfloor x \rfloor$ is the largest integer not bigger than x. As the dimension of the S^z eigenspace changes by 1 at every second ℓ, we conclude that only every second spin-s irrep is present in the decomposition Eq. (5.9) of $(\mathbb{C}^3)^{\vee N}$, and with a multiplicity of 1. Therefore,

$$D^{\mathrm{SU}(3)}_{(\lambda_1,0)}\Big|_{\mathrm{SU}(2)} = \begin{cases} \bigoplus_{s=0}^{\lfloor \lambda_1/2 \rfloor} D^{\mathrm{SU}(2)}_{2s+1} & \text{if } \lambda_1 \text{ is odd,} \\ \bigoplus_{s=0}^{\lambda_1/2} D^{\mathrm{SU}(2)}_{2s} & \text{if } \lambda_1 \text{ is even.} \end{cases} \tag{5.16}$$

In terms of multiplicities this means

$$m_s^{(\lambda_1,0)} = \begin{cases} 1 - (s + \lambda_1) \bmod 2 & \text{if } 0 \leq s \leq \lambda_1, \\ 0 & \text{otherwise,} \end{cases} \tag{5.17}$$

where $n \bmod 2$ is the reminder after the division of n by 2.

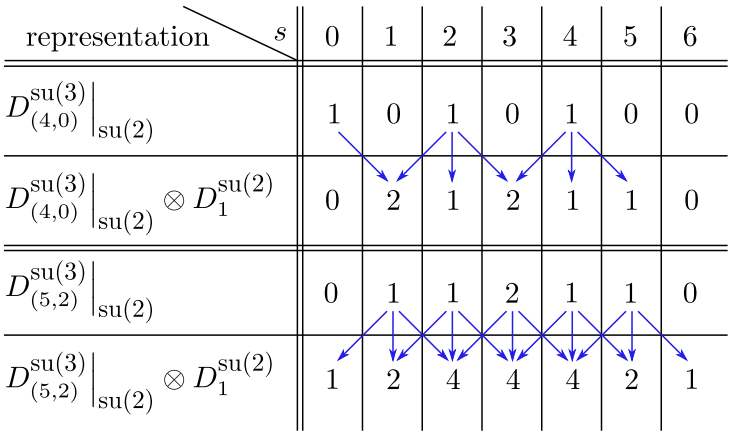

FIGURE 5.2: Illustration of the calculation of the multiplicities in the decomposition Eq. (5.20).

Before continuing with the more complicated cases, we reintroduce the irrep decomposition of the tensor product of an arbitrary SU(3) irrep with the defining representation. According to the fusion rules of SU(3), as discussed in Section 3.7, this reads as:

$$D^{\mathrm{SU}(3)}_{(\lambda_1,\lambda_2)} \otimes D^{\mathrm{SU}(3)}_{(1,0)} = D^{\mathrm{SU}(3)}_{(\lambda_1+1,\lambda_2)} \oplus D^{\mathrm{SU}(3)}_{(\lambda_1,\lambda_2+1)} \oplus D^{\mathrm{SU}(3)}_{(\lambda_1-1,\lambda_2-1)}. \tag{5.18}$$

Let us restrict both sides of the equation to SU(2). The left-hand side decomposes into SU(2) irreps according to the usual spin addition rule,

$$D^{\mathrm{SU}(2)}_j \otimes D^{\mathrm{SU}(2)}_1 = \bigoplus_{s=|j-1|}^{j+1} D^{\mathrm{SU}(2)}_s. \tag{5.19}$$

Furthermore, applying Eq. (5.9) gives us,

$$\begin{aligned} D^{\mathrm{SU}(3)}_{(\lambda_1,\lambda_2)}\Big|_{\mathrm{SU}(2)} \otimes D^{\mathrm{SU}(3)}_{(1,0)}\Big|_{\mathrm{SU}(2)} &\cong \bigoplus_{s=0}^{\infty} m_s^{(\lambda_1,\lambda_2)} D^{\mathrm{SU}(2)}_s \otimes D^{\mathrm{SU}(2)}_1 \\ &= m_1^{(\lambda_1,\lambda_2)} D^{\mathrm{SU}(2)}_0 \oplus \bigoplus_{s=1}^{\infty} \left[m_{s-1}^{(\lambda_1,\lambda_2)} + m_s^{(\lambda_1,\lambda_2)} + m_{s+1}^{(\lambda_1,\lambda_2)} \right] D^{\mathrm{SU}(2)}_s. \end{aligned} \tag{5.20}$$

This step is illustrated in Fig. 5.2. After applying Eq. (5.9), the right-hand side of the restriction of Eq. (5.18) becomes

$$\begin{aligned} &D^{\mathrm{SU}(3)}_{(\lambda_1+1,\lambda_2)}\Big|_{\mathrm{SU}(2)} \oplus D^{\mathrm{SU}(3)}_{(\lambda_1,\lambda_2+1)}\Big|_{\mathrm{SU}(2)} \oplus D^{\mathrm{SU}(3)}_{(\lambda_1-1,\lambda_2-1)}\Big|_{\mathrm{SU}(2)} \\ &\qquad \cong \bigoplus_{s=0}^{\infty} \left[m_s^{(\lambda_1+1,\lambda_2)} + m_s^{(\lambda_1,\lambda_2+1)} + m_s^{(\lambda_1-1,\lambda_2-1)} \right] D^{\mathrm{SU}(2)}_s. \end{aligned} \tag{5.21}$$

Combining Eqs. (5.20) and (5.21) gives us a recurrence relation for the $m_s^{(\lambda_1,\lambda_2)}$ multiplicities,

$$(1-\delta_{s,0})\left(m_{s-1}^{(\lambda_1,\lambda_2)}+m_s^{(\lambda_1,\lambda_2)}\right)+m_{s+1}^{(\lambda_1,\lambda_2)} = m_s^{(\lambda_1+1,\lambda_2)}+m_s^{(\lambda_1,\lambda_2+1)}+m_s^{\lambda_1-1,\lambda_2-1}. \quad (5.22)$$

This equation can be extended to apply to the empty diagram, $(0,0)$, of the trivial representation, by setting $m_s^{(\lambda_1,-1)} = 0$.

The recurrence relation Eq. (5.22), together with Eq. (5.17) as initial condition, uniquely determines the multiplicities $m_s^{(\lambda_1,\lambda_2)}$. One can show by, e.g., by direct substitution, that the solution is the following:

$$m_s^{(\lambda_1,\lambda_2)} = \mathrm{Min}\left\{m_{1,s}^{(\lambda_1,\lambda_2)}, m_{2,s}^{(\lambda_1,\lambda_2)}\right\} \quad (5.23a)$$

with

$$m_{1,s}^{(\lambda_1,\lambda_2)} = \left\lceil \frac{1}{4}\mathrm{Min}\left\{2s-1, 2\lambda_1-(2s-1)\right\} + \left((s+1) \bmod 2 - \frac{1}{2}\right)\left((\lambda_1+1)(\lambda_2+1) \bmod 2\right) \right\rceil \quad (5.23b)$$

$$m_{2,s}^{(\lambda_1,\lambda_2)} = \left\lceil \frac{1}{4}\left(2\mathrm{Min}\left\{(\lambda_1-\lambda_2),\lambda_2\right\}-1\right) \right\rceil + \left((s+\lambda_1+1)(\lambda_1+\mathrm{Max}\{\lambda_2,\lambda_1-\lambda_2\}+1) \bmod 2\right). \quad (5.23c)$$

According to Eq. (5.9), the explicit knowledge of the multiplicities (5.23) means that we have obtained the direct sum expansion of the $\mathfrak{su}(3)$ irreps into $\mathfrak{su}(2)$ irreps. In the following, we will see how it can be used to diagonalize the Hamiltonian in Eq. (5.3).

5.4 The phase diagram of the model

In order to obtain the ground-state energy of the Hamiltonian in Eq. (5.3), we need to find the compatible λ_1, λ_2 and s quantum numbers that minimize its eigenvalue, Eq. (5.11b). To describe these compatibility conditions, let us first note that $(\mathbb{C}^3)^{\otimes N}$ factorizes into SU(3) irreducible subspaces according to Eq. (5.8). Hence, the possible $\lambda = (\lambda_1,\lambda_2)$ pairs are the ones that appear with nonzero m_λ multiplicities in Eq. (5.7b). Furthermore, for each such (λ_1,λ_2) pair, the compatible s values are those with $m_s^{(\lambda_1,\lambda_2)} \neq 0$ in Eq. (5.9). Given the optimal $\lambda = (\lambda_1,\lambda_2)$ and s values, the ground-state eigenspace of the Hamiltonian is $\mathcal{K}_\lambda \otimes \mathcal{K}_s^{(\lambda)} \otimes \mathcal{H}_s^{(\lambda)}$ from Eq. (5.10), which is usually degenerate.

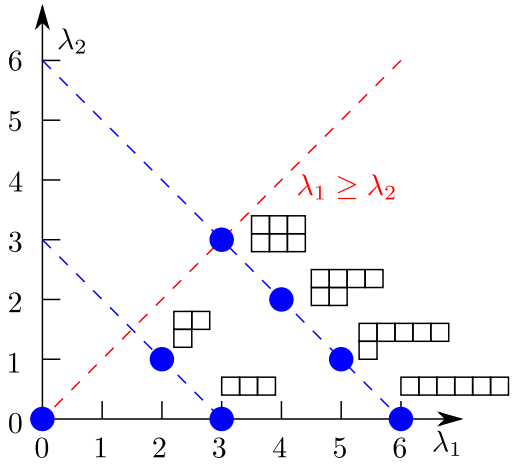

FIGURE 5.3: The (λ_1, λ_2) pairs (blue circles) corresponding to the SU(3) irreps with nonzero multiplicity appearing in the decomposition Eq. (5.7b) for $N = 6$.

The solution of the ground-state energy problem is the simplest when the number of spins is divisible by 6. Thus, we consider this situation first and explain the $N \bmod 6 \neq 0$ case later. The reason why divisibility by 6 is important, is that both the SU(2) and SU(3) singlet subspaces are present in the composite Hilbert space, iff N is divisible by 6. As explained in Section 5.2, the (λ_1, λ_2) irreducible subspaces present in the decomposition of the Hilbert space $(\mathbb{C}^3)^{\otimes N}$ correspond to Young diagrams with at most 2 rows and $N-3i$ boxes with $i = 0, 1, \ldots, N/3$. (See Fig. 5.3, for an illustration of the $N = 6$ case.) Consequently, the $(0, 0)$ diagram, or in other words, the SU(3) singlet is present iff N is divisible by 3. Similarly, it follows directly from the spin addition rules that the total SU(2) singlet subspace is present iff N is even. In the corresponding singlet subspace, the energy contribution of the $C_N^{\mathrm{SU}(2)}$ and $C_N^{\mathrm{SU}(3)}$ terms in the Hamiltonian is 0, therefore in the cases when the lowest energy state is in a singlet subspace, some θ dependent terms are cleared out from the expression of the ground state energy.

The signs of the sine and the cosine prefactors are important in deciding the nature of the ground state, so we divide the phase diagram into four quarters using the angle θ, see Fig. 5.4 (a). To minimize the second term of the energy (5.11b) in the second and third quarters with a given (λ_1, λ_2), where $\cos\theta < 0$, we need to find the maximum possible s value, while in the first and fourth quarters, where $\cos\theta > 0$, we need to find the smallest allowed s. According to Eq. (5.23),

$$\max\{s | m_s^{\lambda_1,\lambda_2} \neq 0\} = \lambda_1, \tag{5.24a}$$

$$\min\{s | m_s^{\lambda_1,\lambda_2} \neq 0\} = \begin{cases} 0 & \text{if both } \lambda_1 \text{ and } \lambda_2 \text{ are even,} \\ 1 & \text{otherwise.} \end{cases} \tag{5.24b}$$

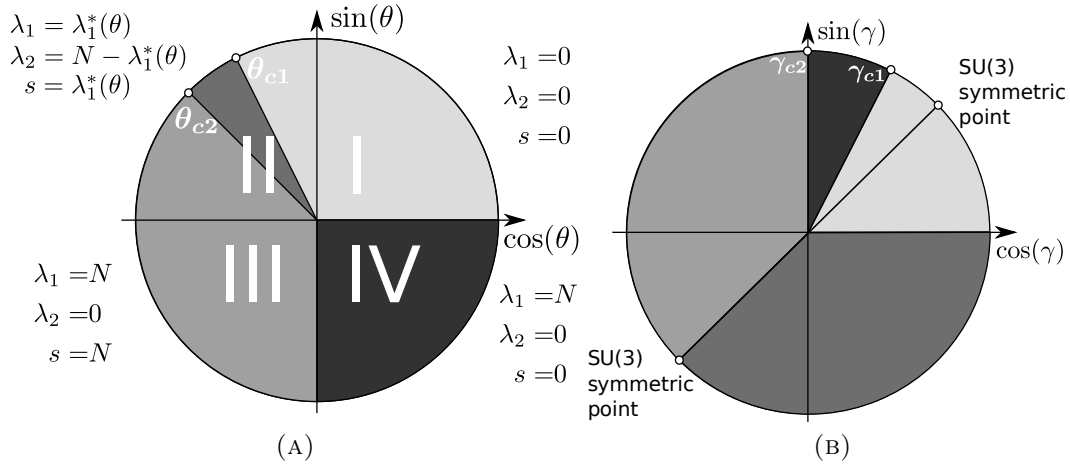

FIGURE 5.4: The ground-state phase diagram of the BLBQ model on the complete graph. In subfigure (a) the phase diagram is plotted with the θ parameter used in Eq. (5.2). The quantum numbers are plotted next to the phase they belong to. In subfigure (b) we used the mapping Eq. (5.5) to represent the phase diagram with the more conventional γ parameter of the bilinear-biquadratic interaction.

This means that in the second and third quarters we need to substitute $s = \lambda_1$ into Eq. (5.11b), then minimize the resulting expression:

$$E_{\lambda_1}^{(\lambda)} = \left(\frac{2}{3}\sin\theta + \cos\theta\right)\lambda_1^2 + (2\sin\theta + \cos\theta)\lambda_1 + \frac{2}{3}\sin\theta\lambda_2(\lambda_2 - \lambda_1). \tag{5.25}$$

On the other hand, in the first and fourth quarters, $s = 0$ or $s = 1$ has to be used according to Eq. (5.24b). We will see shortly, that in the present case of N being the multiple of 6, both λ_1 and λ_2 are even in the ground state, so we use $s = 0$ in Eq. (5.11b), and finally arrive to the polynomial

$$E_0^{(\lambda)} = \frac{2}{3}\sin\theta(\lambda_1^2 + \lambda_2^2 - \lambda_1\lambda_2 + 3\lambda_1). \tag{5.26}$$

Let us now describe what happens in each of these quarters one by one.

In the first quarter ($0 < \theta < \pi/2$), both the sine and the cosine prefactors are positive in Eq. (5.11b) and $s = 0$ can be taken. Hence, we need to minimize Eq. (5.26). Its minimum belongs to the SU(3) singlet ($\lambda_1 = 0, \lambda_2 = 0$), which appears since N is divisible by 3. Therefore, the ground state in the whole region is both an SU(3) and an SU(2) singlet. Obviously, any SU(3) singlet is also an SU(2) singlet, thus the ground-state subspace is plainly the entire SU(3)-singlet

subspace. Using the hook length formula, Eq. (3.32), the dimension of the ground-state subspace is

$$\dim(\mathrm{GS}) = \frac{2N!}{(N/3+2)(N/3+1)^2(N/3!)^3}. \tag{5.27}$$

In the fourth quarter ($3\pi/2 < \theta < 2\pi$), $\sin(\theta)$ is negative but $\cos(\theta)$ is positive. Now Eq. (5.26) is minimized by the irrep $(\lambda_1, \lambda_2) = (N, 0)$. Since N is even, our earlier assumption that the ground state is in the $s = 0$ subspace is justified. The single-row, N-box diagram labels the trivial representation of the permutation group, which is supported on $(\mathbb{C}^3)^{\vee N}$. According to Eq. (5.23), $m_0^{(N,0)} = 1$, i.e., there is only one SU(2) singlet in the symmetric subspace, implying that the ground state is non-degenerate, $\dim(\mathrm{GS}) = 1$.

In the third quarter ($\pi < \theta < 3\pi/2$), both the sine and the cosine are negative, and Eq. (5.25) has to be minimized. Its minimum is at $(\lambda_1, \lambda_2) = (N, 0)$. The symmetric subspace naturally contains the maximum spin ($s = N$) representation, $m_N^{(N,0)} = 1$, which hence spans the ground-state subspace, yielding $\dim(\mathrm{GS}) = 2N + 1$.

In the second quarter ($\pi/2 < \theta < \pi$), the two terms in Eq. (5.11b) are in competition with each other with different signs. In this case, the ground state is polarized according to Eq. (5.24a), i.e., $s = \lambda_1$. Again, we need to minimize Eq. (5.25). Interestingly, the quantum numbers characterizing the ground state in the neighboring quarters extend quite a bit into the second quarter. The $\lambda_1 = \lambda_2 = s = 0$ singlet phase is still the ground state for $\pi/2 < \theta < \theta_{c1}$, while for $\theta_{c2} < \theta < \pi$ the ground state is in the subspace with $\lambda_1 = s = N$, $\lambda_2 = 0$ as in the third quarter. In other words, the two phase boundaries move from $\pi/2$ and π to θ_{c1} and θ_{c2}. The phase boundary θ_{c1} is a complicated function of N. However, when N approaches infinity, it is approximated by

$$\theta_{c1} = \pi - \arctan(2). \tag{5.28}$$

The other phase boundary, for any value of N, is given by

$$\theta_{c2} = \pi - \arctan((2N+1)/(2N+2)). \tag{5.29}$$

Between θ_{c1} and θ_{c2}, the quantum numbers gradually change between those of the two neighboring phases. If (λ_1, λ_2) were allowed to vary continuously, the pair that minimizes the energy would move on the $(x(\theta), N - x(\theta))$ line with

$$x(\theta) = \frac{(2N-2)\tan(\theta) - 1}{4\tan(\theta) + 2}. \tag{5.30}$$

Since only integer pairs are allowed, and the value of the energy (5.11a) on the $\lambda_1 + \lambda_2 = N$ line as a function of λ_1 is a positive parabola with its minimum at $x(\theta)$. The value of λ_1 in the ground state will be the closest integer value to $x(\theta)$, which is $\lambda_1^*(\theta) = \lceil x(\theta) - 1/2 \rceil$. This means that the optimal quantum numbers are $(\lambda_1, \lambda_2) = (\lambda_1^*(\theta), N - \lambda_1^*(\theta))$ and $s = \lambda_1^*(\theta)$. The dimension of the ground state subspace is

$$\dim(\mathrm{GS}) = \frac{N!(2\lambda_1^*(\theta) - N + 1)!}{(N - \lambda_1^*(\theta))!(\lambda_1^*(\theta) + 1)!}(2\lambda_1^*(\theta) + 1). \tag{5.31}$$

In summary, we have found an SU(3) singlet phase, in the region $0 \leq \theta \leq \theta_{c1}$, a partially magnetized phase between $\theta_{c1} \leq \theta \leq \theta_{c2}$, a ferromagnetic phase between $\theta_{c2} \leq \theta \leq 3\pi/2$, and a symmetric SU(2) singlet phase between $3\pi/2 \leq \theta \leq 2\pi$. The complete phase diagram is illustrated in Fig. 5.4, both in terms of θ, and in terms of the original parameter γ used in Eq. (5.4). In terms of the γ angle, when N is asymptotically large, the phase-transition points are at $\gamma = 0, \arctan(2), \pi/2, 5\pi/4$. It is worth to note that the boundaries of the ferromagnetic phase are at the same γ angles than for the one-dimensional BLBQ chain.

It is also worth to discuss some special points of the phase diagram. When $\theta = \pi/2, 3\pi/2$ the Hamiltonian is SU(3) invariant. The $\theta = 3\pi/2$ point is at a phase boundary separating two phases within the symmetric subspace: the ferromagnetic and the symmetric singlet phases. At this point there is an even bigger degeneracy than in the two neighboring phases, all symmetric states are ground states. On the contrary, the SU(3) symmetry at $\theta = \pi/2$ does not result in additional degeneracy of the ground state. This is because the ground state in this case is an SU(3) singlet, which means it also must be an SU(2) singlet. Consequently, this phase extends over the $\theta = \pi/2$ point into the second quarter. The situation is similar with the $\theta = 0, \pi$ points, where the Hamiltonian, Eq. (5.3), contains only the SU(2) Casimir operator. On the one hand, $\theta = 0$ separates the two SU(2) singlet phases, and at this point all SU(2) singlet states are ground states. On the other hand, for $\theta = \pi$ we have an SU(2) ferromagnetic state with maximal spin, which is always contained in the symmetric subspace, thus, it does not result in an additional degeneracy and does not separate phases.

Finally, let us turn to the case when the number of spins is not divisible by 6. It is then possible that the Hilbert space does not have an SU(3) singlet subspace, or that the $(N, 0)$ Young diagram has no SU(2) Singlet subspace. In these cases one cannot separately optimize the $C_N^{\mathrm{SU}(2)}$ and $C_N^{\mathrm{SU}(3)}$ parts of the Hamiltonian in the second and the fourth quarters. Instead, there is a competition between two different ground states with almost optimal SU(3) and SU(2) Quantum numbers.

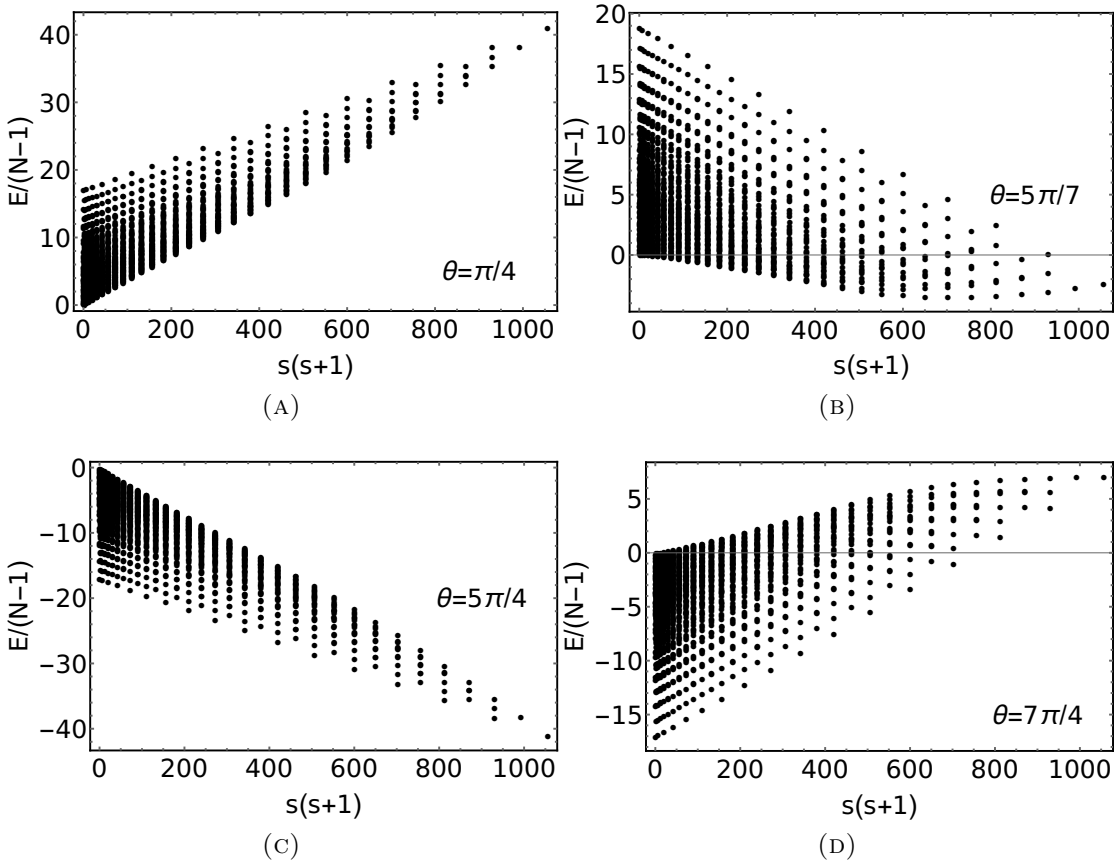

FIGURE 5.5: The energy spectrum of the Hamiltonian (5.3) as a function of the total spin square. Each subfigure represents one of the four ground state phases. The spectrum is evaluated for $N = 36$ sites.

For example, in the first quarter when $N \bmod 3 = 1$, the ground state for $0 < \theta < \arctan(1/6)$ has the quantum numbers $\lambda_1 = 2$, $\lambda_2 = 2$, $s = 0$. When $\arctan(1/6) < \theta < \pi/2$ this is replaced by the state with $\lambda_1 = 1$, $\lambda_2 = 0$, $s = 1$. The difference in the quantum numbers is of the order of 1, and thus it is unimportant for large N.

5.5 Energy spectrum

Lastly, we discuss the full energy spectrum of our model. Let us first note, that as a consequence of the infinite range interaction, the energy given by Eq. (5.3) is not an extensive quantity. In order to make it extensive in the thermodynamic limit, we normalize our Hamiltonian with an additional $1/(N-1)$ factor. Fig. 5.5 illustrates the energy spectrum as a function of $s(s+1)$ for representative values of the θ parameter for each of the ground-state phases. In Fig. 5.5a, we have chosen the representative angle $\theta = \pi/4$ from the SU(3) singlet phase. As expected, the lowest energy belongs to $s = 0$, and the next level is very close in energy to the

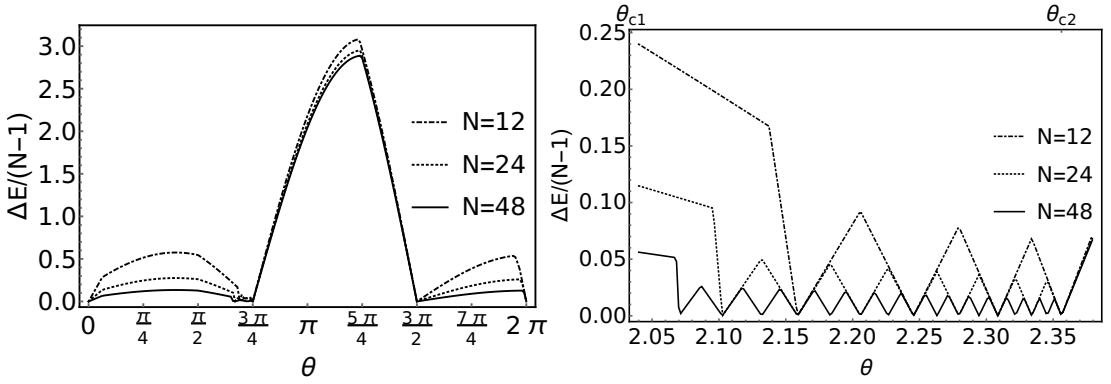

(A) (B)

FIGURE 5.6: The difference between the two lowest energy levels of the Hamiltonian (5.3) for $N = 32$ sites.

ground state. In Fig. 5.5b, we have chosen $\theta = 5\pi/7$ representing the partially magnetized phase. Here, the lowest energy belongs to an intermediate value of the total spin given by $\lambda_1^*(5\pi/7)$. Fig. 5.5c with $\theta = 5\pi/4$ corresponds to the ferromagnetic phase. The lowest energy is for $s = N$. The next lowest energy level is separated by a gap, which does not vanish when N goes to infinity. Finally, Fig. 5.5d is plotted for $\theta = 7\pi/4$ representing the symmetric SU(2) singlet phase. The minimal energy level is at $s = 0$ and the separation between the two lowest levels vanishes in the thermodynamic limit.

We further note, that by the transformation $\theta \to \theta + \pi$ the Hamiltonian (5.3) changes sign. Therefore, the spectra also get reflected under such a transformation. A reminiscent behavior is approximately present when comparing Figs. 5.5a and 5.5c, as well as 5.5b and 5.5d, although the four representative θ angles were intentionally chosen not to be symmetric on the circle.

Let us take a closer look at the energy gap, i.e., the separation of the two lowest lying energy levels, see Fig. 5.6. The gap remains finite as N tends to infinity only in the ferromagnetic region. Both in the SU(3) singlet phase and in the symmetric SU(2) singlet phase, the gap tends to 0 as $\mathcal{O}(1/N)$. The situation is quite delicate in the partially magnetized phase. For any finite N, there is a series of ground-state level crossings, the number of which is proportional to N, see Fig. 5.6b. As N tends to infinity these level-crossings get increasingly dense, and the phase becomes gapless in the thermodynamic limit even without the $1/(N-1)$ normalization of the Hamiltonian.

5.6 Summary and outlook

We determined the ground-state phase diagram and energy spectrum of the spin-1 bilinear-biquadratic model on the complete graph. In this simple setting, the Hamiltonian is a linear combination of the quadratic Casimir operators of the SU(2) and SU(3) Lie algebras. These two Casimir operators commute, thus the diagonalization of the Hamiltonian reduces to the representation theoretic problem of identifying the embedding of SU(2) irreducible representations into SU(3) ones. Solving this problem is one of the main results of this part of the thesis. By diagonalizing the Hamiltonian, we found that the model has four phases belonging to different symmetry sectors. With respect to SU(2) two of the phases are singlets, there is also a partially magnetized and a ferromagnetic phase. One of the SU(2)-singlet phases is also SU(3)-singlet, while the other one belongs to the completely symmetric subspace and is thus characterized by a maximal $\lambda_1 = N$ quantum number. The ferromagnetic ground state is also symmetric, i.e., $s = \lambda_1 = N$. The most interesting part of our phase diagram is the gapless partially magnetized phase between the ferromagnetic and the SU(3)-singlet phase. The λ_1, λ_2 and s quantum numbers change gradually within this phase, while they stay constant within the other phases. At all phase boundaries the quantum numbers have a discontinuity proportional to N, except at the boundary between the partially magnetized and the ferromagnetic phase (θ_{c2}).

Spin models on complete graphs are generally believed to mimic the properties of their counterparts on regular lattices in sufficiently high dimensions. However, for the BLBQ model, already some aspects of low-dimensional lattice models are reflected in the complete graph results. A natural example is the case of ferromagnetic coupling, for which the ground-state space is the $\lambda_1 = s = N$ maximally polarized subspace, independently of the underlying geometry. A more interesting observation is that the symmetric SU(2) singlet, $(\lambda_1, \lambda_2) = (N, 0), s = 0$, appears as a limiting ground state also in the one-dimensional BLBQ model at the boundary of the dimerized SU(2)-singlet and the ferromagnetic phase [132]. In contrast, dimerization and trimerization, which are important features of the BLBQ-model on bipartite and tripartite lattices, cannot be described on complete graphs. Thus, a natural generalization of our problem would be to consider the model on k-partite complete graphs. Already in the bipartite case, one can expect the appearance of symmetry-breaking antiferromagnetism.

Finally, let us comment about the possible experimental relevance of this model. In Ref. [46], an experiment with ultracold atoms was proposed for the realization of the SU(3) symmetric point of the BLBQ Hamiltonian on a complete graph.

It would be desirable to extend this approach to the entire phase diagram. An experimental realization would not only mean that one can study these quantum phases of matter in the lab, but one would also obtain metrologically useful states. In this respect, particularly the singlet phases can be of interest, as macroscopic singlet states have been proposed for gradient magnetometry [135, 136].

Chapter 6

Collective SU(3) spin systems with bipartite symmetry

6.1 Introduction

In this chapter, we expand upon the theme started in Chapter 5, and investigate another highly permutation symmetric 3-level quantum system. As we have pointed out in Section 5.1, the most general SU(3) symmetric two-particle interaction is given by a linear combination of two SU(3) symmetric, linearly independent two-particle operators, e.g.:

$$H = \alpha C_2^{\mathrm{SU}(3)} + \beta \mathbb{1}. \tag{6.1}$$

Nonetheless, it gives more physical intuition to choose an operator different from $C_2^{\mathrm{SU}(3)}$: The swap operator F_{ij} defined with $F_{ij}|\alpha\rangle|\beta\rangle = |\beta\rangle|\alpha\rangle$ for any product vector. This makes it clear that the most general SU(3) symmetric two-particle interaction is the humble exchange interaction.

In Section 5.1 we argued that this exchange interaction yields a trivial Hamiltonian when paired with complete permutation invariance. Chiefly for this reason, in Chapter 5 we broke the complete SU(3) invariance with an SU(2) symmetric term in the interaction. In this chapter, we chose a different approach: Instead of breaking the SU(3) symmetry, we break the complete permutation invariance in a minimal fashion, keeping large enough subsystems permutation invariant so that our techniques remain usable. We divide the entire system into two equal-sized permutation symmetric subsystems; in this way, we introduce a bipartite structure in a mean-field type model. It is reasonable to expect that this will make the phase structure more interesting, since it relaxes the extreme frustration of the complete graph, and makes the model able to admit the bipartite symmetry breaking ground states normally associated with antiferromagnetism.

We denote the two subsystems by A, B and AB, and set the strength of

the interaction between two arbitrary spins on the same subsystem to J_1, while on different subsystems to J_2. With this, the Hamiltonian describing the entire system reads as,

$$H = (J_1 - J_2) \sum_{\substack{i,j\in \mathrm{A} \\ i<j}} C_{2\ ij}^{\mathrm{SU}(3)} + (J_1 - J_2) \sum_{\substack{i,j\in \mathrm{B} \\ i<j}} C_{2\ ij}^{\mathrm{SU}(3)} + J_2 \sum_{\substack{i,j\in \mathrm{AB} \\ i<j}} C_{2\ ij}^{\mathrm{SU}(3)}. \tag{6.2}$$

We point out that unless J_1 or J_2 equals 0, our model still has complete connectivity between the spins, we just imposed a bipartite symmetry by changing the connection strengths. The graph describing the connections becomes bipartite only when $J_1 = 0$.

Dropping unnecessary indexes, we introduce the quadratic SU(3) Casimir operators of the two subsystems C_{A}, C_{B}, and the entire Hilbert space C_{AB},

$$C_X = \sum_{\alpha,\beta=1}^{3} \left(\sum_{i\in X} E_i^{\alpha,\beta} \right) \left(\sum_{j\in X} E_j^{\beta\alpha} \right) = \sum_{\substack{i,j\in \mathrm{X}, \\ i<j}} C_{2\ ij}^{\mathrm{SU}(3)} - \frac{8}{3} \left(|\mathrm{X}| - 2 \right) |\mathrm{X}| \mathbb{1}. \tag{6.3}$$

From here on, we use X as a placeholder that can mean either A, B or AB, and |X| denotes the number of sites in X. The second equation is a consequence of applying Schur's lemma to the one-site quadratic Casimir operators $C_{2\ i}^{\mathrm{SU}(3)} = \sum_{\alpha\beta} E_i^{\alpha\beta} E_i^{\beta\alpha}$. We define the parameter θ with $\tan(\theta) = J_2/(J_1 - J_2)$ and rescale the Hamiltonian of Eq. (6.2), in order to measure the energy in units of $\sqrt{J_1^2 + 2J_2^2 - 2J_1 J_2}$. With the newly introduced notations, the rescaled Hamiltonian takes a form that is more easily tacked with representation theoretic techniques:

$$H_{\mathrm{CBE}} = \sin(\theta) C_{\mathrm{AB}} + \cos(\theta) \left(C_{\mathrm{A}} + C_{\mathrm{B}} \right). \tag{6.4}$$

The physical intuition we can gain from this form is that the right parameters that characterize the system are not the strengths of the interaction within and between the subsystems, but rather the strength of the "baseline" uniform exchange interaction on the entire system represented by C_{AB}, and the strength of the additional uniform interaction on the subsystems superposed with the former, which is represented by C_{A} and C_{B}. In a way, we can think about this as adjusting the zero-point of the coupling constant J_1 of the intra-subsystem interactions to match the baseline J_2. With these uniform interactions, the spins on the subsystems and the entire system act in a mean-field-like collective manner. Thus, throughout the paper we will call it the spin-1 *collective bipartite exchange Hamiltonian*, or *CBE Hamiltonian* for short.

Such a system may look quite artificial for the first glance, however, experimental techniques with ultracold atoms and cavity electrodynamics represent a promising way towards its realization. One may expect, that a dual system of ultracold ensembles inside lossy optical cavities [137–139] can actually be used to realize SU(3) symmetric Mott insulators on a bipartite lattice, where the permutation invariant infinite-range interaction is provided by the cavity photons. The two ensembles can be realized by different electric configurations of the ultracold atomic gas, e.g., the two 3-component $F = 1$ hyperfine states on the two sides of the rubidium D_1 transition[1].

This chapter is structured as the following: In Section 6.2, we formally diagonalize the Hamiltonian using representation theoretic tools. In Section 6.4, we explicitly construct and explore the ground state phase diagram. Finally, in Section 6.5, we summarize the results and provide an outlook.

6.2 The eigenspace decomposition of the Hamiltonian

Thanks to the invariance of the Hamiltonian to the permutations of the subsystems A and B, it's eigenspace decomposition, similarly to Section 5.2 for the BLBQ model, can be obtained entirely through representation theoretic considerations. More precisely, by finding the compatible eigenspaces of the three Casimir operators in Eq. (6.4). In this section, we give this decomposition.

We set the number of sites in each subsystem to N. The full Hilbert space, $\mathcal{H}^{(\mathrm{AB})} \cong (\mathbb{C}^3)^{\otimes 2N}$, decomposes into a direct sum of irreducible subspaces under global SU(3) transformations. The Hilbert spaces $\mathcal{H}^{(\mathrm{A})} \cong \mathcal{H}^{(\mathrm{B})} \cong (\mathbb{C}^3)^{\otimes N}$ also have a similar decomposition under their respective N-fold SU(3) transformations. More explicitly, according to Eq. (3.27), the irreps that appear in these decompositions correspond to the $\lambda \vdash_3 2N$ and $\lambda \vdash_3 N$ partitions:

$$\mathcal{H}^{(\mathrm{AB})} \cong \mathcal{H}^{(\mathrm{A})} \otimes \mathcal{H}^{(\mathrm{B})} \cong \bigoplus_{\lambda \vdash_3 2\mathrm{N}} \mathcal{K}_\lambda^{(\mathrm{AB})} \otimes \mathcal{H}_\lambda^{(\mathrm{AB})} \cong \left(\bigoplus_{\lambda \vdash_3 \mathrm{N}} \mathcal{K}_\lambda^{(\mathrm{A})} \otimes \mathcal{H}_\lambda^{(\mathrm{A})} \right) \otimes \left(\bigoplus_{\lambda \vdash_3 \mathrm{N}} \mathcal{K}_\lambda^{(\mathrm{B})} \otimes \mathcal{H}_\lambda^{(\mathrm{B})} \right). \quad (6.5)$$

Here $\mathcal{H}_\lambda^{(\mathrm{X})}$ are subspaces where the respective N-fold or $2N$-fold SU(3) transformations act irreducibly, and $\mathcal{K}_\lambda^{(\mathrm{X})}$ are subspaces where the same transformations act

[1] D. A. Steck, "Rubidium 87 D Line Data", available online at http://steck.us/alkalidata (revision 2.2.1, 21 November 2019).

as identity. The dimensions of these $\mathcal{K}_\lambda^{(\mathrm{X})}$ subspaces are equal to the multiplicities of the SU(3) irreducible representations, $D_\lambda^{\mathrm{SU}(3)}$, in the irrep decomposition of the $2N$-fold (AB) or N-fold (A, B) tensor product of the defining representation. This multiplicity can be calculated directly with the hook length formula, Eq. (3.32). The dimension of $\mathcal{H}_\lambda^{(\mathrm{X})}$ is the dimension of the $D_\lambda^{\mathrm{SU}(3)}$ irrep, which is the number of semistandard Young tableaux with shape λ and dimension 3, or equivalently, $\dim\left(D_\lambda^{\mathrm{SU}(3)}\right) = (p+1)(q+1)(p+q+2)/2$, where p and q are the Dynkin labels describing the diagram $\lambda = [p, q]$.

The eigenspaces of C_{AB}, C_{A} and C_{B} are precisely the degenerate subspaces of the form $\mathcal{K}_\lambda^{(\mathrm{X})} \otimes \mathcal{H}_\lambda^{(\mathrm{X})}$ in Eq. (6.5); thus, the diagonalization of the CBE Hamiltonian (6.4) turns into a representation theoretic problem. Since the Casimir operators appearing in the CBE Hamiltonian commute with each other, their eigenspaces must be compatible. This compatibility manifests by the tensor products of C_{A} and C_{B} eigenspaces decomposing into direct sums of C_{AB} eigenspaces, i.e.:

$$\left(\mathcal{K}_{\lambda^{(\mathrm{A})}}^{(\mathrm{A})} \otimes \mathcal{H}_{\lambda^{(\mathrm{A})}}^{(\mathrm{A})}\right) \otimes \left(\mathcal{K}_{\lambda^{(\mathrm{B})}}^{(\mathrm{B})} \otimes \mathcal{H}_{\lambda^{(\mathrm{B})}}^{(\mathrm{B})}\right) \cong \mathcal{K}_{\lambda^{(\mathrm{A})}}^{(\mathrm{A})} \otimes \mathcal{K}_{\lambda^{(\mathrm{B})}}^{(\mathrm{B})} \otimes \left(\bigoplus_{\lambda^{(\mathrm{AB})} \in \lambda^{(\mathrm{A})} \otimes \lambda^{(\mathrm{B})}} \mathcal{H}_{\lambda^{(\mathrm{AB})}}^{(\mathrm{AB})}\right). \tag{6.6}$$

As a result, we are able to label the eigenspaces of the CBE Hamiltonian by $(\lambda^{(\mathrm{A})}, \lambda^{(\mathrm{B})}, \lambda^{(\mathrm{AB})})$ triples of SU(3) irreps. In this sense, however, not all SU(3) irreps are compatible with each other. A valid triple of irreps has to fulfill two conditions:

1. As the direct sum in Eq. (6.6) is over the $\lambda^{(\mathrm{AB})}$ partitions that appear in the irrep decomposition of $D_{\lambda^{(\mathrm{A})}}^{\mathrm{SU}(3)} \otimes D_{\lambda^{(\mathrm{B})}}^{\mathrm{SU}(3)}$, this condition must be true for any valid triple.

2. The partitions must appear in the irrep decompositions of the N-fold and $2N$-fold tensor products of the defining representation of SU(3), i.e., $\lambda^{(\mathrm{A})}, \lambda^{(\mathrm{B})} \vdash_3 N$ and $\lambda^{(\mathrm{AB})} \vdash_3 2N$.

6.3 Determining the ground state subspace

Now that we have described how to characterize the eigenspaces the CBE Hamiltonian, we move on to determine the triple of SU(3) irreps, $(\lambda^{(A)}, \lambda^{(B)}, \lambda^{(\mathrm{AB})})$, that corresponds to the subspace of the ground states, i.e., the lowest energy eigenspace. We progress towards this goal through the following steps: We fix two arbitrary irreps on the subsystems, $\lambda^{(\mathrm{A})}$ and $\lambda^{(\mathrm{B})}$, and then determine the

irrep $\lambda^{*(\mathrm{AB})}(\lambda^{(\mathrm{A})}, \lambda^{(\mathrm{B})}, \theta)$ which appears in the decomposition of $D^{\mathrm{SU}(3)}_{\lambda^{(\mathrm{A})}} \otimes D^{\mathrm{SU}(3)}_{\lambda^{(\mathrm{B})}}$ and minimizes the term proportional to C_{AB} in the CBE Hamiltonian (6.4). Depending on the sign of the sine prefactor, this is equivalent to finding the irrep $\check{\lambda}^{(\mathrm{AB})}(\lambda^{(\mathrm{A})}, \lambda^{(\mathrm{B})}) \cong (\check{\lambda_1}^{(\mathrm{AB})}, \check{\lambda_2}^{(\mathrm{AB})})$ that minimizes or the irrep $\hat{\lambda}^{(\mathrm{AB})}(\lambda^{(\mathrm{A})}, \lambda^{(\mathrm{B})}) \cong (\hat{\lambda_1}^{(\mathrm{AB})}, \hat{\lambda_2}^{(\mathrm{AB})})$ that maximizes the eigenvalue of C_{AB}. After $\lambda^{*(\mathrm{AB})}$ is known, the problem of determining the ground state subspace reduces to finding irreps $\lambda^{(A)}$ and $\lambda^{(B)}$ for which the triple $(\lambda^{(\mathrm{A})}, \lambda^{(\mathrm{B})}, \lambda^{*(\mathrm{AB})}(\lambda^{(\mathrm{A})}, \lambda^{(\mathrm{B})}, \theta))$ minimizes the eigenvalue of the CBE Hamiltonian.

6.3.1 The dominance order of partitions

In order to be able to derive $\check{\lambda}^{(\mathrm{AB})}(\lambda^{(\mathrm{A})}, \lambda^{(\mathrm{B})})$ and $\hat{\lambda}^{(\mathrm{AB})}(\lambda^{(\mathrm{A})}, \lambda^{(\mathrm{B})})$, it is necessary to introduce the dominance order of partitions. Sometimes also called majoriziation order, dominance order is a partial order on the integer partitions of a positive integer N.

Definition 2. Suppose $\lambda = (\lambda_1, \lambda_2, \ldots, \lambda_l)$, $\mu = (\mu_1, \mu_2, \ldots \mu_m) \vdash N$. Then λ dominates μ, which we denote as $\lambda \trianglerighteq \mu$, if

$$\lambda_1 + \lambda_2 + \cdots + \lambda_i \geq \mu_1 + \mu_2 + \cdots + \mu_i, \tag{6.7}$$

for all $i \geq 1$. If $i > l$ $(i > m)$ we take λ_i (μ_i) as 0.

To give some intuition, if $\lambda \trianglerighteq \mu$ then one can imagine the Young diagram of λ as short and fat, while μ as long and skinny. E.g.: $(3,3) \trianglerighteq (2,2,1,1)$, but $(3,3)$ and $(4,1,1)$ are not related.

In a partially ordered set (poset), comparable elements that are immediate neighbors are said to have a covering relation. That is, the partition $\lambda \vdash N$ covers $\mu \vdash N$ iff $\lambda \triangleright \mu$, where by $\triangleright$ we mean a dominance relation with at least one strict inequality, and there is no partition $\nu \vdash N$ such that $\lambda \triangleright \nu \triangleright \mu$. The following condition for a covering relation between partitions is introduced in [140].

Proposition 15. *The partition $\lambda \vdash N$ covers $\mu \vdash N$ in dominance order iff there is a pair of indices $1 \leq i < k \leq N$ such that:*

1. *$\lambda_i = \mu_i + 1, \lambda_k = \mu_k - 1$, and $\lambda_j = \mu_j$ for all $k \neq j, k \neq i$.*
2. *$k = i + 1$ or $\mu_i = \mu_k$.*

Thinking in Young diagrams, this means that one can get the diagram λ from μ, by removing a box from the end of row k, and appending it to the immediately preceding row, or to row $i < k$ if the rows i through k of the diagrams all have the

same length, but row $i-1$ is different. Using Proposition 15, we can introduce an alternative, visual definition for dominance order: $\lambda \rhd \mu$ iff one can get to the Young diagram of λ starting from μ, by moving boxes between rows one-by-one only upwards.

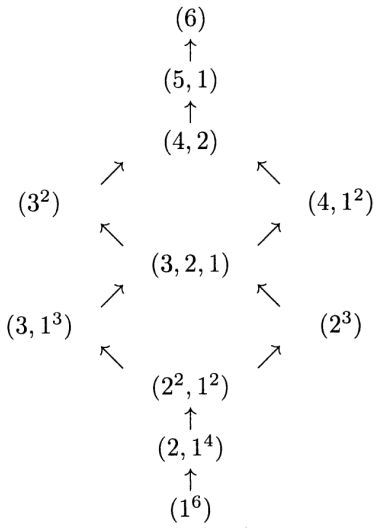

FIGURE 6.1: The Hasse diagram of the partitions of 6. A Hasse diagram displays the covering relations between the elements of a poset.

Now, we are ready to give the reason why dominance order is important for our effort: The eigenvalues of the quadratic Casimir operator of SU(d) are arranged in dominance order. That is, if $\lambda \rhd \mu$ then $c_2^{\mathrm{SU}(d)}(\lambda) > c_2^{\mathrm{SU}(d)}(\mu)$. This can be confirmed by using the definition of $c_2^{\mathrm{SU}(d)}(\lambda)$ in Eq. (3.57). It is enough to check the case where λ covers μ. Let the indices i and k be such that in Proposition 15. Then, we have

$$c_2^{\mathrm{SU}(d)}(\lambda) - c_2^{\mathrm{SU}(d)}(\mu) = (k-i) + (\tilde{\lambda}_i - \tilde{\lambda}_k) - 2 = (k-i) + (\mu_i - \mu_k) \geq 1. \quad (6.8)$$

Here, we temporally took back our previous convention of labeling SU(d) irreps with $d-1$-row Young diagrams, and used the full d-row diagrams. This way, the Young diagrams in the irrep decompositions of $D^{\mathrm{SU}(d)}_{\lambda^{(\mathrm{A})}} \otimes D^{\mathrm{SU}(d)}_{\lambda^{(\mathrm{B})}}$ are all integer partitions of the same number, and therefore form a poset w.r.t. dominance order. We determine $\check{\lambda}^{(\mathrm{AB})}(\lambda^{(A)}, \lambda^{(B)})$ and $\hat{\lambda}^{(\mathrm{AB})}(\lambda^{(A)}, \lambda^{(B)})$ by showing that this poset has both a minimum and maximum, and finding these elements.

6.3.2 The maximum product diagram

We start with the easier task of finding the maximum diagram in the irrep decomposition of $D^{\mathrm{SU}(d)}_{\lambda^{(\mathrm{A})}} \otimes D^{\mathrm{SU}(d)}_{\lambda^{(\mathrm{B})}}$. This means finding the most "short and fat" diagram in the set constructed by attaching the boxes of $\lambda^{(\mathrm{B})}$ to $\lambda^{(\mathrm{A})}$ in the way described by the Littlewood-Richardson algorithm in Section 3.7.1. According to this algorithm, boxes labeled with the number j, i.e. boxes from the j-th row of $\lambda^{(\mathrm{B})}$, can only appear in the j-th row of the constructed tableau or below. In addition to this, we always create a valid tableau by attaching every box with label j to the j-th row; therefore, the corresponding diagram is always present in the irrep decomposition of the product. This diagram dominates all other product diagrams, as starting from it, we can reach any other product diagram by moving boxes only downwards. Thus, the maximum diagram is given by,

$$\hat{\lambda}^{(\mathrm{AB})}_i(\lambda^{(\mathrm{A})}, \lambda^{(\mathrm{B})}) = \lambda^{(\mathrm{A})}_i + \lambda^{(\mathrm{B})}_i. \tag{6.9}$$

6.3.3 The minimum product diagram

Finding the minimum diagram in the irrep decomposition of $D^{\mathrm{SU}(d)}_{\lambda^{(\mathrm{A})}} \otimes D^{\mathrm{SU}(d)}_{\lambda^{(\mathrm{B})}}$ with respect do dominance order is much less straightforward than finding the maximum. When we searched for the maximum, we had to find the most "top heavy" distribution for each type of labeled box in the Littlewood-Richardson algorithm. For each label, this distribution was independent of the distributions of the rest of the labels. Unfortunately, this is not the case when we search for the minimum, and the most "bottom heavy" distributions. The most bottom heavy distribution for the boxes with label j depends heavily on the distributions of boxes with labels $i < j$, and the shape of the diagrams $\lambda^{(\mathrm{A})}, \lambda^{(\mathrm{B})}$. For this reason, although we could find the maximum diagram independently of the dimension, for the minimum we restrict ourselves to the original problem of $d = 3$.

Proposition 16. *The minimum diagram w.r.t. dominance order in the irrep decomposition of* $D^{\mathrm{SU}(3)}_{\lambda^{(\mathrm{A})}} \otimes D^{\mathrm{SU}(3)}_{\lambda^{(\mathrm{B})}}$*, is the last diagram that the direct sum in the closed formula, Eq.* (3.53)*, for the irrep decomposition loops through. That is, the diagram*

$$\begin{aligned}\lambda(k_{2,1}, k_{2,2}, k_{1,1}) = \\ (\lambda^{(\mathrm{A})}_1 + \lambda^{(\mathrm{B})}_1 - k_{2,1} - k_{2,2}, \lambda^{(\mathrm{A})}_2 + \lambda^{(\mathrm{B})}_2 - k_{1,1} + k_{2,2}, k_{2,1} + k_{1,1}),\end{aligned} \tag{6.10}$$

for which all three running indices take their maximum values:

$$
\begin{aligned}
k_{2,1} &= u(1,1) = min\{\mu_1 - \mu_2, \lambda_2^{(\mathrm{A})}\} \\
k_{2,2} &= u(1,2)|_{u(1,1)} = min\{\lambda_1^{(\mathrm{A})} - \lambda_2^{(\mathrm{A})}, \lambda_1^{(\mathrm{B})} - u(1,1)\}, \\
k_{1,1} &= u(2,1)|_{u(1,1),u(1,2)} = min\{\lambda_2^{(\mathrm{A})} + u(1,2) - u(1,1), \lambda_2^{(\mathrm{B})}\}.
\end{aligned}
\tag{6.11}
$$

We prove this proposition in Appendix D, where for every diagram in the product, labeled by the indices $(k'_{2,1}, k'_{2,2}, k'_{1,1})$, we construct a sequence of diagrams starting from our proposed minimum diagram, and ending with the diagram labeled by $(k'_{2,1}, k'_{2,2}, k'_{1,1})$, then show that every diagram in the sequence dominates the previous one.

Substituting Eq. (6.11) into Eq. (6.10), converting the result back to the two-row notation using the equivalence relation described in Proposition 8, then separating and simplifying the different cases created by the three layers of embedded min functions, gives us an expression for the row lengths of the minimum diagram:

$$
\check{\lambda}^{(\mathrm{AB})}(\lambda^{(\mathrm{A})}, \lambda^{(\mathrm{B})}) \quad = \quad \begin{cases} (X, Y) & \text{if } Y > 0 \text{ and } X > Y \\ (Y, X) & \text{if } X > 0 \text{ and } X \leq Y \\ (Y - X, -X) & \text{if } X \leq 0 \text{ and } Y > 0 \\ (X - Y, -Y) & \text{if } X > 0 \text{ and } Y \leq 0 \\ (-Y, X - Y) & \text{if } X \leq 0 \text{ and } X > Y \\ (-X, Y - X) & \text{if } Y \leq 0 \text{ and } X \leq Y, \end{cases}
\tag{6.12}
$$

where, we define $X = \lambda_1^{(\mathrm{A})} - \lambda_2^{(\mathrm{A})} - \lambda_2^{(\mathrm{B})}$ and $Y = \lambda_1^{(\mathrm{B})} - \lambda_2^{(\mathrm{B})} - \lambda_2^{(\mathrm{A})}$. Take note that all the conditions in Eq. (6.12) can be interpreted as the requirement that the corresponding row lengths should describe a valid integer partition, i.e.: $\check{\lambda}_1^{(\mathrm{AB})} \geq \check{\lambda}_2^{(\mathrm{AB})} \geq 0$. For any choice of $\lambda^{(\mathrm{A})}$ and $\lambda^{(\mathrm{B})}$, either only a single case describes a valid diagram, or all cases that describe a valid diagram are equal.

6.4 The ground-state-phases

In this section, using the results of Section 6.3, we determine the different ground state phases of our model; there are five of these in total. The model becomes gapless in two phases and at the phase-boundaries, while it remains gapped within the other phases. Interestingly, in one of the gapped phases the bipartite sub-lattice symmetry is broken in a strong sense: namely, for the ground state subspace the irreps λ_{A} and λ_B corresponding to the two subsystems are non-identical. We are

mainly concerned with the thermodynamic limit, however, some of our results also apply to finite system sizes.

In Section 6.3, we diagonalized the CBE Hamiltonian and determined the optimal product irrep $\lambda^{*(\mathrm{AB})}(\lambda_\mathrm{A}, \lambda_B, \theta)$. Thus, the identification of the ground state subspace simplifies to finding the irreps λ_A and λ_B for which the triple $(\lambda_\mathrm{A}, \lambda_\mathrm{B}, \lambda^{*(\mathrm{AB})}(\lambda_\mathrm{A}, \lambda_\mathrm{B}, \theta))$ has minimal energy. When λ_A and λ_B are fixed, $\lambda^{*(\mathrm{AB})}$ depends only on the sign of the prefactor of the Casimir operators C_A, C_B, and C_AB, i.e., on the sign of $\sin(\theta)$ and $\cos(\theta)$. Hence, it is useful to investigate the ground state separately in the four quarters of the domain of our angle parameter θ; we number these quarters clockwise, starting with $0 \leq \theta \leq \pi/2$, as seen in Fig. 6.2.

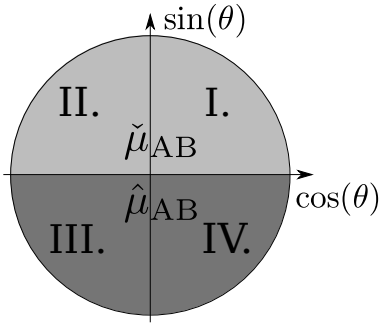

FIGURE 6.2: The numbering of the quarters of the parameter region with the corresponding choice of the irrep $\lambda^{*(\mathrm{AB})}$.

It will sometimes be practical to switch from the standard parameters of SU(3) irreps to a different set that we can treat as continuous variables in the thermodynamic limit, $N \to \infty$:

$$\lambda_1 = \frac{Nv}{2}(1+x), \quad \lambda_2 = \frac{Nv}{2}(1-x). \tag{6.13}$$

Here, Nv describes the number of boxes in the diagram and x expresses how the boxes are divided up between the two rows, it is defined in such a way that $\lambda_1 \geq \lambda_2$ is automatically enforced. Ideally we would like these pseudo-continuous variables to vary between 0 and 1, but the circumstances add some extra restrictions. Taking the irrep decomposition of the composite Hilbert space into account, v takes values between $(N \bmod 3)/N$ and 1 in steps of $3/N$. In the case of x, we have to consider that the two rows cannot be equal sized when the number of boxes is odd. Therefore, for every fixed value of v, x takes values between $(Nv \bmod 2)/(Nv)$ and 1 in steps of $2/Nv$.

By substituting Eq. (6.13) into the eigenvalue of the quadratic SU(3) Casimir operator, Eq. (3.58), one can see that the eigenvalue corresponding to (λ_1, λ_2) only contains terms that are either quadratic or linear in N. In the thermodynamic

limit it is sufficient to consider only the contributions of the quadratic part, given by

$$c_{qu}(\lambda_1, \lambda_2) = \frac{2}{3}(\lambda_1^2 + \lambda_2^2 - \lambda_1\lambda_2). \tag{6.14}$$

As an unexpected coincidence, for the minimum product diagram, $\check{\lambda}^{(\mathrm{AB})}(\lambda^{(\mathrm{A})}, \lambda^{(\mathrm{B})})$, the value of this quadratic part of the Casimir eigenvalue is described by the same formula in all 6 cases of Eq. (6.12).

$$\begin{aligned} &c_{qu}(\check{\lambda}_1^{(\mathrm{AB})}, \check{\lambda}_2^{(\mathrm{AB})}) = \\ &\quad c_{qu}(\lambda_1^{(\mathrm{A})}, \lambda_2^{(\mathrm{A})}) + c_{qu}(\lambda_1^{(\mathrm{B})}, \lambda_2^{(\mathrm{B})}) - (\lambda_1^{(\mathrm{A})}\lambda_1^{(\mathrm{B})} + \lambda_2^{(\mathrm{A})}\lambda_1^{(\mathrm{B})} + \lambda_1^{(\mathrm{A})}\lambda_2^{(\mathrm{B})} - 2\lambda_2^{(\mathrm{A})}\lambda_2^{(\mathrm{B})}). \end{aligned} \tag{6.15}$$

This greatly reduces the effort required to map out the phases of the ground state.

6.4.1 First quarter $(0 < \theta < \pi/2)$

We start with the regions where there is no competition between the two types of interactions (the terms with C_{AB} and $C_{\mathrm{A/B}}$) and thus, determining the ground state is the easiest. This means the parameter regions where the signs of the sine and cosine prefactors in the CBE Hamiltonian (6.4), are the same, i.e., the first quarter and third quarters. We begin with the former.

In this region of the parameter space, the eigenvalues of all the Casimir operators have to be minimized. From Eq. (3.58) one can immediately see that this is done by the singlet representation on all subspaces, $(\lambda_1^{(\mathrm{A})}, \lambda_2^{(\mathrm{A})}) = (\lambda_1^{(\mathrm{B})}, \lambda_2^{(\mathrm{B})}) = (\lambda_1^{(\mathrm{AB})}, \lambda_2^{(\mathrm{AB})}) = (0, 0)$, whenever it is available. The $\lambda \vdash_3 N$ partition equivalent to the SU(3) singlet is $(N/3, N/3, N/3)$ which appears in the decomposition of the Hilbert spaces $\mathcal{H}^{(\mathrm{A})}$ and $\mathcal{H}^{(\mathrm{B})}$ only when N is divisible by 3. In the other cases, i.e., when $N \bmod 3 \neq 0$, the ground state is labeled by the smallest available values of the λ_1 and λ_2 quantum numbers. These depend only on the value of N mod 3 and otherwise do not scale with N. The difference between the energy of these states and that of the singlet is also of order $O(1)$; therefore when later we give results about the thermodynamic limit, we will only consider the $N \bmod 3 = 0$ case.

$N \bmod 3$	$(\lambda_1^{(\mathrm{A})}, \lambda_2^{(\mathrm{A})})$	$(\lambda_1^{(\mathrm{B})}, \lambda_2^{(\mathrm{B})})$	$(\lambda_1^{(\mathrm{AB})}, \lambda_2^{(\mathrm{AB})})$
0	$(0, 0)$	$(0, 0)$	$(0, 0)$
1	$(1, 0)$	$(1, 0)$	$(1, 1)$
2	$(1, 1)$	$(1, 1)$	$(1, 0)$

TABLE 6.1: The ground state for $(0 < \theta < \pi/2)$

The ground state of an antiferromagnetic Heisenberg model is a global singlet both on a complete graph connection layout and, according to Marshall's theorem [8, 9], on a bipartite lattice with equal sized sublattices. The ground state we have here also falls in line with this behavior.

6.4.2 Third quarter $(\pi < \theta < 3\pi/2)$

The other region in the parameter space with no competition between the two types of interactions is the third quarter, i.e., $0 < \theta < \pi/2$. Here, we need to maximize the eigenvalues of all the Casimir operators. Consider the decomposition of the Hilbert space of the entire system into SU(3) irreps. With no regard to the restrictions coming from fixing the irreps on the A and B subsytems, the irrep that maximizes the eigenvalue of C_{AB} is $(\lambda_1^{(\mathrm{AB})}, \lambda_2^{(\mathrm{AB})}) = (2N, 0)$. The irreps that maximize the eigenvalues of C_{A} and C_{B} are $(\lambda_1^{(\mathrm{A})}, \lambda_2^{(\mathrm{A})}) = (\lambda_1^{(\mathrm{B})}, \lambda_2^{(\mathrm{B})}) = (N, 0)$. These representations are compatible with each other. From Eq. (6.9) one can see that $\hat{\lambda}^{(\mathrm{AB})}((N,0),(N,0)) = (2N,0)$; therefore, the ground states of the CBE Hamiltonian in this quarter of the parameter space belong to the subspace labeled by the triple $(\lambda^{(A)}, \lambda^{(B)}, \lambda^{(AB)}) = ((N,0),(N,0),(2N,0))$. Chapter 3 on the Schur-Weyl duality gives us a straightforward interpretation of these numbers: the ground state subspace is the symmetric part of the Hilbert space, spanned by vectors that are invariant to all permutations of sites. Since in this quarter both types of interactions are ferromagnetic, we expect the ground state to be similar to the ferromagnetic ground state of $SU(2)$ Heisenberg models. This matches both the interpretation from the Schur-Weyl duality and the maximal eigenvalues of the Casimir operators.

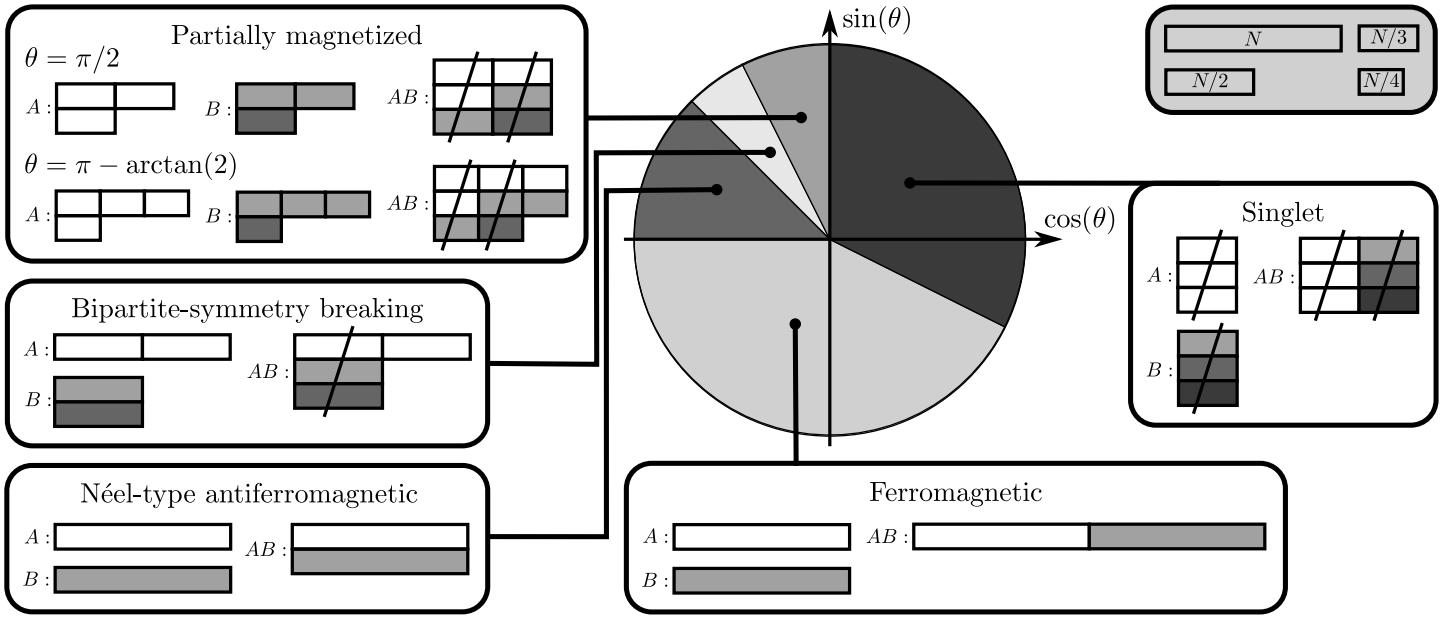

FIGURE 6.3: The ground state phase diagram of the CBE Hamiltonian. Each ground state subspace is labeled by three SU(3) Young diagrams corresponding to the two subsystems and the entire system. The different lengths of the rectangular blocks in the Young diagrams represent the number of boxes in the rows as shown in the legend in the top right corner. In order to display how the Littlewood-Richardson rules apply to the product diagram on the entire system (AB), we have colored the rows of the diagrams of the B subsystem and added a third line indicating SU(3)singlets in the system. With this third line, the number of boxes in each diagram is equal to the number of sites in the corresponding (sub-) system. In order to recover the standard two-row SU(3) diagrams, one needs to remove all the columns with three boxes. This is indicated by these columns being crossed out. The diagram with all boxes crossed out corresponds to the label $(0, 0)$, i.e., the singlet representation. Starting from $\theta = 0$ and going clockwise we have the singlet phase ($-\arctan((1 + 3/N)/(2 + 3/N)) \leq \theta \leq \pi/2$), the ferromagnetic phase ($\pi \leq \theta \leq 2\pi - \arctan((1+3/N)/(2+3/N))$), the Néel-type antiferromagnetic phase ($3\pi/4 \leq \theta \leq \pi$), the bipartite-symmetry breaking phase ($\pi - \arctan(2(N+2)/(N+6)) \leq \theta \leq 3\pi/4$), and the partially magnetized critical phase ($\pi/2 \leq \theta \leq \pi - \arctan(2(N+2)/(N+6))$). The ground state in the partially magnetized phase shifts many times with the value of θ, in the diagram we only displayed the ground states at the two ends of the region (in the thermodynamic limit).

6.4.3 Fourth quarter $(3\pi/2 < \theta < 2\pi)$

In this region of the parameter space, the two interactions in the CBE Hamiltonian (6.4) are competing with each other. The eigenvalues of the Casimir operators of the A and B subsystems needs to be minimized, while the Casimir for the entire Hilbert space needs to be maximized. According to Eq. (6.9), this latter means that $\lambda^{*(\mathrm{AB})} = (\lambda_1^{(\mathrm{A})}+\lambda_1^{(\mathrm{B})}, \lambda_2^{(\mathrm{A})}+\lambda_2^{(\mathrm{B})})$. Using the new variables defined in Eq. (6.13) for the energy of the CBE Hamiltonian, we obtain

$$E = (\cos(\theta) + \sin(\theta))\left(c_{qu}(v_\mathrm{A}, x_\mathrm{A}) + c_{qu}(v_\mathrm{B}, x_\mathrm{B})\right) + \sin(\theta)N^2 v_\mathrm{A} v_\mathrm{B}\left(\frac{1}{3} + x_\mathrm{A}x_\mathrm{B}\right). \quad (6.16)$$

From this, one can see that the solution simplifies when the coefficients of both terms are negative, i.e., in the region $3\pi/2 < \theta < 7\pi/4$. Here, the absolute value of both terms needs to be maximized, and the irreps that maximizes both is labeled by $x_\mathrm{A} = x_\mathrm{B} = 1$ and $v_\mathrm{A} = v_\mathrm{B} = 1$. In other words, the previously discussed ground state of the quarter $\pi < \theta < 3\pi/2$ extends into this region.

This brings up two other questions: Could this symmetric ground state extend any further, and is it possible that the singlet ground state of the first quarter extends similarly into this parameter region? This last case could be feasible for values of θ for which the interaction $C_\mathrm{A} + C_\mathrm{B}$ dominates the term C_AB. Since the energy of the singlet is 0, it can be the ground state only when the energies of all other irrep combinations are positive. The inequality $E(v_\mathrm{A}, x_\mathrm{A}, v_\mathrm{B}, x_\mathrm{B}) \geq 0$ yields a condition for θ that has to apply to all possible values of $v_\mathrm{A}, x_\mathrm{A}, v_\mathrm{B}$ and x_B:

$$-\mathrm{ctg}(\theta) \geq 1 + \frac{2 + 6x_\mathrm{A}x_\mathrm{B}}{\frac{v_\mathrm{A}}{v_\mathrm{B}}(1+3x_\mathrm{A}^2) + \frac{v_\mathrm{B}}{v_\mathrm{A}}(1+3x_\mathrm{B}^2)}. \quad (6.17)$$

In order to extract the critical value of parameter θ, two observations should be made: First, when $v_\mathrm{A} = v_\mathrm{B}$, and $x_\mathrm{A} = x_\mathrm{B}$, the right-hand-side of (6.17) is equal to 2; and second, by utilizing $xa + b/x \geq 2\sqrt{ba}$ and the inequality between the arithmetic and geometric means, one obtains that the right-hand side of (6.17) always has to be less or equal to 2. Thus, the singlet subspace is the ground state subspace in this region iff $-\mathrm{ctg}(\theta) \geq 2$, which means that it extends from $\theta = 2\pi$ until $\theta = 2\pi - \arctan(1/2)$.

Next, we check whether the symmetric ground state extends any further. The inequality $E(1,1,1,1) \leq E(v_\mathrm{A}, x_\mathrm{A}, v_\mathrm{B}, x_\mathrm{B})$ provides the following condition for θ:

$$-\mathrm{ctg}(\theta) \leq 1 + \frac{2v_\mathrm{A}v_\mathrm{B}(1+3x_\mathrm{A}x_\mathrm{B}) - 8}{v_\mathrm{A}^2(1+3x_\mathrm{A}^2) + v_\mathrm{B}^2(1+3x_\mathrm{B}^2) - 8}. \quad (6.18)$$

We follow a reasoning analogous to the one after Eq. (6.17). Using the relation between the geometric and arithmetic means, it is easy to see that 2 is a strict lower bound of the right-hand side of Eq. (6.18). Moreover, the right-hand side reaches this lower bound iff $x_{\mathrm{A}} = x_{\mathrm{B}}$ and $v_{\mathrm{A}} = v_{\mathrm{B}}$. We conclude that the symmetric ground state extends until $\theta = 2\pi - \arctan(1/2)$ and therefore, there is a direct transition between the symmetric and the singlet ground states at this parameter value.

6.4.4 Second quarter $(\pi/2 < \theta < \pi)$

In the remaining quarter of the parameter space, $\pi/2 < \theta < \pi$, the two types of interactions are again competing. This time, the coefficient of C_{AB} in the CBE Hamiltonian (6.4) is positive, therefore, we use the irrep corresponding to the minimal eigenvalue of C_{AB}, $\lambda^{*(\mathrm{AB})} = \check{\lambda}^{(\mathrm{AB})}$, and substitute Eq. (6.15) into the energy,

$$E = (\cos(\theta) + \sin(\theta))\left(c_{qu}(v_{\mathrm{A}}, x_{\mathrm{A}}) + c_{qu}(v_{\mathrm{B}}, x_{\mathrm{B}})\right) - \sin(\theta)\frac{N^2}{6} v_1 v_2 \left(1 + 3x_1 + 3x_2 - 3x_1 x_2\right). \quad (6.19)$$

It is clear that when the coefficients of both terms are negative, that is, when $3\pi/4 < \theta < \pi$, the irreps on the A and B subspaces which minimize this expression are labeled by $v_{\mathrm{A}} = v_{\mathrm{B}} = x_{\mathrm{A}} = x_{\mathrm{B}} = 1$. However, this ground state subspace is not an extension of that of the quarter $\pi < \theta < 3\pi/2$, even though the x and v parameters are identical. This is due to the difference in $\lambda^{*(\mathrm{AB})}$. In the present case, we have to choose the SU(3) irrep in the product $(N, 0) \otimes (N, 0)$ that corresponds to the minimal eigenvalue of the C_{AB} Casimir operator, which according to Eq. (6.12) is $\lambda^{(\mathrm{AB})} = (0, N)$. This ground state is similar to a Néel-type antiferromagnetic order in the sense that the two sublattices of a bipartite lattice are ferromagnetically aligned, but the value of the quadratic Casimir operator on the entire lattice, is minimized. Another detail that complements this correspondence with the Néel order is that the parameter region where this ground state appears coincides with the part where the intra-subsystem interaction J_1 is ferromagnetic, while the inter-subsystem one J_2 is antiferromagnetic. With SU(2) spins, a regular Néel ordered ground state would appear under these same circumstances.

In the remaining part of the domain of θ, i.e., $\pi/2 < \theta < 3\pi/4$, finding the ground state becomes somewhat more complicated. Unlike the previous cases, we cannot immediately tell the value of the v_{A} and v_{B} variables in the ground state. Instead, we have to find the minima of a polynomial of four variables on the convex

set describing the domain of these variables. Using a scaling argument, we can reduce the number of variables to three. First, we remark that for a suitably large value of N the ground state energy of the CBE Hamiltonian is guaranteed to be negative in the parameter region we are currently investigating. Indeed, in the case of $N \bmod 3 = 0$, there exists at least one combination of irreps for which the energy is negative, we select a pair of conjugate representations, (λ_1, λ_2) and $(\lambda_1, \lambda_1 - \lambda_2)$ on the A and B subspaces. The product of these contains the SU(3) singlet $(0,0)$, thus the contribution of the term proportional to C_{AB} to the energy is 0 [2]. Second, we use the fact that the ground state energy is negative to get rid of one variable in the optimization problem. Assume that in the ground state $v_{\mathrm{A}} \leq v_{\mathrm{B}}$. Since $c_{qu}(v_{\mathrm{A}}, x_{\mathrm{A}})$ contains only terms proportional to N^2, the ground state energy given by Eq. (6.19) scales quadratically when we scale both v_{A} and v_{B} by the same constant, hence,

$$E(\frac{v_{\mathrm{A}}}{v_{\mathrm{B}}}, x_{\mathrm{A}}, 1, x_{\mathrm{B}}) = \frac{1}{v_{\mathrm{B}}^2} E(v_{\mathrm{A}}, x_{\mathrm{A}}, v_{\mathrm{B}}, x_{\mathrm{B}}) \leq E(v_{\mathrm{A}}, x_{\mathrm{A}}, v_{\mathrm{B}}, x_{\mathrm{B}}), \tag{6.20}$$

where the last inequality holds as E is negative and $v_{\mathrm{B}}^2 \leq 1$. It follows that when searching for the ground state we can set v_{B} to 1. In the following we determine the minimum of the polynomial $E(v_{\mathrm{A}}, x_{\mathrm{A}}, 1, x_{\mathrm{B}})$ inside the domain of the remaining three variables. This minimum has different qualities depending on the value of θ.

In the region $\pi/2 < \theta < \pi - \arctan 2$ the minimum inside the domain of the variables is a local minimum of the polynomial $E(v_{\mathrm{A}}, x_{\mathrm{A}}, 1, x_{\mathrm{B}})$. At this local minimum $v_{\mathrm{A}} = v_{\mathrm{B}} = 1$, and $x_{\mathrm{A}} = x_{\mathrm{B}} = x(\theta)$, a smooth function of θ. Up to this stage of the calculation, we could handle x_{A} and x_{B} as continuous variables. Yet, when extracting the discrete (p, q) values labeling the ground state, we need to take into account that in the case of $v_{\mathrm{A}} = v_{\mathrm{B}} = 1$ they can only take the values $((N \bmod 2) + 2i)/N$, with i being an integer between 0 and $N/2$; That is, among the two proper values neighboring $x(\theta)$, the ground state is the one with the lower energy. Since the energy Eq. (6.19) as a function of $x_{\mathrm{A}} = x_{\mathrm{B}} = x$ is a parabola, we can simply round $x(\theta)$ to its closest integer value. After doing this and using Eq. (6.15) to determine the corresponding irrep, $(\lambda^{(\mathrm{AB})}, \lambda^{(\mathrm{AB})})$, on the

[2] In the cases when $N \bmod 3 \neq 0$, we can always choose a pair of irreps that are almost conjugates of each other and for which the term proportional to $C_{\mathrm{A}} + C_{\mathrm{B}}$ has an energy contribution of $O(N^2)$. In the irreducible decomposition of the direct product of these two irreps, the irrep with the lowest C_{AB} eigenvalue is either $(1,1)$ or $(1,0)$, both of which have an energy contribution of $O(1)$. Thus, we can again conclude that the ground state energy has to be negative.

entire Hilbert space, we arrive at the irreps labeling the ground state [3]:

$$\begin{aligned}
\lambda_1^{(\mathrm{A})} =& \lambda_1^{(\mathrm{B})} = \frac{N}{2} + \left\lceil \frac{1}{2}\left(\frac{N}{3+2\mathrm{ctg}(\theta)}\right)\right\rfloor, \\
\lambda_2^{(\mathrm{A})} =& \lambda_2^{(\mathrm{B})} = \frac{N}{2} - \left\lceil \frac{1}{2}\left(\frac{N}{3+2\mathrm{ctg}(\theta)}\right)\right\rfloor, \\
\lambda_1^{(\mathrm{AB})} =& 3\left\lceil \frac{1}{2}\left(\frac{N}{3+2\mathrm{ctg}(\theta)}\right)\right\rfloor - \frac{N}{2}, \\
\lambda_2^{(\mathrm{AB})} =& 3\left\lceil \frac{1}{2}\left(\frac{N}{3+2\mathrm{ctg}(\theta)}\right)\right\rfloor - \frac{N}{2},
\end{aligned} \tag{6.21}$$

where $\lceil x \rfloor$ denotes the closest integer value of x.

In the region $\pi - \arctan 2 < \theta < 3\pi/4$, the polynomial $E(v_\mathrm{A}, x_\mathrm{A}, 1, x_\mathrm{B})$ has no local minimum inside the domain of its variables, therefore, the minimum has to be on the border of the domain. In fact there are two minima occupying two different extremal points of the domain, they are located at $(v_\mathrm{A}, x_\mathrm{A}, v_\mathrm{B}, x_\mathrm{B}) = (1, 1, 1, 0)$ and $(v_\mathrm{A}, x_\mathrm{A}, v_\mathrm{B}, x_\mathrm{B}) = (1, 0, 1, 1)$. The most peculiar quality of the ground states associated with these minima is that unlike all previously discussed ground states, they break the bipartite symmetry of the CBE Hamiltonian. This also explains why these ground states come as a pair, when the A and B subsystems are swapped the two minima are transformed into each other. After taking into account the discrete nature of our variables and rounding the location of the minima appropriately, then extracting $\lambda_1^{(\mathrm{AB})}$ and $\lambda_2^{(\mathrm{AB})}$ from Eq. (6.15), we arrive at the two sets of SU(3) irreps labeling the ground state. The first one is $(\lambda_1^{(\mathrm{A})}, \lambda_2^{(\mathrm{A})}) = (N, 0)$, $(\lambda_1^{(\mathrm{B})}, \lambda_2^{(\mathrm{B})}) = (\lceil N/2 \rceil, \lfloor N/2 \rfloor)$, $(\lambda_1^{(\mathrm{AB})}, \lambda_2^{(\mathrm{AB})}) = (\lceil N/2 \rceil, N \bmod 2)$, and the second one is obtained from the former by swapping the A and B subsystems.

6.4.5 Special parameter values

For generic values of the parameter θ, the ground state subspace of the CBE Hamiltonian (6.4) belongs to a fixed set of quantum numbers, i.e., irrep labels $(\lambda^{(\mathrm{A})}, \lambda^{(\mathrm{B})}, \lambda^{(\mathrm{AB})})$. However, at the borders of the different phases, the ground state subspace becomes more degenerate incorporating states with different irrep labels, or in other words, multiple sets of quantum numbers become degenerate in energy. For example, at the borders of the phases at least two sets of labels correspond to

[3] For simplicity, we gave here the result for the case when N is even. For the case when N is odd, the ground state labels are given by almost the same equations, only the floor function has to be used instead of rounding the terms to the nearest integer in Eq. (6.21), furthermore one has to add the constant $1/2$ to $\lambda_1^{(\mathrm{A})}$ and $\lambda_1^{(\mathrm{B})}$, $-1/2$ to $\lambda_2^{(\mathrm{A})}$ and $\lambda_2^{(\mathrm{B})}$, and $3/2$ to $\lambda_2^{(\mathrm{AB})}$.

the ground state energy, but further degeneracies are also possible depending on the form the energy takes at the given parameter. If this happens we have to keep in mind that when determining the ground state energies, we have neglected the parts of the Casimir operators eigenvalue, Eq. (3.58), that are only linear in N. So far this has been acceptable because we were only interested in the thermodynamic limit, and the other terms scale with $O(N^2)$. However, at the values of θ where the quantum numbers describing the ground state subspace become degenerate, there is a possibility that the linear terms break the degeneracy. We should also note that at the parameter values $\theta = 0, \pi/2, \pi, 3\pi/2$ either the $\lambda^{(AB)}$ or the $\lambda^{(A)}$ and $\lambda^{(B)}$ ceases being a relevant quantum number which could also lead to degeneracies; two of these values ($\theta = \pi/2, \pi$) are also phase boundaries, but the other two should be considered separately. In this subsection, we check each of these special parameter values.

Let us start with the two special points that are not at a phase boundary, i.e., $\theta = 0$ and $\theta = 3\pi/2$. At $\theta = 0$, the irreps $\lambda^{(\mathrm{A})}$ and $\lambda^{(\mathrm{B})}$ labeling the ground state are the same as those inside the singlet phase, listed in Table 6.1. However, since at this point the CBE Hamiltonian is governed solely by the interaction within the A and B subsystems, $\lambda^{(\mathrm{AB})}$ stops being a relevant quantum number and the ground state subspace extends to the entire $\lambda^{(\mathrm{A})} \otimes \lambda^{(\mathrm{B})}$ subspace. In practice, this means that there is no additional degeneracy when $N \bmod 3 = 0$, but in the other two cases the ground state subspace is slightly enlarged. The situation at $\theta = 3\pi/2$ is in some sense the dual to the previous case, as the CBE Hamiltonian takes the form $H = -C_{\mathrm{AB}}$, and the only relevant label is $\lambda^{(\mathrm{AB})}$. However, since the irrep $\lambda^{(\mathrm{AB})} = (2N, 0)$ is compatible only with the irreps $\lambda^{(\mathrm{A})} = \lambda^{(\mathrm{B})} = (N, 0)$ on the subsystems, there is no additional degeneracy of the ground state.

The parameter value $\theta = \pi/2$ is at the boundary of the singlet and the partially magnetized phases. Here, the CBE Hamiltonian takes the form $H = C_{\mathrm{AB}}$, thus, $\lambda^{(\mathrm{A})}$ and $\lambda^{(\mathrm{B})}$ are not relevant labels of the energy eigenstates. The irrep $\lambda^{(\mathrm{AB})}$ corresponding to the ground state is the one appearing in Table 6.1, and the ground state is extended to the entire $\lambda^{(\mathrm{AB})}$ subspace. Compared to the case at $\theta = 0$, the degeneracy here is a lot more extensive.

At the boundary point of the ferromagnetic and Néel-type antiferromagnetic phase, $\theta = \pi$, the CBE Hamiltonian takes the form $H = -(C_{\mathrm{A}} + C_{\mathrm{B}})$. Here, since only $\lambda^{(\mathrm{A})}$ and $\lambda^{(\mathrm{B})}$ are relevant labels, the ground state subspace is enlarged to the entire $(N, 0) \otimes (N, 0)$ subspace.

At the point $\theta = 2\pi - \arctan(1/2)$, where the singlet and the ferromagnetic phases meet, the expression of the energy in the fourth quarter, shown in Eq. (6.16)

takes the form:

$$E = \frac{\sqrt{5}}{30} N^2 \left[(v_\mathrm{A} - v_\mathrm{B})^2 + 3(v_\mathrm{A} x_\mathrm{A} - v_\mathrm{B} x_\mathrm{B})^2 \right]. \tag{6.22}$$

At this point, the ground state subspace encompasses all irreducible subspaces for which the two subsystems are symmetric to exchange and the energy contribution of C_AB is maximized. In other words, $(\lambda_1^{(\mathrm{A})}, \lambda_2^{(\mathrm{A})}) = (\lambda_1^{(\mathrm{B})}, \lambda_2^{(\mathrm{B})}) = (\lambda_1, \lambda_2)$ and $(\lambda_1^{(\mathrm{AB})}, \lambda_2^{(\mathrm{AB})}) = (2\lambda_1, 2\lambda_2)$. In this situation however, we must take into account the previously omitted parts of the energy that are linear in N, since these might break the degeneracy. By checking the energy contributions of these linear terms one can make two important conclusions. First, the value of the parameter θ where the shift between the two types of ground state occurs receives a correction for finite values of N, $\theta = 2\pi - \arctan((1+3/N)/(2+3/N))$. Second, the degeneracy is broken, and the ground state subspace consists only of the two types of ground states neighboring the critical point: the singlet subspace and the symmetric subspace.

The Néel-type antiferromagnetic and the bipartite symmetry breaking phases border at $\theta = 3\pi/4$, here the CBE Hamiltonian is proportional to $C_\mathrm{AB} - C_\mathrm{A} - C_\mathrm{B}$. At this point, the J_1 coupling constant of the interactions within the subsystems vanishes, and the connection layout of the spins becomes bipartite in the strong sense. The subspace where the ground state energy, Eq. (6.19), is minimal is larger than the span of the ground state subspaces of the two adjacent phases. It encompasses all subspaces with labels of the form $(\lambda_1^{(\mathrm{A})}, \lambda_2^{(\mathrm{A})}) = (N, 0)$, $(\lambda_1^{(\mathrm{B})}, \lambda_2^{(\mathrm{B})}) = (N/2(1+x), N/2(1-x))$ $(\lambda_1^{(\mathrm{AB})}, \lambda_2^{(\mathrm{AB})}) = (N/2(1+x), Nx)$ with $x \in [0,1]$, and those one gets form the former set by swapping the A and B subsystems. The energy contribution of the $O(N)$ parts of the Casimir operators is constant in the entire ground state subspace, therefore this degeneracy remains. A peculiarity one should take note of here is that the SU(3) singlet subspace has no intersection with this ground state subspace, which demonstrates how Marshall's theorem doesn't apply to antiferromagnetic bipartite SU(3) systems in general.

The border of the bipartite symmetry breaking and the partially magnetized phases is at $\theta = \pi - \arctan 2$. At this point, according to the part of the energy that scales quadratically with N, the ground state subspace is the span of a number of irreducible subspaces which break the bipartite symmetry. The labels for these take the form $(\lambda_1^{(\mathrm{A})}, \lambda_2^{(\mathrm{A})}) = (N/2(1+x), N/2(1-x))$, $(\lambda_1^{(\mathrm{B})}, \lambda_2^{(\mathrm{B})}) = (N(1-x/2), Nx/2)$ and $(\lambda_1^{(\mathrm{AB})}, \lambda_2^{(\mathrm{AB})}) = (N/2(1/2+|1/2-x|), N/2(1/2-|1/2-x|))$, with $x \in [0,1]$. However, the energy contribution of the linear terms breaks this degeneracy and, away from the thermodynamic limit, adjusts the critical parameter value where

the ground state phases change by a correction of magnitude $O(1/N)$. The new value is $\theta = \pi - \arctan(2(N+2)/(N+6))$ and the ground state subspace is the span of the ground state subspaces of the two adjacent phases.

6.4.6 Energy gaps

From a many-body point of view, it is important to know whether the different quantum phases of our model are gapped or gapless in the thermodynamic limit. As a consequence of the infinite range interaction, the eigenvalues of the CBE Hamiltonian, Eq. (6.4), are not extensive quantities. In order to make the energy extensive and meaningfully define a gap, we normalize the Hamiltonian by a factor of $1/N$, which is a usual procedure in models on complete graphs [141].

Let us now investigate the energy gaps taking this normalization factor into account. In the singlet phase, corresponding to the region $-\arctan((1+3/N)/(2+3/N)) \leq \theta \leq \pi/2$, the Casimir eigenvalues of both the ground state subspace, and the states with the second lowest energy, are constant in N; (Apart from the mod 3 oscillations.) therefore, the normalized CBE Hamiltonian in this phase is gapless.

The three different phases in the parameter region $\pi - \arctan(2(N+2)/(N+6)) \leq \theta \leq 2\pi - \arctan((1+3/N)/(2+3/N))$ have the unifying feature that the Casimir eigenvalues of the ground state subspace and the second lowest energy states (which we can obtain from the ground state by a small constant modification of the appropriate quantum numbers) are of order $O(N^2)$, and their difference is of order $O(N)$. Taking the normalization into account, we obtain that these phases are gapped.

Finally, in the parameter region $\pi/2 \leq \theta \leq \pi - \arctan(2(N+2)/(N+6))$, the quantum numbers describing the ground state change many times. The behavior of the gap in this phase is shown in Fig. 6.4. According to Eq. (6.21), there is a ground state level crossing at each θ where the number $N/(6+4\mathrm{ctg}(\theta))$ is half-integer. The state with the second lowest energy is always given by rounding the number $N/(6+4\mathrm{ctg}(\theta))$ in Eq. (6.21) to the next closest integer. The density of these level crossings increases linearly with N. Additionally, the local maximums of the gap between the level crossings are enveloped by a smooth function which gives us an upper bound for the value of the gap Δ:

$$\Delta \leq \frac{1}{N}\left(4\cos(\theta) + 6\sin(\theta)\right). \tag{6.23}$$

Therefore, the continuous phase is gapless in the thermodynamic limit.

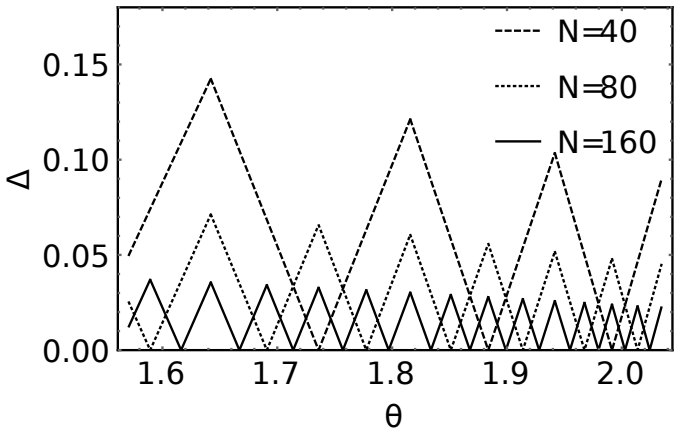

FIGURE 6.4: The normalized energy gap Δ in the parameter region $\pi/2 \leq \theta \leq \pi - \arctan(2)$ for different system sizes.

6.5 Summary and outlook

Studying spin systems on complete graphs has a long history in many-body physics. Such models have been considered in the past mainly as infinite-dimensional mean-field versions of their finite-dimensional lattice counter-parts, examples include the Curie-Weiss-model [141] and the Sherrington-Kirkpatrick version of spin-glass models [102]. With the advent of cold atomic systems, long-range interactions, including complete-graph interactions could also be realized in the lab [46]. In this chapter, we have considered a slight modification of this approach by studying a quantum spin model on a bipartite complete graph, which could be regarded as a mean-field approach that captures also the effects that stems from the bipartition of a lattice. Moreover, such a bipartite model might also be realized using experimental techniques with ultracold atoms and cavity electrodynamics.

We have identified five quantum phases of this model, as shown in Fig. 6.3. There are two gapless phases, the antiferromagnetic singlet phase and the partially magnetized critical phase; and three gapped phases, the ferromagnetic phase, the Néel-type of antiferromagnetic phase with ferromagnetically aligned subsystems, and a bipartite-symmetry-breaking phase. Concerning this last phase, it is interesting to note, that already such a simple bipartite long-range model provides a phase that is absent in the literature on short-ranged bipartite models. In this phase, although the two subsystems transform under the same representation of SU(3), the ground state of this phase restricted to the subsystems belongs to different representations. Our results for the partially magnetized, and bipartite symmetry breaking phases only apply in the thermodynamic limit, however, the rest is also relevant for finite system sizes.

There are a number of ways how one can extend the present study. A straightforward modification would be to consider subsystems with different sizes, in particular, one could study the limiting case of a central spin (or spin-star) model, where one subsystem is simply a single spin-1 particle. The topology of the couplings could also be changed more drastically, for example by extending the bipartite system discussed here into a multipartite mean-field model by considering k subsystems with collective spin-spin interactions within and across the subsystems. Furthermore, one could also relax the complete connectivity, and study similar models with decaying long-range interactions. Symmetric collective spin states have been studied, due to their experimental feasibility, also from a quantum metrology point of view [135, 142], it would be interesting to study also bipartite models especially in the light of the experiment reported in [143]. A further direction would be to investigate not only static properties, but time-evolutions, e.g., different quench protocols. Such quench studies would also be of great interest if one would be able to experimentally realize such collective models, as discussed earlier, and then observe the quench dynamics in the lab.

Chapter 7

The shareability of Werner and isotropic states

7.1 Introduction

In this chapter, we undertake the problem of shareability for Werner and isotropic states, as it was outlined in Chapter 4. Our goal is to obtain the lowest parameter value, $\alpha_{n_{\mathrm{L}},n_{\mathrm{R}}}$, that corresponds to an n_{L}-n_{R} shareable Werner state in the parametrization Eq. (4.12), and the highest parameter value, $\beta_{n_{\mathrm{L}},n_{\mathrm{R}}}$, that corresponds to an n_{L}-n_{R} shareable isotropic state in the parametrization Eq. (4.19). The results we present are an extension of the partial results of Johnson and Viola, who in their work [78], identified these parameter values for the case of 1-n shareability as,

$$\alpha_{1,n} = -\frac{d-1}{n}, \qquad \beta_{1,n} = 1 + \frac{d-1}{n}. \tag{7.1}$$

We solve the general shareability problem for both families of states.

The reason why this topic is connected to the rest of the thesis is the bipartite permutation symmetry inherent to the structure of the shareability problem. For a valid sharing state, all bipartite reduced states between the two subsystems must be identical. The mixture of this bipartite permutation invariance, and the global unitary invariance of Werner states crates a structure of symmetries that generalizes that of the spin system we investigated in Chapter 6 to arbitrary dimensions. Indeed, as it will turn out, in order to obtain the shareability of Werner states, we need to solve an eigenproblem of a linear operator very similar to the CBE Hamiltonian in Eq. (6.4); thus we can apply the set of tools that we used in Chapter 6, generalized to higher dimensions. Our method can be adapted also for isotropic states with minor modifications.

This chapter is structured as follows: In Section 7.2, we map the shareability problem into an eigenproblem of a linear operator that we express with various representations of the quadratic Casimir operator of SU(d). In Section 7.3, we give

a solution to the combinatorial problem of finding the smallest (w.r.t. dominance order) Young diagram in the Littlewood-Richardson product of two arbitrary diagrams. This is the generalization of the problem that we solved in Section 6.3.3 for arbitrary dimensions, and it allows us to take the same approach for solving the eigenproblem that we used for the CBE Hamiltonian. Finally, in Sections 7.4 and 7.5, we give our solution of the shareability problem for Werner and isotropic states respectively.

7.2 Mapping the problem of shareability into an eigenproblem

As the first step, we show that the problem of finding the most entangled, n_{L}-n_{R} shareable Werner or isotropic state is equivalent to finding extremal eigenvalues of certain linear operators; for Werner states, we retrace the calculation in [78]. If a sharing state, $\hat{\rho}^{\mathrm{W}}(\alpha)$, for the Werner state $\rho^{\mathrm{W}}(\alpha)$ exists, there must also be a sharing state that is symmetric to both global unitary transformations and bipartite permutations from $S_{n_{\mathrm{L}}} \times S_{n_{\mathrm{R}}}$. As a matter of fact, the twirled state,

$$\sum_{\pi \in S_{n_{\mathrm{L}}} \times S_{n_{\mathrm{R}}}} \int_{\mathrm{U}(d)} \mathrm{d}U (U^{\dagger})^{\otimes (n_{\mathrm{L}}+n_{\mathrm{R}})} D^{(S_{n_{\mathrm{L}}+n_{\mathrm{R}}})}_{n_{\mathrm{L}}+n_{\mathrm{R}}}(\pi^{-1}) \hat{\rho}^{\mathrm{W}}(\alpha) D^{(S_{n_{\mathrm{L}}+n_{\mathrm{R}}})}_{n_{\mathrm{L}}+n_{\mathrm{R}}}(\pi) U^{\otimes (n_{\mathrm{L}}+n_{\mathrm{R}})}, \tag{7.2}$$

shares the same Werner state as $\hat{\rho}^{\mathrm{W}}(\alpha)$. Conversely, all states with such symmetries share some Werner state. We construct sharing states with these symmetries by using the flip operator that has a distinguished role in our parametrization of Werner states. Consider the operator,

$$H^{\mathrm{W}} = \frac{1}{n_{\mathrm{L}} n_{\mathrm{R}}} \sum_{i \in L, j \in R} F_{ij}. \tag{7.3}$$

Since F_{ij} is invariant to $U \otimes U$ transformations and H^{W} has bipartite permutation symmetry, the eigenprojectors of H^{W} n_{L}-n_{R} share Werner states. Moreover, for any state $\hat{\rho}^{\mathrm{W}}(\alpha)$ that n_{L}-n_{R} shares the Werner state $\rho^{\mathrm{W}}(\alpha)$,

$$\mathrm{Tr}\left(\hat{\rho}^{\mathrm{W}}(\alpha) H^{\mathrm{W}}\right) = \alpha. \tag{7.4}$$

Consequently, the smallest eigenvalue of H^{W} must be the parameter of the most entangled n_{L}-n_{R} shareable Werner state, $\alpha_{n_{\mathrm{L}},n_{\mathrm{R}}}$. Indeed, the existence of an n_{L}-n_{R} sharing state for some $\alpha < \min \mathrm{Spect}(H^{\mathrm{W}})$ would make Eq. (7.4) lead to a contradiction.

We can construct an operator analogous to H^{W} also for isotropic states. In this case, the entanglement of $\rho^{\mathrm{I}}(\beta)$ increases with the parameter β, and the partial transpose of the flip operator serves the same function as the flip operator does for Werner states. By the same argument we used for Werner states, the largest eigenvalue of

$$H^{\mathrm{I}} = \frac{1}{n_{\mathrm{L}} n_{\mathrm{R}}} \sum_{i \in L, j \in R} F_{ij}^{t_R}, \tag{7.5}$$

is the parameter of the most entangled n_{L}-n_{R} shareable isotropic state $\beta_{n_{\mathrm{L}}, n_{\mathrm{R}}}$.

In order to apply a representation theoretic treatment similar to what we used in chapters 5 and 6 to the problem, we must express H^{W} and H^{I} in terms of Casimir operators. As an SU(d) invariant two-site operator, we can express F_{ij} with the two-site quadratic Casimir operator,

$$F_{ij} = \frac{1}{2} C_{ij}^{SU(d)} + \left(\frac{2}{d} - d \right) \mathbb{1}. \tag{7.6}$$

In addition to this, we use the relationship between the two-site and N-site representations of the Casimir,

$$C_N^{SU(d)} = \sum_{i<j} C_{ij}^{SU(d)} - N(N-2) \left(d - \frac{1}{d} \right) \mathbb{1}, \tag{7.7}$$

to express H^{W} with the Casimir represented on the left (L), right (R) and entire composite Hilbert space (LR),

$$H^{\mathrm{W}} = \frac{1}{2 n_{\mathrm{L}} n_{\mathrm{R}}} \left(C_{\mathrm{LR}}^{SU(d)} - C_{\mathrm{L}}^{SU(d)} - C_{\mathrm{R}}^{SU(d)} \right) + \frac{\mathbb{1}}{d}. \tag{7.8}$$

In the isotropic case, the partial transposition in $F_{ij}^{t_{\mathrm{R}}}$ translates to one of the generators being transposed compared to Eq (7.6).

$$H^{\mathrm{I}} = \frac{1}{n_{\mathrm{L}} n_{\mathrm{R}}} \sum_{i \in \mathrm{L}} \sum_{j \in \mathrm{R}} E_i^{\alpha\beta} E_j^{\alpha\beta} + \frac{1}{d} \mathbb{1}. \tag{7.9}$$

Since the generators of SU(d) are antihermitian[1], we can relate these transposed generators to the complex conjugate, i.e dual of the defining representation: The generators of the dual representation are $\{-(E^t)^{\alpha\beta}\}_{\alpha,\beta=1}^{d}$. We deal with the $E_i^{\alpha\beta} E_j^{\alpha\beta}$

[1] As a matter of fact, the generators we defined in Eq. (3.54) are not antihermitian. This is because we use the generators of the det 1 subgroup of GL(d) in place of the genuine, antihermitian SU(d) generators. However, the Casimir operators expressed using the generators $-(E^t)^{\alpha\beta}$, can only differ from the ones expressed with the antihermitian generators by a constant multiplication factor.

term in Eq. (7.9) by introducing the quadratic Casimir operator $\tilde{C}_{\mathrm{LR}}$ in the representation $(D_{(1)}^{SU(d)})^{\otimes n_{\mathrm{L}}} \otimes (\overline{D}_{(1)}^{SU(d)})^{\otimes n_{\mathrm{R}}}$:

$$\tilde{C}_{\mathrm{LR}} = \left(\sum_{k\in\mathrm{L}} E_k^{\alpha\beta} - \sum_{l\in\mathrm{R}} E^{\beta\alpha}\right)\left(\sum_{k\in\mathrm{L}} E_k^{\beta\alpha} - \sum_{l\in\mathrm{R}} E_l^{\alpha\beta}\right) = -2\sum_{k\in\mathrm{L}}\sum_{l\in\mathrm{R}} E_k^{\alpha\beta}E_l^{\alpha\beta} + C_{\mathrm{L}} + C_{\mathrm{R}}. \tag{7.10}$$

This way, we are able to re-express H^{I} with $\mathrm{SU}(d)$ Casimir operators,

$$H^{\mathrm{I}} = \frac{1}{2n_{\mathrm{L}}n_{\mathrm{R}}}\left(C_{\mathrm{L}}^{\mathrm{SU}(d)} + C_{\mathrm{R}}^{(\mathrm{SU}(d))} - \tilde{C}_{\mathrm{LR}}^{\mathrm{SU}(d)}\right) + \frac{\mathbb{1}}{d}. \tag{7.11}$$

Thus, we were able to convert the problem of shareability into the ground state problem of "Hamiltonians" that are eerily similar to the Hamiltonian of the bipartite spin system that we investigated in Chapter 6. In fact, for $d = 3$ and $n_{\mathrm{L}} = n_{\mathrm{R}} = n$, H^{W} is equivalent to the CBE Hamiltonian at the parameter $\theta = 3\pi/4$, which belongs to one of the phase boundaries of the model. By substituting the ground state energy, we can immediately tell that for $d = 3$, $\alpha_{n,n} = -1/n$.

7.3 The minimum product diagram

We will search for the optimal eigenvalues of H^{W} and H^{I} using the same approach as we did with the CBE Hamiltonian of Chapter 6; i.e., we first optimize the contribution of the $C_{\mathrm{LR}}^{\mathrm{SU}(d)}$ and $\tilde{C}_{\mathrm{LR}}^{\mathrm{SU}(d)}$ terms constrained to fixed $C_{\mathrm{L}}^{\mathrm{SU}(d)}$ and $C_{\mathrm{R}}^{\mathrm{SU}(d)}$ are eigenspaces. In order to be able to do this, we first have to find a general solution to a problem we already solved in the case of $d = 3$ in Section 6.3.3: Identifying the diagram in the irrep decomposition of the tensor product of two arbitrary $\mathrm{SU}(d)$ irreps that is the minimum w.r.t. dominance order. The solution we present in this section is based on the works of T. Y. Lam [144] and O. Azenhas [145].

7.3.1 Conjugate and difference partitions

First, we must introduce some new concepts related to partitions. The row lengths of a skew diagram do not, in general, describe an integer partition. We call the "partitionification" of a skew diagram a *difference partition*: The difference partition, $\lambda - \mu$, of the skew diagram λ/μ is the integer partition created by arranging the numbers $\lambda_i - \mu_i$ in decreasing order, i.e,

$$\lambda - \mu = \mathrm{sort}\{\lambda_i - \mu_i\}_{i=1}^{d}. \tag{7.12}$$

The *conjugate*, λ^*, of the Young diagram λ, is the transposition of λ as a diagram. Described with the row lengths, this translates to

$$\lambda_i^* = \#\{\lambda_j : \lambda_j \geq i\}. \tag{7.13}$$

For skew diagrams, conjugation is defined with $(\lambda/\mu)^* = \lambda^*/\mu^*$, which coincides with visual transposition.

Conjugating two dominance ordered partitions reverses their order, i.e.,

$$\lambda \trianglerighteq \mu \Leftrightarrow \mu^* \trianglerighteq \lambda^*. \tag{7.14}$$

This is in accordance with the visual aid, that one can imagine λ as tall and skinny while μ as short and fat; we leave the proper reasoning to the reader.

We define the *vertical strips*, $v_i(\lambda/\mu)$, of the skew diagram λ/μ analogously to the horizontal strips introduced in Proposition 9: $v_i(\lambda/\mu)$ is the skew diagram composed of the i-th cell in each row of λ/μ counted from *right to left*. While for the length of the strips, we have $|h_i(\lambda/\mu)| = |v_i(\lambda^*/\mu^*)|$, the strips $h_i(\lambda/\mu)$ and $v_i(\lambda^*/\mu^*)$ are, in general, not conjugates of each other.

Using conjugation and strip sequences, we have a visual method for determining a difference partition from the corresponding skew diagram without resorting to the explicit sorting of the rows:

$$(\lambda-\mu)_i^* = \#\{(\lambda-\mu)_j : (\lambda-\mu)_j \geq i\} = \\ \#\{(\lambda/\mu)_j : (\lambda/\mu)_j \geq i\} = |v_i(\lambda/\mu)|, \tag{7.15}$$

i.e, in order to obtain $\lambda - \mu$, one simply has to "straighten" the i-th vertical strips of λ/μ into the i-th column, as in the following example where we label the boxes of v_i with i,

$$\lambda/\mu = \begin{array}{|c|c|c|}\hline \multicolumn{1}{c}{} & \multicolumn{1}{c}{} & 2 & 1 \\ \cline{3-4} \multicolumn{1}{c}{} & \multicolumn{1}{c}{} & 1 \\ \cline{3-3} 3 & 2 & 1 \\ \cline{1-3} 1 \\ \cline{1-1} \end{array}, \quad \lambda - \mu = \begin{array}{|c|c|c|}\hline 1 & 2 & 3 \\ \cline{1-3} 1 & 2 \\ \cline{1-2} 1 \\ \cline{1-1} 1 \\ \cline{1-1} \end{array}. \tag{7.16}$$

Applying the same method to the conjugate diagrams, we get $(\lambda^* - \mu^*)_i^* = |v_i(\lambda^*/\mu^*)| = |h_i(\lambda/\mu)|$. We must emphasize that in general, $(\lambda^* - \mu^*)^* \neq (\lambda - \mu)$ due to the shuffling of rows in the definition of the difference partition. As a matter of fact, we can say more than this about the relation of the two partitions:

Proposition 17.

$$(\lambda - \mu) \trianglelefteq (\lambda^* - \mu^*)^*. \tag{7.17}$$

Proof. We show that we can transform $(\lambda - \mu)$ into $(\lambda^* - \mu^*)^*$ by only moving boxes upwards or sideways. First, we sort the rows of the skew diagram λ/μ by their lengths in decreasing order, without changing the horizontal position of any of the boxes. We call this intermediary diagram $(\lambda/\mu)'$. One can get to $(\lambda - \mu)$ from $(\lambda/\mu)'$ by only moving boxes to the left. Since transforming λ/μ into $(\lambda/\mu)'$ does not change the height of any column, the lengths of the horizontal strip sequences are also invariant to the transformation. In order to transform $(\lambda/\mu)'$ into $(\lambda^* - \mu^*)^*$ by moving boxes only upwards or sideways, move the boxes of $h_i((\lambda/\mu)')$ to the i-th row, e.g.,

$\lambda/\mu =$ 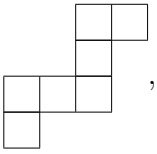 , $(\lambda/\mu)' =$ 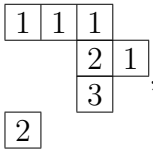 , $(\lambda^* - \mu^*)^* =$ 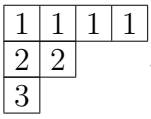 . (7.18)

□

7.3.2 The extremal contents of Littlewood-Richardson tableaux

To find the minimum product diagram, one must first look at the problem from a different angle, by fixing a different pair of diagrams in the Littlewood-Richardson product. For a given skew shape λ/μ, we define $LR(\lambda, \mu)$ as the set of all partitions ν, for which a Littlewood-Richardson skew tableau of shape λ/μ and content ν exists; i.e, λ is an irreducible constituent of $\mu \otimes \nu$. We can make a statement about the maximal element of $LR(\lambda, \mu)$.

Proposition 18. *For all $\nu \in LR(\lambda, \mu)$,*

$$\nu \trianglelefteq (\lambda^* - \mu^*)^*. \tag{7.19}$$

Proof. Since the numbers in the columns of a Littlewood-Richardson skew tableau, read from top to bottom, are strictly increasing, all instances of the number i must be inside the first i horizontal strips of λ/ν; therefore for all $1 \leq i \leq d$ we have,

$$\sum_{j=1}^{i} (\lambda^* - \mu^*)_j^* \geq \sum_{j=1}^{i} \nu_i. \tag{7.20}$$

□

Let us take a look at the conjugate of Proposition 18. If a Littlewood-Richardson skew tableau with shape λ^*/μ^* and content ν^* exists, then $\nu^* \trianglelefteq (\lambda - \mu)^*$ and therefore $(\lambda - \mu) \trianglelefteq \nu$. The heart of our argument for obtaining the minimum element of $LR(\lambda, \mu)$, is Theorem 6 of [145].

Theorem 4. *There exists a bijection between the set of Littlewood-Richardson skew tableaux of shape λ/μ, content ν, and those of shape λ^*/μ^*, content ν^*.*

As a consequence of this theorem, for every $\nu \in LR(\lambda, \mu)$,

$$\lambda - \mu \trianglelefteq \nu \trianglelefteq (\lambda^* - \mu^*)^*. \tag{7.21}$$

To finish the argument about the extremal elements of $LR(\lambda, \mu)$, we have to show two examples of Littlewood-Richardson skew tableaux with shape λ/μ and contents $(\lambda^* - \mu^*)^*$ and $\lambda - \mu$.

For the first case, consider the tableau obtained by filling the i-th horizontal strip of λ/μ with the symbol i. This is the single Littlewood-Richardson tableau with shape λ/μ and content $(\lambda^* - \mu^*)^*$, as this is the only way one can place all instances of the symbol i within the first i horizontal strips while keeping the columns strictly increasing.

For the second case, the required content can be achieved by filling the i-th vertical strip of λ/μ with the increasing sequence $1, 2, \ldots |v_i(\lambda/\mu)|$. Some concrete examples for the two types of fillings are,

$$\begin{array}{|c|c|c|c|}\hline \multicolumn{1}{c}{} & \multicolumn{1}{c}{} & 1 & 1 \\ \cline{3-4} \multicolumn{1}{c}{} & 1 & 2 & \multicolumn{1}{c}{} \\ \cline{2-3} 1 & 2 & 3 & \multicolumn{1}{c}{} \\ \cline{1-3} 2 & \multicolumn{1}{c}{} & \multicolumn{1}{c}{} & \multicolumn{1}{c}{} \\ \cline{1-1} \end{array} \quad \text{and} \quad \begin{array}{|c|c|c|c|}\hline \multicolumn{1}{c}{} & \multicolumn{1}{c}{} & 1 & 1 \\ \cline{3-4} \multicolumn{1}{c}{} & 2 & 2 & \multicolumn{1}{c}{} \\ \cline{2-3} 1 & 3 & 3 & \multicolumn{1}{c}{} \\ \cline{1-3} 4 & \multicolumn{1}{c}{} & \multicolumn{1}{c}{} & \multicolumn{1}{c}{} \\ \cline{1-1} \end{array} \quad . \tag{7.22}$$

7.3.3 The dual symmetry of the SU(d) fusion rules

We obtain the minimum diagram with non-zero multiplicity in the product $D_\mu^{\mathrm{SU}(d)} \otimes D_\nu^{\mathrm{SU}(d)}$ from the minimum of $LR(\lambda, \mu)$, by making use of the dual symmetry of the fusion rules of SU(d).

Contrarily to conjugating diagrams, taking the duals leaves dominance order unchanged. If $\lambda, \mu \vdash_d n$ and $\lambda \trianglerighteq \mu$ then,

$$n - \sum_{i=l+1}^{d} \mu_i = \sum_{i=1}^{l} \mu_i \leq \sum_{i=1}^{l} \lambda_i = n - \sum_{i=l+1}^{d} \lambda_i. \tag{7.23}$$

Assuming that we take the M-dual of λ and μ for the same M, so as to make sure that dominance order is well defined between the results, this proves our statement.

The coefficient $m_\lambda^{\mu,\nu}$ of the SU(d) fusion rules in Eq. (3.41) has a symmetry for exchanging λ with ν, and taking the dual of both partitions. This is evident if we express $m_\lambda^{\mu,\nu}$ with the inner product of characters,

$$\begin{aligned} m_\lambda^{\mu,\nu} = \langle \chi_\mu \chi_\nu, \chi_\lambda \rangle &= \int \mathrm{d}u \chi_\mu(u) \chi_\nu(u) \chi_\lambda^*(u) \\ &= \int \mathrm{d}u \chi_\mu(u) \chi_{\overline{\lambda}}(u) \chi_{\overline{\nu}}(u)^* = m_{\overline{\nu}}^{\mu,\overline{\lambda}}. \end{aligned} \tag{7.24}$$

We can use this symmetry to derive the minimum product diagram from the minimum of $LR(\lambda, \mu)$ described in Eq. (7.21),

$$\lambda - \mu = \min\{\nu : m_\lambda^{\mu,\nu} > 0\} = \min\{\nu : m_{\overline{\nu}}^{\mu,\overline{\lambda}} > 0\}. \tag{7.25}$$

As the dual does not influence dominance order, we can relabel the indices which yields,

$$\min\{\lambda : m_\lambda^{\mu,\nu}\} = \overline{(\overline{\nu} - \mu)}. \tag{7.26}$$

At this step, we must make sure that the difference partition $\overline{\nu} - \mu$ is well defined, by choosing the dual diagram to be an appropriate M-dual with $M \geq \max\{\mu_i + \nu_i^r\}_{i=1}^d$. This makes no difference in terms of SU(d) representations. Substituting the definitions of the dual and difference partitions gives us a more intuitive picture of the minimum diagram,

$$\overline{(\overline{\nu} - \mu)} = \mathrm{sort}\{(\nu_{d-i+1} + \mu_i)\}_{i=1}^d := \mathrm{sort}\{(\nu_i^r + \mu_i)\}_{i=1}^d, \tag{7.27}$$

Essentially, we obtain $\overline{(\overline{\nu} - \mu)}$ by attaching ν upside down to μ and sorting the rows of the result.

7.4 The shareability of Werner states

In the following, we use the knowledge of the minimum product diagram, Eq. (7.26), to derive the optimal eigenvalues of H^{W} and H^{I}, and thus obtain the sets of n_{L}-n_{R} shareable Werner and isotropic states. We start our discussion with the former.

Being aware of the minimum diagram significantly reduces the number of variables we have to deal with, as we search for the smallest eigenvalue of the operator H^{W} from Eq. (7.8). Substituting Eq. (7.27) into the eigenvalue of Eq. (7.8) gives us the objective function, E^{W}, of our constrained minimization problem,

$$E^{\mathrm{W}}(\mu,\nu) = \frac{1}{2n_{\mathrm{L}}n_{\mathrm{R}}}\left[c(\overline{(\overline{\nu}-\mu)}) - c(\mu) - c(\nu)\right] + \frac{1}{d} = \frac{1}{n_{\mathrm{L}}n_{\mathrm{R}}}\sum_{i=1}^{d}\left(\tilde{\mu}_i\tilde{\nu}_i^r + (d-i)\left[\mathrm{sort}(\{\tilde{\mu}_j+\tilde{\nu}_j^r\}_{j=1}^{d})_i - (\tilde{\mu}_i+\tilde{\nu}_i)\right]\right) + \frac{1}{d}, \tag{7.28}$$

Where according to the definition of the Casimir operator eigenvalues in Eq. (3.57), $\tilde{\mu}_i = \mu_i - n_{\mathrm{L}}/d$ and $\tilde{\nu}_i = \nu_i - n_{\mathrm{R}}/d$. Since both $\tilde{\mu}$ and $\tilde{\nu}$ sum up to 0, we can drop all the terms that are proportional to $d\tilde{\mu}_i$ and $d\tilde{\nu}_i$. The constant terms introduced by $\tilde{\cdot}$ extinguish each other in the remaining terms of E^{W} that are linear in $\tilde{\mu}$ and $\tilde{\nu}$. Moreover, we have,

$$\sum_{i=1}^{d}\tilde{\mu}_i\tilde{\nu}_i^r = \sum_{i=1}^{d}\mu_i\nu_i^r - \frac{n_{\mathrm{L}}n_{\mathrm{R}}}{d}, \tag{7.29}$$

and therefore we can drop the $\tilde{\cdot}$ and the $1/d$ term completely. In summary, E^{W} simplifies to,

$$E^{\mathrm{W}}(\mu,\nu) = \frac{1}{n_{\mathrm{L}}n_{\mathrm{R}}}\sum_{i=1}^{d}\left[\mu_i\nu_i^r - i(\mathrm{sort}(\{\mu_j+\nu_j^r\}_{j=1}^{d})_i - (\mu_i+\nu_i))\right]. \tag{7.30}$$

It is possible to chose the diagrams μ and ν in such a way that there are no overlapping rows between μ and ν^r, and thus the contribution of the first term in Eq. (7.30) is 0. Since this is the only quadratic term, it is reasonable to expect that the smallest eigenvalue of $H^{(W)}$ corresponds to a pair of non-overlapping diagrams. Restricting ourselves to such pairs, makes it easier to obtain the diagrams that minimize the remaining terms, as in this case the only coupling between the diagrams μ and ν is given by $\mathrm{sort}(\{\mu_j+\nu_j^r\}_{j=1}^{d}) = \mathrm{sort}(\mu\cup\nu)$. In the following, we will show that among the pairs of diagrams that minimize E^{W}, there has to be at least one with certain special, non-overlapping shapes.

Proposition 19.

$$\min_{\mu\vdash_d n_{\mathrm{L}},\nu\vdash_d n_{\mathrm{R}}} E^{\mathrm{W}}(\mu,\nu) = E^{\mathrm{W}}(\mu^*(d_{\mathrm{L}}),\nu^*(d_{\mathrm{R}})) \tag{7.31}$$

for at least one of the diagram pairs,

$$\begin{aligned}\mu^*(d_{\mathrm{L}}) &= \left(\left\lceil\frac{n_{\mathrm{L}}}{d_{\mathrm{L}}}\right\rceil^{n_{\mathrm{L}} \bmod d_{\mathrm{L}}}, \left\lfloor\frac{n_{\mathrm{L}}}{d_{\mathrm{L}}}\right\rfloor^{d_{\mathrm{L}}-n_{\mathrm{L}} \bmod d_{\mathrm{L}}}\right),\\ \nu^*(d_{\mathrm{R}}) &= \left(\left\lceil\frac{n_{\mathrm{R}}}{d_{\mathrm{R}}}\right\rceil^{n_{\mathrm{R}} \bmod d_{\mathrm{R}}}, \left\lfloor\frac{n_{\mathrm{R}}}{d_{\mathrm{R}}}\right\rfloor^{d_{\mathrm{R}}-n_{\mathrm{R}} \bmod d_{\mathrm{R}}}\right),\end{aligned} \tag{7.32}$$

where $d_{\mathrm{L}}, d_{\mathrm{R}}$ are positive integers such that $d_{\mathrm{L}} + d_{\mathrm{R}} = d$.

Proof. We will create a path of diagram pairs starting from any $\mu \vdash_d n_{\mathrm{L}}$ and $\nu \vdash_d n_{\mathrm{R}}$, that terminates in one of the pairs described by Eq (7.32), along which the value of E^{W} is weakly decreasing.

We denote the number of overlapping rows between μ and ν^r by d_{LR}, and the numbers of non-overlapping rows of μ and ν^r by d_{L} and d_{R} respectively. Therefore, the number of rows of μ is $d_{\mathrm{L}} + d_{\mathrm{LR}} \leq d$ and that of ν is $d_{\mathrm{R}} + d_{\mathrm{LR}} \leq d$, where $d_{\mathrm{L}} + d_{\mathrm{R}} + d_{\mathrm{LR}} = d$ and $\mu_i \nu_i^r \neq 0$ iff $d_{\mathrm{L}} + 1 \leq i \leq d_{\mathrm{L}} + d_{\mathrm{LR}}$, see Figure 7.1. Moreover, we denote the number of boxes in the non-overlapping parts by $n'_{\mathrm{L}} = \sum_{i=1}^{d_{\mathrm{L}}} \mu_i$ and $n'_{\mathrm{R}} = \sum_{i=1}^{d_{\mathrm{R}}} \nu_i$. We build the path from two different types of steps. In the first one, we transform the non-overlapping parts of the two diagrams into a certain standard form. In the second one, we take a pair of diagrams for which the non-overlapping parts are in the standard form, and move boxes from the overlapping into the non-overlapping parts.

Consider the transformation that consists of moving a single box downward within the non-overlapping part of μ, in a way that results in a valid integer partition. I.e., we transform μ into μ', where $\mu'_i = \mu_i - 1$, $\mu'_j = \mu_j + 1$ for some $1 \leq i < j \leq d_{\mathrm{L}}$ and all other rows of μ stay unchanged, see Figure 7.1. An important detail to take note of here, is that we can always choose the order of rows of $\mathrm{sort}(\{\mu_j + \nu_j^r\}_{j=1}^d)$ in a way to make it invariant to the transformation. If there is ambiguity in the order, i.e., $\{\mu_j + \nu_j^r\}_{j=1}^d$ has multiple elements equal to μ_i or μ_j, we choose μ_i to be the bottommost, and μ_j to be the topmost of them.

Let us compute the change in E^{W} after transforming μ to μ'. Since the overlapping part stays unchanged, the quadratic term of Eq. (7.30) has no contribution. The contribution of the remaining terms depends on the distance between the two changed rows in μ, and in $\mathrm{sort}(\{\mu_j + \nu_j^r\}_{j=1}^d)$,

$$\begin{aligned}E^{\mathrm{W}}(\mu', \nu) - E^{\mathrm{W}}(\mu, \nu) = \frac{1}{n_{\mathrm{L}} n_{\mathrm{R}}} \Big[j - i - \\ \Big(\mathrm{first}(\mu_j, \mathrm{sort}(\{\mu_j + \nu_j^r\}_{j=1}^d)) - \mathrm{last}(\mu_i, \mathrm{sort}(\{\mu_j + \nu_j^r\}_{j=1}^d))\Big)\Big] \leq 0,\end{aligned} \tag{7.33}$$

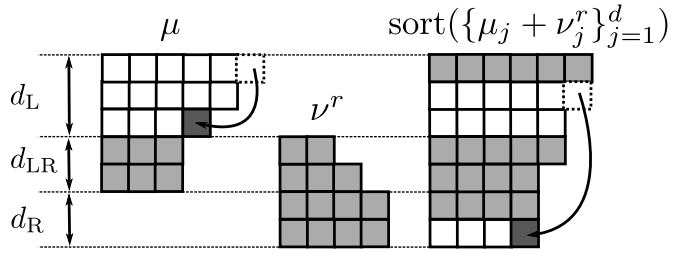

FIGURE 7.1: An example for a transformation that decreases the non-overlapping part of μ in dominance order. The distance between the two affected rows in $\mathrm{sort}(\{\mu_j + \nu_j^r\}_{j=1}^d)$ is always larger than or equal to that in μ, as the sorting can shuffle in additional rows between the ones present in μ. These are indicated with a darker color.

where $\mathrm{first}(x, y)$ and $\mathrm{last}(x, y)$ denote the first and last positions of x in the sequence y. The distance between the last occurrence of μ_i and the first occurrence of μ_j in $\mathrm{sort}(\{\mu_j + \nu_j^r\}_{j=1}^d)$ must be at least $j-i$, since $\mu_{i+1}, \mu_{i+2}, \ldots, \mu_{j-1}$ all lie between the two elements. Additionally, since $\mathrm{sort}(\{\mu_j + \nu_j^r\}_{j=1}^d) = \mathrm{sort}(\{\mu_j^r + \nu_j\}_{j=1}^d)$, performing the analog of this transformation on ν weakly decreases E^W as well.

Repeating the transformation just described on both μ and ν, creates sequences of diagrams that are strictly decreasing in dominance order. Continuing until there is no legal way left to move boxes downwards within the non-overlapping parts of μ and ν, transforms these parts into the minimum elements of $\{\lambda \vdash_{d_\mathrm{L}} n'_\mathrm{L}\}$ and $\{\lambda \vdash_{d_\mathrm{R}} n'_\mathrm{R}\}$ respectively, i.e., the end results of the repeated transformations are,

$$\begin{aligned} \mu'' &= \left(\left\lceil \frac{n'_\mathrm{L}}{d_\mathrm{L}} \right\rceil^{n'_\mathrm{L} \bmod d_\mathrm{L}}, \left\lfloor \frac{n'_\mathrm{L}}{d_\mathrm{L}} \right\rfloor^{d_\mathrm{L} - n'_\mathrm{L} \bmod d_\mathrm{L}}, \mu_{d_\mathrm{L}+1}, \mu_{d_\mathrm{L}+2}, \ldots \mu_d \right) \text{ and} \\ \nu'' &= \left(\left\lceil \frac{n'_\mathrm{R}}{d_\mathrm{R}} \right\rceil^{n'_\mathrm{R} \bmod d_\mathrm{R}}, \left\lfloor \frac{n'_\mathrm{R}}{d_\mathrm{R}} \right\rfloor^{d_\mathrm{R} - n'_\mathrm{R} \bmod d_\mathrm{R}}, \nu_{d_\mathrm{R}+1}, \nu_{d_\mathrm{R}+2}, \ldots, \nu_d \right). \end{aligned} \tag{7.34}$$

In this way, we are able to transform any pair of diagrams into this standard form without increasing E^W.

We define a second type of transformation that acts on pairs of diagrams, μ, ν of the form described in Eq. (7.34); we further assume that $d_\mathrm{LR} > 0$. Consider the transformation that takes a single box from the bottommost overlapping row of μ, and attaches it to the non-overlapping part in the way that makes the resulting diagram the smallest w.r.t. dominance order. I.e., we transform μ to μ' where $\mu'_{d_\mathrm{L}+d_\mathrm{LR}} = \mu_{d_\mathrm{L}+d_\mathrm{LR}} - 1$, $\mu'_{n'_\mathrm{L} \bmod d_\mathrm{L}+1} = \mu_{n'_\mathrm{L} \bmod d_\mathrm{L}+1} + 1$, and all other rows stay unchanged, see Figure 7.2.

Now let us express the change in E^W prompted by this transformation. The

contributions of the terms of Eq. (7.30) proportional to $\sum_i \mu_i \nu_i^r$ and $\sum_i i\mu_i$ are always negative, what remains is the term that depends on the diagram $\mathrm{sort}(\{\mu_j + \nu_j^r\}_{j=1}^d)$. This diagram is composed of four rectangular portions that contain only rows of lengths $\lceil n'_{\mathrm{L}}/d_{\mathrm{L}} \rceil$, $\lfloor n'_{\mathrm{L}}/d_{\mathrm{L}} \rfloor$, $\lceil n'_{\mathrm{R}}/d_{\mathrm{R}} \rceil$ and $\lfloor n'_{\mathrm{R}}/d_{\mathrm{R}} \rfloor$, which correspond to the non-overlapping parts of μ and ν^r. Above, between, and below these rectangular parts, the sort shuffles in the d_{LR} overlapping rows of $\mu + \nu^r$ in some unknown order, as shown in the example in Figure 7.2.

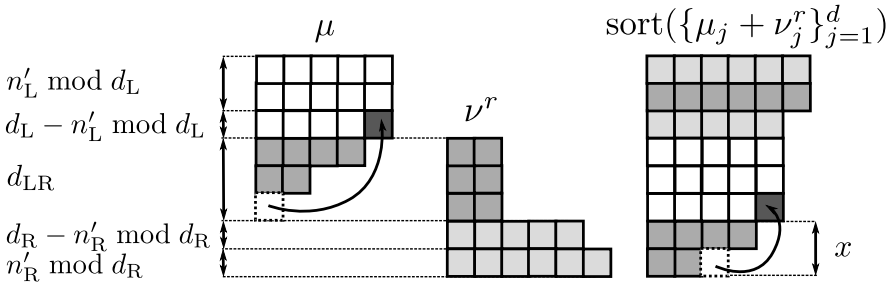

FIGURE 7.2: A transformation of a pair of diagrams of the standard form described by Eq. (7.34), that moves a box form the bottom row of μ into the non-overlapping part. In the diagram μ, $d_{\mathrm{LR}} - 1$ overlapping rows are between the original and new positions of the box, while in $\mathrm{sort}(\{\mu_j + \nu_j^r\}_{j=1}^d)$, these overlapping rows are not necessarily between the two positions.

When our transformation moves the box downwards in $\mathrm{sort}(\{\mu_j + \nu_j^r\}_{j=1}^d)$, the contribution of every term in $E^{\mathrm{W}}(\mu', \nu) - E^{\mathrm{W}}(\mu, \nu)$ is non-positive; therefore, we need only be concerned with the cases in which the box moves upwards. Without loss of generality, we can assume that $n'_{\mathrm{L}}/d_{\mathrm{L}} \leq n'_{\mathrm{R}}/d_{\mathrm{R}}$, thus, we move the box into the top row of the bottommost rectangular section of $\mathrm{sort}(\{\mu_j + \nu_j^r\}_{j=1}^d)$. In the case of the contrary, we simply apply the transformation to ν instead of μ. This means, that the only arrangements in which the box moves upwards, are the ones where it is taken from one of those rows that are shuffled below all the non-overlapping rows. Let us assume that we take the box from the x-th row below the bottommost non-overlapping row, i.e., it moves $x + d_{\mathrm{L}} - n'_{\mathrm{L}} \bmod d_{\mathrm{L}} - 1$ rows upward in $\mathrm{sort}(\{\mu_j + \nu_j^r\}_{j=1}^d)$, and $d_{\mathrm{LR}} + d_{\mathrm{L}} - n'_{\mathrm{L}} \bmod d_{\mathrm{L}} - 1$ upwards in μ. This way, the change in E^{W} is,

$$E^{\mathrm{W}}(\mu', \nu) - E^{\mathrm{W}}(\mu, \nu) = -\nu_{d_{\mathrm{R}}+1} + x - d_{\mathrm{LR}} \leq 0. \tag{7.35}$$

Starting from any pair of diagrams, by first rearranging the non-overlapping rows into the standard form in Eq. (7.34), then moving the boxes from the overlapping rows into the non-overlapping ones with the method just described, we

eventually reach one of the diagrams in the proposition without increasing the value of E^{W}. □

As a consequence of Proposition 19, in order to obtain the shareability, it is enough to compare the values of E^{W} for the $d-1$ diagram pairs in Eq. (7.32). Substituting the pair $\mu^*(d_{\mathrm{L}}), \nu^*(d_{\mathrm{R}})$ into Eq. (7.30), we get

$$E^{\mathrm{W}}(\mu^*(d_{\mathrm{L}}), \nu^*(d_{\mathrm{R}})) = \begin{cases} -\min\left\{\frac{d_{\mathrm{L}}}{n_{\mathrm{L}}}, \frac{d_{\mathrm{R}}}{n_{\mathrm{R}}}\right\} & \text{if} \quad \left\lfloor \frac{n_{\mathrm{L}}}{d_{\mathrm{L}}} \right\rfloor \neq \left\lfloor \frac{n_{\mathrm{R}}}{d_{\mathrm{R}}} \right\rfloor \\ -\frac{1}{n_{\mathrm{L}} n_{\mathrm{R}}}\left[d_{\mathrm{L}} d_{\mathrm{R}} \left\lfloor \frac{n_{\mathrm{L}}}{d_{\mathrm{L}}} \right\rfloor - (n_{\mathrm{L}} \bmod d_{\mathrm{L}})(n_{\mathrm{R}} \bmod d_{\mathrm{R}})\right] & \text{if} \quad \left\lfloor \frac{n_{\mathrm{L}}}{d_{\mathrm{L}}} \right\rfloor = \left\lfloor \frac{n_{\mathrm{R}}}{d_{\mathrm{R}}} \right\rfloor \end{cases} . \tag{7.36}$$

In the first case of Eq. (7.36), one can obtain $\mathrm{sort}(\{\mu_j + \nu_j^r\}_{j=1}^d)$ by simply attaching the shorter one of the diagrams $\mu^*(d_{\mathrm{L}})$ and $\nu^*(d_{\mathrm{R}})$ below the longer one. Contrarily, in the second case, the rows of the diagrams $\mu^*(d_{\mathrm{L}})$ and $\nu^*(d_{\mathrm{R}})$ are reshuffled in $\mathrm{sort}(\{\mu_j + \nu_j^r\}_{j=1}^d)$, which results in the peculiar expression containing modulos.

The modulos in the second case of Eq. (7.36) make it difficult to tell exactly which bipartition of d minimizes $E^{\mathrm{W}}(\mu^*(d_{\mathrm{L}}), \nu^*(d - d_{\mathrm{L}}))$, but we can reduce the number of candidates a little bit further. If we temporarily disregard the second case of Eq. (7.36), the expression is minimized by choosing d_{L} in a way that $d_{\mathrm{L}}/n_{\mathrm{L}}$ and $(d - d_{\mathrm{L}})/n_{\mathrm{R}}$ are the closest to each other, i.e., $d_{\mathrm{L}} = \lfloor d n_{\mathrm{L}}/(n_{\mathrm{L}} + n_{\mathrm{R}}) \rceil$ in the case this value is within the bounds 1 and $d-1$, and $d_{\mathrm{L}} = 1$ or $d_{\mathrm{L}} = d - 1$ otherwise. When we also take the second case of Eq. (7.36) into account, considering the magnitude of the term containing modulos, we get that the value of d_{L} that minimizes $E^{\mathrm{W}}(\mu^*(d_{\mathrm{L}}), \nu^*(1 - d_{\mathrm{L}}))$ differs from the one just described by at most 1. In other words, the parameter corresponding to the most entangled n_{L}-n_{R} shareable Werner states is,

$$\begin{aligned} &\alpha_{n_{\mathrm{L}}, n_{\mathrm{R}}} = \min_{d_{\mathrm{L}} \in A} E^{\mathrm{W}}(\mu^*(d_{\mathrm{L}}), \nu^*(d - d_{\mathrm{L}})), \text{ where} \\ &A = \left\{ \left\lfloor \frac{n_{\mathrm{L}}}{n_{\mathrm{L}} + n_{\mathrm{R}}} \right\rceil - 1, \left\lfloor \frac{n_{\mathrm{L}}}{n_{\mathrm{L}} + n_{\mathrm{R}}} \right\rceil, \left\lfloor \frac{n_{\mathrm{L}}}{n_{\mathrm{L}} + n_{\mathrm{R}}} \right\rceil + 1 \right\} \cap [1, d-1] . \end{aligned} \tag{7.37}$$

We visualize this result in Figure 7.3.

7.5 The shareability of isotropic states

In order to derive the shareability of isotropic states, one has to find the Young diagrams μ, ν and λ corresponding the eigenvalues of $C_{\mathrm{L}}, C_{\mathrm{R}}$ and $\tilde{C}_{\mathrm{LR}}$ from Eq. (7.11),

that maximize the eigenvalue of H^{I}. These diagrams have to fulfill $\mu \vdash_d n_{\mathrm{L}}, \nu \vdash_d n_{\mathrm{R}}$ and λ must appear in the irrep decomposition of $D_{\mu}^{\mathrm{SU}(d)} \otimes D_{\overline{\nu}}^{\mathrm{SU}(d)}$. Taking the dual of one of the diagrams in the product is the principal difference compared to the shareability problem of Werner states; and it makes the solution significantly easier to derive for isotropic states. The reason for this, is that the dual almost completely erases the competition between the terms of H^{I}, that are proportional to $\tilde{C}_{\mathrm{LR}}$ and $C_{\mathrm{L}} + C_{\mathrm{R}}$.

The most striking example is the case of $n_{\mathrm{L}} = n_{\mathrm{R}} = n$. As the eigenvalues of the Casimir operators follow the dominance order of the corresponding partitions, the contribution of $C_{\mathrm{L}}+C_{\mathrm{R}}$ to the eigenvalue of H^{I} is maximized by the same single-line diagram on both sides, $\mu = \nu = (n, 0^{d-1})$. Furthermore, as Proposition 9 states, the Littlewood-Richardson product of a diagram and its dual always contains the SU(d) singlet diagram that minimizes the contribution of the $\tilde{C}_{\mathrm{LR}}$ term of H_I. Substituting this result into the eigenvalue of H_I immediately gives us the maximal value for the parameter β of n-n shareable isotropic states,

$$\beta_{n,n} = 1 + \frac{d-1}{n}. \tag{7.38}$$

In the case of $n_{\mathrm{L}} \neq n_{\mathrm{R}}$, we use the result for the minimum product diagram. According to Eq. (7.26), the diagram that is the minimum in dominance order among the diagrams that appears in the decomposition of $D_{\mu}^{\mathrm{SU}(d)} \otimes D_{\overline{\nu}}^{\mathrm{SU}(d)}$ is $\lambda = \overline{\nu' - \mu}$. Here, ν' denotes a diagram that differs from ν only by columns of height d, the number of these columns is set by choosing the M-dual appearing in Eq. (7.26) in a way to make $\nu' - \mu$ well defined. When substituting these diagrams into the eigenvalues of the Casimir operators in H^{I}, we do not have to worry about the details related to the dual, as the Casimir operators themselves are invariant to it. Thus, instead of $\overline{\nu' - \mu}$ we use the formal integer partition $\lambda = \nu - \mu$, that we get by extending the definition of the difference partition to allow negative numbers.

After substituting into the eigenvalue of H^{I}, and repeating the same simplifications that we described after Eq. (7.28), the objective function for our maximization problem takes the form,

$$\begin{aligned} E^{\mathrm{I}}(\mu,\nu) = \frac{1}{2n_{\mathrm{L}}n_{\mathrm{R}}}(c(\mu) + c(\nu) - c(\nu-\mu)) + \frac{1}{d} = \\ \frac{1}{n_{\mathrm{L}}n_{\mathrm{R}}} \sum_{i=1}^{d} [\mu_i\nu_i + i((\nu-\mu)_i - \nu_i - \mu_i)] + \frac{1+d}{n_{\mathrm{R}}}. \end{aligned} \tag{7.39}$$

Observe the interaction of $\sum_i i(\ldots)$, and the sorting of elements implicit in $\mu - \nu$. The index $i = 1$ is paired with the largest number in $\{\nu_j - \mu_j\}_{j=1}^{d}$, $i = 2$ with

the second largest, and so on. The value of the expression is the same as if, instead of sorting, we chose the permutation $\sigma \in S_d$, that permutes the elements of $\{\nu_j - \mu_j\}_{j=1}^d$ in such a way that the value of the sum is minimal. As a result, we can rewrite E^{I} as follows,

$$\begin{aligned} E^{\mathrm{I}}(\mu,\nu) &= \min_{\sigma\in S_d} E^{\mathrm{I}}_\sigma(\mu,\nu) \\ E^{\mathrm{I}}_\sigma(\mu,\nu) &= \frac{1}{n_{\mathrm{L}} n_{\mathrm{R}}} \sum_{i=1}^{d} \left[\mu_i\nu_i + i(\nu_{\sigma(i)} - \mu_{\sigma(i)} - \nu_i - \mu_i)\right] + \frac{1+d}{n_{\mathrm{R}}}. \end{aligned} \tag{7.40}$$

In the following, we temporarily extend the domains of μ and ν from integer partitions into real partitions; we denote the resulting convex sets with $\mathcal{L} = \mu \vdash_d^{\mathbb{R}} n_{\mathrm{L}}$ and $\mathcal{R} = \nu \vdash_d^{\mathbb{R}} n_{\mathrm{R}}$. After this modification, it is clear from Eq. (7.40), that as a pointwise minimum of a set of bilinear functions, E^{I} is biconcave. I.e., if one fixes the value of either μ or ν, E^{I} is concave as a function of the remaining variable. We will use this property to show that the maximum of E^{I} is always in an extreme point of $\mathcal{L} \times \mathcal{R}$.

Let us start by expressing the elements of $Ext(\mathcal{L} \times \mathcal{R})$. It is easiest to do this by using Dynkin labels, since in this scheme, the only constraint the labels have to obey is the fixed system size. Thus, with Dynkin labels, the extreme points of $\mathcal{L}$ and $\mathcal{R}$ are proportional to unit vectors, and we can index the elements of $Ext(\mathcal{L} \times \mathcal{R})$ with a pair of integers,

$$\begin{aligned} &\mathrm{Ext}(\mathcal{L} \times \mathcal{R}) = \left\{(\mu^{(k)}, \nu^{(l)})\right\}_{k,l=1}^{d}, \text{ where} \\ &\mu^{(k)} = [0^{k-1}, n_{\mathrm{L}}/k, 0^{d-k}], \quad \nu^{(l)} = [0^{l-1}, n_{\mathrm{R}}/l, 0^{d-l}]. \end{aligned} \tag{7.41}$$

Thinking in diagrams, $\mu^{(k)}$ corresponds to the rectangle with height k and width n_{L}/k.

As E^{I}_σ is bilinear, and $\mathcal{L} \times \mathcal{R}$ is a product of two convex sets, E^{I}_σ must be maximal in at least one point in $\mathrm{Ext}(\mathcal{L} \times \mathcal{R})$. However, it does not yet follow that the same is true for E^{I}. It may be the case, that for any permutation σ, none of the extreme points where E^{I}_σ is maximal are located within the polytope in which $E^{\mathrm{I}}_\sigma(\mu,\nu) = E^{\mathrm{I}}(\mu,\nu)$. We can get a sufficient condition for the maximum being at a particular extreme point by showing the contrary.

Lemma 5. *If there exists an extreme point, $(\mu^{(i)},\nu^{(j)}) \in Ext(\mathcal{L}\times\mathcal{R})$, and a permutation, $\sigma \in S_d$, for which*

$$\begin{aligned} E^{\mathrm{I}}_{\sigma}(\mu^{(i)},\nu^{(j)}) &\leq E^{\mathrm{I}}_{\sigma'}(\mu^{(i)},\nu^{(j)}) \qquad \forall \sigma' \in S_d \text{ and} \\ E^{\mathrm{I}}_{\sigma}(\mu^{(i)},\nu^{(j)}) &\geq E^{\mathrm{I}}_{\sigma}(\mu^{(k)},\nu^{(l)}) \qquad \forall k,l = 1,2,\dots d, \text{ then} \\ \max_{\mu\in\mathcal{L},\nu\in\mathcal{R}} E^{\mathrm{I}}(\mu,\nu) &= E^{\mathrm{I}}(\mu^{(i)},\nu^{(j)}). \end{aligned} \tag{7.42}$$

Proof. If the two inequalities of Eq. (7.42) hold then,

$$E^{\mathrm{I}}(\mu^{(i)},\nu^{(j)}) = E^{\mathrm{I}}_{\sigma}(\mu^{(i)},\nu^{(j)}) \geq E^{\mathrm{I}}_{\sigma}(\mu,\nu) \geq E^{\mathrm{I}}(\mu,\nu) \quad \forall(\mu,\nu)\in\mathcal{L}\times\mathcal{R}. \tag{7.43}$$

□

Proposition 20.

$$\max_{\mu\in\mathcal{L},\nu\in\mathcal{R}} E^{\mathrm{I}}(\mu,\nu) = E^{\mathrm{I}}(\mu^{(1)},\nu^{(1)}). \tag{7.44}$$

Proof. We only have to find an appropriate permutation σ that fulfills the conditions of Lemma 5 for $i = j = 1$. In order to decide whether these conditions hold, it is enough to evaluate E^{I} at the extreme points. Substituting Eq. (7.41) into Eq. (7.40) we get,

$$\begin{aligned} E^{\mathrm{I}}_{\sigma}(\mu^{(k)},\nu^{(l)}) = \frac{1}{kl}\min\{k,l\} - \frac{1}{kn_{\mathrm{R}}}\sum_{i=1}^{k}(\sigma^{-1}(i)+i) + \\ \frac{1}{ln_{\mathrm{L}}}\sum_{i=1}^{l}(\sigma^{-1}(i)-i) + \frac{1+d}{n_{\mathrm{R}}}. \end{aligned} \tag{7.45}$$

Without loss of generality, we can assume $n_{\mathrm{R}} \geq n_{\mathrm{L}}$. In the case of the contrary, the commutativity of the tensor product allows us to swap the two subsystems. With this assumption, the first inequality of Eq. (7.42) is fulfilled iff $\sigma(1) = 1$. An example for such a permutation, that fulfills the second inequality is the identity, $\mathrm{Id} = (1,2,\dots,d)$ since,

$$E^{\mathrm{I}}_{\mathrm{Id}}(\mu^{(k)},\nu^{(l)}) = \frac{1}{kl}\min\{k,l\} + \frac{d-k}{n_{\mathrm{R}}}. \tag{7.46}$$

□

The extreme point $(\mu^{(1)},\nu^{(1)})$ corresponds to a pair of single-line diagrams, which is in line with the previous result for n-n shareability. Since this extreme point is always an integer partition, the maximal value of the parameter β for

n_{L}-n_{R} shareable isotropic states immediately follows from Proposition 20.

$$\beta_{n_{\mathrm{L}},n_{\mathrm{R}}} = E^{\mathrm{I}}(\mu^{(1)},\nu^{(1)}) = 1 + \frac{d-1}{\max\{n_{\mathrm{L}},n_{\mathrm{R}}\}}. \tag{7.47}$$

An equivalent way to frame this result, is that the isotropic state with parameter β is n_{L}-n_{R} shareable for all $n_{\mathrm{L}}, n_{\mathrm{R}} \leq (d-1)/(\beta-1)$. This means, that contrarily to the case of Werner states, every isotropic state has a unique, maximum shareability, $n_{\mathrm{L}} = n_{\mathrm{R}} = \lfloor (d-1)/(\beta-1) \rfloor$ w.r.t. the partial order of $n_{\mathrm{L}}, n_{\mathrm{R}}$ pairs.

7.6 Summary and Outlook

In this chapter, we have determined the sets n_{L}-n_{R} shareable Werner and isotropic states for arbitrary values of n_{L} and n_R and local dimension d.

In our derivation, we used the set of symmetries inherent to the shareability problem to translate it into finding the extremal eigenvalues of certain linear operators that exhibit the same symmetries. The eigenvalues of these operators can be labeled by triples of Young diagram that must be compatible with one another w.r.t. the Littlewood-Richardson product of diagrams. We relied on the works of Azenhas [145] and Lam [144] to determine the minimum, in dominance order, diagram in the product of two arbitrary diagrams, which reduced the set of variables enough for the problem to be exactly solvable.

We obtained the result, that the range of n_{L}-n_{R} shareable Werner states has a non-trivial tradeoff between n_{L} and n_{R}, that depends of the divisibilities of the two values. In contrast, the conjugate unitary symmetry of isotropic states makes the Hamiltonian of the corresponding ground state problem unfrustrated; the result of this is, that the range of n_{L}-n_{R} shareable isotropic states has no tradeoff for increasing the smaller value of the $n_{\mathrm{L}}, n_{\mathrm{R}}$ pair.

By reason of the similarity between the linear operator we had to minimize as part of the derivation of our Werner state result, and the CBE Hamiltonian of Chapter 6, we can also interpret $\beta_{n_{\mathrm{L}},n_{\mathrm{R}}}$ as the ground state energy of a spin Hamiltonian. In the system corresponding to this Hamiltonian, d-level spins interact by exchange interaction, and the structure of connectivity is described by a bipartite complete graph with bipartite subsets of sizes n_{L} and n_{R}. In the context of the CBE Hamiltonian, this translates to the case in which there is no coupling within the subsystems.

A straightforward direction one could develop this topic further, is the investigation of multipartite Werner state shareabilities. In this scenario, an n-partite

Werner state is shared between n composite Hilbert spaces in a permutation symmetric way. In a way analogous to Section 7.2, it is possible to map the multipartite shareability problem into an eigenproblem of a linear operator composed of various tensor product representations of the quadratic SU(d) Casimir operator. The knowledge of these multipartite shareabilities could serve as a way to characterize the entanglement of multipartite Werner states.

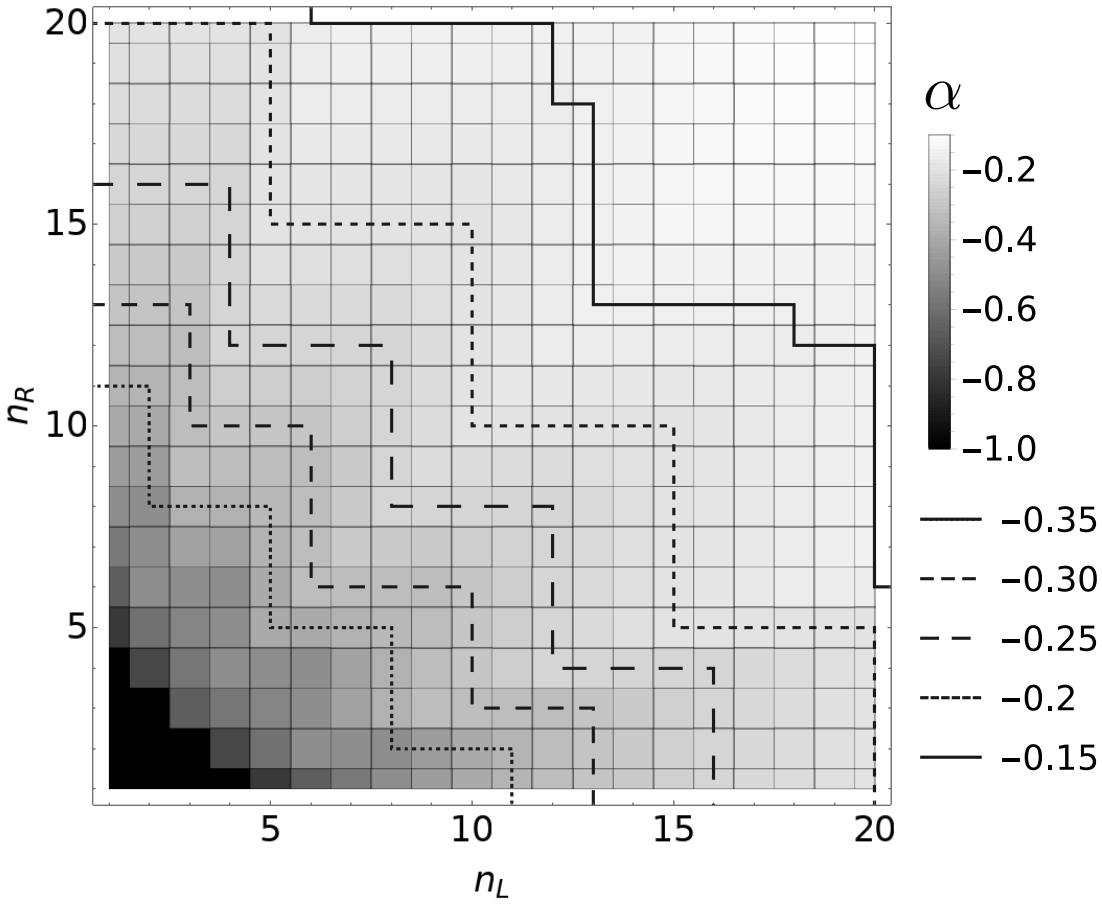

FIGURE 7.3: The extreme parameters of n_{L}-n_{R} shareable Werner states up to 20-20 shareability in the case of $d = 5$. The colors temperature of the squares represents the value of $\alpha_{n_{\mathrm{L}},n_{\mathrm{R}}}$. In particular, squares with black color indicate that all Werner states are extendible for the corresponding n_{L} and n_{R}. These values are a consequence of the fact that the Werner state $\rho^{\mathrm{W}}(-1)$ is a partial trace of the completely antisymmetric pure state on $\mathcal{H}^{\otimes d}$, thus, all Werner states must be extendible for $n_{\mathrm{L}}+n_{\mathrm{R}} \leq d$. The various lines denote the border between the regions of $(n_{\mathrm{L}}, n_{\mathrm{R}})$-pairs for which the Werner state with the corresponding α parameter is and is not extendible.

Chapter 8

Összefoglaló (Summary in Hungarian)

A disszertációban három különböző kérdéskört vizsgáltam. A közös motívum ami ezek mindegyikében megjelenik, a permutáció és SU(d) szimmetriák összjátéka. Az első két projektben erősen szimmetrikus mágneses rendszerek alapállapoti problémáit vizsgáltam, a harmadikban pedig megoldottam a kvantumos megoszthatóság problémáját két különböző kétrészű kvantumállapot család esetére.

Az 5. fejezetben egy három-szintű, SU(2)-szimmetrikus kéttest kölcsönhatással ellátott, permutáció-szimmetrikus spinrendszer alapállapotait tanulmányoztam. Ez a Heisenberg-modell egyik lehetséges három-szintű általánosítása. A kéttest Hilbert-tér SU(2) transzformációk alatt felbomlik a 0, 1 és 2-es spinek által címkézett irreduciblis alterekre. Ennek megfelelően, a legáltalánosabb, előírt szimmetriákkal rendelkező kölcsönhatás előállítható az identitás, és két másik SU(2) invariáns, lineárisan független kéttest operátor lineáris kombinációjaként. Ezt a két operátort az SU(2) és SU(3) csoportok kvadratikus Casimir-operátorainak választom a kétrészecske reprezentációban. Az így eredményül kapott kölcsönhatás normálás után egyedül a θ szabad paramétert tartalmazza.

$$H_{ij} = \sin(\theta) C_{ij}^{\mathrm{SU}(3)} + \cos(\theta) C_{ij}^{\mathrm{SU}(2)}. \tag{8.1}$$

Ez a kétrészecske kölcsönhatás régóta ismert a szilárdtest fizikában bilineáris-bikvadratikus (BLBQ) kölcsönhatás néven. A hagyományos alakjában Casimir-operátorok helyett két másik SU(2)-szimmetrikus operátorral fejezik ki,

$$H_{ij} = \cos(\gamma) \mathbf{S}_i \mathbf{S}_j + \sin(\gamma) (\mathbf{S}_i \mathbf{S}_j)^2. \tag{8.2}$$

A teljes permutáció szimmetria egy kéttest-kölcsönható spin modell esetében azt jelenti, hogy a spinek kapcsolatát egy rács helyett a teljes gráf írja le. A teljes gráfon értelmezett klasszikus spin modellek, például a Sherrington–Kirkpatrick [102],

vagy a Curie–Weiss modell, fontos szerepet játszanak a statisztikus mechanikában. Ennek az oka, hogy az ilyen permutáció-szimmetrikus modellek könnyen kezelhetőek, ugyanakkor mégis jó becsléseket adnak a megfelelő kölcsönhatások tulajdonságaira magas-dimenziós rácsok esetén. Az átlagtér elméletként való hasznosíthatóság mellett, az ultrahideg atomokkal végzett kísérletek lehetőséget adnak a teljes gráfon értelmezett SU(d)-szimmetrikus modellek kísérleti megvalósítására is, például abban a formában amit [46]-ben indítványoznak.

A modell teljes permutáció szimmetriájának következménye, hogy az egész rendszert leíró Hamilton-operátorban a 8.1. egyenlet két Casimir-operátorának N-részecskés ábrázolásai jelennek meg,

$$H_{\mathrm{BLBQ}} = \sin(\theta) C_N^{\mathrm{SU}(3)} + \cos(\theta) C_N^{\mathrm{SU}(2)}. \tag{8.3}$$

Ennek a Hamilton-operátornak az alapállapotát az SU(2) és SU(3)-szimmetrikus tagok közötti versengés határozza meg, a sajátérték problémája pedig megoldható tisztán csoportelméleti módszerekkel. Mivel a 8.3. egyenlet Casimir operátorai kommutálnak, és a sajátaltereik az N-részecske Hilbert-tér SU(2) és SU(3) irreducibilis alterei, H_{BLBQ} sajátaltereit egy SU(2) és egy SU(3) irreducibilis ábrázolásból (irrepből) álló párokkal tudjuk címkézni. A sajátérték probléma megoldásának kulcsa annak a meghatározása, hogy mik az egymással kompatibilis SU(2) és SU(3) irrepek. Az SU(2) csoport 1-es spinű ábrázolásának képe egy részcsoportja SU(3)-nak. Ebből kifolyólag, amikor megszorítjuk erre a részcsoportra, minden SU(3) irrep felbomlik valamilyen SU(2) irrepek direkt összegére. Ezt a felbontást az 5.9. egyenlet írja le formálisan; az egyenletben megjelenő, $m_s^{(\lambda)}$ multiplicítások meghatározása, lásd az 5.23. egyenletet, egy fontos eredménye a dolgozatnak. A kompatibilis, s, λ irrep párok az $m_s^{(\lambda)} \geq 1$ multiplicításoknak felelnek meg; a multiplicítások pontos értékeivel pedig H_{BLBQ} sajátaltereinek dimenzióit is lehetséges megadni.

A H_{BLBQ} Hamilton-operátor spektrumának ismeretében feltérképeztem az alapállapot fázisait a θ szabad paraméter függvényében, lásd az 5.4 ábrát. A modellnek négy, különböző szimmetria szektorokhoz tartozó alapállapoti fázisa van: Két SU(2) szinglet fázis, egy ferromágneses fázis, és egy részlegesen mágnesezett fázis. A két SU(2) szinglet fázis egyike egyben SU(3) szinglet is, míg a másik része a sokrészecske Hilbertert-tér teljesen permutáció-invariáns alterének. A részlegesen mágnesezett fázist, a többivel ellentétben, nem lehet konkrét λ és s kvantumszámokkal jellemezni, ezek ugyanis a közel folytonosan változnak θ függvényeként. Ilyen módon, a termodinamikai limeszben, a θ paraméternek minden ehhez a fázishoz tartozó értékénél egy „level crossing” történik, vagyis a fázis gap nélküli. A

gap a részlegesen mágnesezett fázisban, véges rendszerméretek esetén, az 5.6. ábrán látható.

A 6. fejezetben vizsgált spinmodell az 5. fejezet témájának egy új variációja. Az előző esethez hasonlóan, a Heisenberg-modell egy általánosítását vizsgálom egy erősen permutáció-szimmetrikus felállításban. A különbség az, hogy a spinek most egy SU(3)-szimmetrikus kicserélődési kölcsönhatással hatnak kölcsön; és ahelyett hogy, a korábbi modellhez hasonlóan, megtörném az SU(3) szimmetriát, a permutáció szimmetriát töröm meg részlegesen azzal, hogy a rendszert két, egyenlő nagyságú alrendszerre bontom, és csupán ezeken belül követelek meg permutáció szimmetriát. Ez azt jelenti, hogy a rendszert két, különböző csatolási állandójú kicserélődési kölcsönhatás jellemzi. Egy a részrendszereken belül, egy pedig azok között hat. Egy ilyen kétrészű struktúra bevezetése egy átlagtér modellbe érdekesebbé teszi a fázisstruktúrát, mivel relaxálja a teljes gráfban megjelenő extrém frusztrációt, és megnyitja a lehetőséget a kétrészű kicserélődési szimmetria megsértésére.

Hasonlóan a teljes gráfon értelmezett bilineáris-bikvadratikus modell esetéhez, a permutáció szimmetria lehetővé teszi, hogy a teljes rendszer Hamilton-operátorát Casimir-operátorok lineáris kombinációjaként fejezzük ki. Ebben az esetben SU(3) kvadratikus Casimir-operátora jelenik meg, a teljes rendszeren ($C_{\mathrm{AB}}^{\mathrm{SU(3)}}$), és a részrendszereken ($C_{\mathrm{A}}^{\mathrm{SU(3)}}$, $C_{\mathrm{B}}^{\mathrm{SU(3)}}$) vett szorzatábrázolásokban, a normált Hamilton-operátor pedig egy szabad paramétert tartalmaz,

$$H_{\mathrm{CBE}} = \sin(\theta) C_{\mathrm{AB}}^{\mathrm{SU(3)}} + \cos(\theta) \left(C_{\mathrm{A}}^{\mathrm{SU(3)}} + C_{\mathrm{B}}^{\mathrm{SU(3)}} \right). \tag{8.4}$$

A 8.4. egyenletben megjelenő Casimir-operátorok ismét lehetővé teszik az alapállapoti probléma egzakt megoldását ábrázoláselmélet segítségével. H_{CBE} sajátértékeit SU(3) irrepek hármasaival lehetséges címkézni. Ezek közül kettő az alrendszereknek felel meg, egy pedig a teljes rendszernek. Azt hogy három tetszőleges irrep kompatibilis-e egymással az SU(3) csoport fúziós szabálya, az úgynevezett Littlewood–Richardson szabály határozza meg. Ez egy Young-diagramokkal megfogalmazott kombinatorikai algoritmus.

A Littlewood–Richardson algoritmus eredményének, Schlosser által meghatározott [66], zárt alakú kifejezésének segítségével megadom, hogy két adott, az alrendszerekhez tartozó, SU(3) irrep esetén a 8.4. egyenlet Hamilton-operátorá-nak $C_{\mathrm{AB}}^{\mathrm{SU(3)}}$-vel arányos tagja milyen irrep esetén adja a legalacsonyabb járulékot, lásd a 6.9. és a 6.12. egyenleteket. Ez lecsökkenti az alapállapoti probléma változóinak számát két, egymástól független SU(2) irrepre. Ez után az egyszerűsítés után

az alapállapoti probléma analitikusan kezelhetővé válik. A θ kontroll paraméter függvényében a modellnek öt alapállapoti fázisa van (lásd a 6.3. ábrát): Egy ferromágneses fázis, egy Néel-típusú antiferromágneses fázis ferromágnesesen rendezett alrendszerekkel, egy SU(3) szinglet fázis, egy gap-nélküli részlegesen mágnesezett fázis amiben az alapállapotot leíró kvantumszámok folytonosan változnak a θ paraméter függvényeként, valamint egy kétreszű kicserélési szimmetriát sértő fázis, amiben az alrendszereken különböző SU(3) reprezentációk jelennek meg. Az utóbbi kapcsán figyelemre méltó, hogy már ebben az egyszerű, hosszútávú kölcsönhatást tartalmazó modellben megjelenik egy ilyen szimmetriasértő fázis amire, az eddigi ismereteink alapján, nincs példa rövidtávú kölcsönhatások esetén.

A 7. fejezet a kvantumos megoszthatósági problémával foglalkozik, ennek lényege a következő: Aliz és Bob kapnak egy-egy, n_{A} illetve n_{B} méretű, kompozit kvantumrendszert, amik ugyanannak a Hilbert-térnek a másolataiból állnak. Lehetséges-e, hogy a kettőjük összetett rendszere olyan kvantumállapotban legyen, ami mellett minden kétrészű alrendszer, aminek egyik része Alizé a másik pedig Bobé, ugyanabban a ρ kvantumállapotban van? Ha egy adott ρ kétrészű kvantumállapotra ez lehetséges, akkor ρ-t n_{A}-n_{B} megoszthatónak nevezzük. Egyrészt a tiszta, összefonódott állapotok nyilvánvalóan nem, vagyis a terminológiánk szerint csupán 1-1 megoszthatóak. Másrészt pedig, a szeparábilis állapotok pontosan megegyeznek a tetszőlegesen, vagyis ∞-∞ megoszthető állapotokkal. Általában véve azt lehet elmondani, hogy egy állapot minél jobban összefonódott, annál kevésbé megosztható.

Abból a célból, hogy a problémát némileg megközelíthetőbbé tegyem, leszűkítem a lehetséges ρ kvantumállapotok halmazát két U(d)-szimmetrikus állapotcsaládra: A Werner-állapotokra, amik invariánsak a globális unitér transzformációkra, valamint az izotropikus állapotokra, amik invariánsak az $U \otimes U^*$ alakú transzformációkra, ahol $U \in \mathrm{U}(d)$, és $*$ a komplex konjugálást jelöli. Mindkét állapotcsalád fontos szerepet játszik a kvantum-összefonódás megértésében, különösképp a Werner-állapotok, amiket eredetileg ugyanabban a cikkben definiáltak mint magát az összefonódást [68]. A megoszthatósági probléma inherens kétrészű permutációs szimmetriájának, valamint az általam vizsgált állapotok unitér szimmetriájának köszönhetően, lehetséges a problémát ábrázoláselmélet segítségével megoldani. Korábban ugyanebből a megközelítésből indult ki Johnson és Viola [78], akiknek sikerült szükséges és elégséges feltételeket megadniuk a Werner- és izotropikus állapotok 1-n_{B} megoszthatóságára. A munkám során ezt az eredményt kiterjesztem n_{A} és n_{B} tetszőleges értékeire.

Megmutattam, hogy az n_{A}-n_{B} megoszthető Werner- és izotropikus állapotok

meghatározása ekvivalens bizonyos, a 8.4. egyenlet Hamilton-operátorához hasonó, lineáris operátorok extremális sajátértékeinek megtalálásával. A korábbi, kétrészű spinmodell alapállapoti problémájához hasonlóan, ezeknek a lineáris operátoroknak a sajátértékeit is Young-diagramok hármasaival lehetséges címkézni. A diagramok kompatibilitáshoz szükséges feltételeket pedig ismét a Littlewood–Richardson szabály adja. Az extremális sajátértékek megadásához a kétrészű spinrendszer alapállapoti problémájának megoldásához használt módszert terjesztem ki tetszőleges dimenzióra. Ehhez különösen fontosnak bizonyultak Lam [144] és Azenhas [145] eredményei amik meghatározzák a Littlewood–Richardson algoritmusban megjelenő Young-diagramok parciális rendezését.

A Werner- és az izotropikus állapotokat is lehetséges egyetlen paraméterrel leírni, lásd a 4.12. és a 4.18. egyenleteket. Adott n_{L} és n_{R} esetén az n_{L}-n_{R} megosztható állapotok a megfelelő standard paraméterekben egy-egy intervallumnak felelnek meg amiknek csak az egyik végpontja nem-triviális. Werner-állapotokra ez az intervallum $[\phi_{n_{\mathrm{L}}n_{\mathrm{R}}}, 1]$, izotropikus állapotokra pedig $[0, \psi_{n_{\mathrm{L}}n_{\mathrm{R}}}]$. Az eredményem a $\phi_{n_{\mathrm{L}}n_{\mathrm{R}}}$ (a 7.36. illetve 7.37. egyenletek) illetve $\psi_{n_{\mathrm{L}}bn_{\mathrm{R}}}$ (a 7.47. e-gyenlet) extremális pontok meghatározása.

Thesis points

1. Through representation theoretic considerations, I exactly diagonalized the Hamiltonian of the spin-1 bilinear-biquadratic model on the complete graph (Eq. (5.3)), and analyzed its ground state as a function of the external control parameter θ. I have found that the model has four distinct ground state phases belonging to different symmetry sectors. There is a ferromagnetic phase, a gapless partially magnetized phase in which the quantum numbers describing the ground state change gradually with θ, a completely permutation symmetric SU(2) singlet phase, and a phase in which the ground state is both an SU(2) and SU(3) singlet. I have a published paper in Journal of Physics A about this topic [1].

2. I exactly diagonalized the collective bipartite exchange Hamiltonian (Eq. (6.4)) in the thermodynamic limit, and studied its ground state as a function of the external control parameter θ. The model has five different ground state phases: A ferromagnetic phase, a Néel-type antiferromagnetic phase with ferromagnetically aligned bipartite subsystems, an SU(3) singlet phase, a gapless partially magnetized phase in which the ground state changes gradually with the control parameter, and a bipartite symmetry breaking phase in which two subsystems are characterized by different SU(3) representations. I have published a paper about this topic in Physical Review B [2].

3. I have determined necessary and sufficient conditions for the n_{A}-n_{B} shareability of SU(d) Werner and isotropic states, for arbitrary values of $n_{\mathrm{A}}, n_{\mathrm{B}}$, and d. As of the writing of this thesis, I have a preprint available about this topic [3].

Appendix A

A faithful representation generates the representation ring

This appendix is dedicated to Proposition 7 of the main text. The proposition is essentially a corollary of a Galois correspondence between the representation subrings, and normal, closed subgroups of a compact group. In order to expand on this topic, we have to define the ring of representations, or group characters, and some related concepts. This appendix is entirely optional, we do not refer to these definitions elsewhere in the thesis. First, we recount the proposition in question:

Proposition 21. *For a compact group G, and a faithful, unitary, finite dimensional representation D, every G-irrep appears in the irreducible decomposition of $D^{\otimes N} \otimes \overline{D}^{\otimes M}$ for some $N, M \in \mathbb{N}$.*

The irreps of a compact group are in a one-to-one correspondence with their characters; making use of this, we define the representation ring in terms of characters. We denote the character of the unitary, finite dimensional representation D_μ as χ_{D_μ}. Characters have the properties,

$$\begin{aligned} &\chi_{D_\mu \oplus D_\nu} = \chi_{D_\mu} + \chi_{D_\nu}, \quad \chi_{\overline{D_\mu}} = \chi^*_{D_\mu} \quad \text{and} \\ &\chi_{D_\mu \otimes D_\nu} = \chi_{D_\mu}\chi_{D_\nu}. \end{aligned} \tag{A.1}$$

Let I_G denote the set of characters of irreps, or irreducible characters. A product of characters decomposes into a sum of irreducible characters according to the fusion rules of G:

$$\text{If} \quad D_\mu \otimes D_\nu = \bigoplus_\lambda m^\lambda_{\mu,\nu} D_\lambda \quad \text{then} \quad \chi_{D_\mu}\chi_{D_\nu} = \sum_{\chi_{D_\lambda} \in I_G} m^\lambda_{\mu,\nu}\chi_{D_\lambda}. \tag{A.2}$$

We define the representation ring $\mathcal{R}(G)$, as the set of the pointwise $\mathbb{Z}$-linear combinations of characters of G, a.k.a. generalized characters, equipped with complex

conjugation, and the multiplication given by the $\mathbb{Z}$-linear extension of the fusion rules, Eq. (A.2). In this way, $\mathcal{R}(G)$ carries the same information as the fusion rules.

$\mathcal{R}(G)$ has a natural partial order: For any $\chi_\mu, \chi_\nu \in \mathcal{R}(G)$, $\chi_\mu \prec \chi_\nu$ iff $\chi_\nu - \chi_\mu$ is a character of some representation. This makes the set of characters of G the positive cone, $\mathcal{R}(G)^+$, of $\mathcal{R}(G)$ w.r.t. this partial order.

The irreducible characters, I_G are the minimal elements in $\mathcal{R}(G)^+$, and form a basis of $\mathcal{R}(\mathcal{G})$. A subring $\mathcal{R} \subseteq \mathcal{R}(G)$, is a representation subring if it is spanned by a set of irreducible characters.

Proposition 21 is a straightforward consequence of the following Galois correspondence. This result is originally from [146], but the form we use here is given in [147].

Theorem 6. *Representation subrings $\mathcal{R} \subseteq \mathcal{R}(G)$ and closed normal subgroups $H \subseteq G$ are in a one-one correspondence,*

$$H_R = \{g \in G \mid g \in \ker(\chi), \forall \chi \in R^+\}, \tag{A.3}$$

$$R_H^+ = \{\chi \in \mathcal{R}(G)^+ \mid g \in \ker(\chi), \forall g \in H\}. \tag{A.4}$$

Where in the context of characters, the kernel $\ker(\chi) = \chi^{-1}(\chi(\mathrm{Id}))$. Consider the representation subring with positive cone $R^+_{\ker(\chi)}$ for some character $\chi \in \mathcal{R}(G)^+$. This is the smallest representation subring that contains χ. Indeed, assume that the representation subring corresponding to $R^+_{\ker(\chi)}$ contains an other representation subring. According to Theorem 6, it must then correspond to a closed normal subgroup H such that $\ker(\chi) \subset H \subseteq G$. In this case, $\chi \notin R_H^+$ since $\ker(\chi)$ does not contain H.

Now assume that χ is the character of a faithful representation, i.e., $\ker(\chi) = \{e\}$. This means $\mathcal{R}^+_{\ker(\chi)} = \mathcal{R}(G)^+$, thus the representation subring generated by $\ker(\chi)$ is the entire representation ring of G. This proves Proposition 21, as by definition, the representation subring generated by is spanned by the irreducible characters that appear in the irrep decomposition of $\chi^n(\chi^*)^m$ for some $n, m \in \mathbb{N}$.

Appendix B

A quantum de Finetti bound for shareability

In this appendix, we derive a bound on the trace norm distance between n_{L}-n_{R} shareable and separable states, as outlined in Section 4.1, by applying the technique used in finite quantum de Finetti theorems [53–56].

Proposition 22. *Let $\rho \in \mathcal{S}(\mathcal{H}_{\mathrm{L}} \otimes \mathcal{H}_{\mathrm{R}})$, where $\dim \mathcal{H}_{\mathrm{L}} = \dim \mathcal{H}_{\mathrm{R}}$, be n_{L}-n_{R} shareable. Then there exists a separable state, $\sigma \in \mathcal{S}(\mathcal{H}_{\mathrm{L}} \otimes \mathcal{H}_{\mathrm{R}})$ such that*

$$||\rho - \sigma||_1 \leq 2 - \frac{2n_{\mathrm{L}}n_{\mathrm{R}}}{(d+n_{\mathrm{L}})(d+n_{\mathrm{R}})}. \tag{B.1}$$

Proof. Let $\hat{\rho} \in \mathcal{S}(\mathcal{H}_{\mathrm{L}}^{\vee n_{\mathrm{L}}} \otimes \mathcal{H}_{\mathrm{R}}^{\vee n_{\mathrm{R}}})$ be a left-right permutation symmetric sharing state for $\rho \in \mathcal{S}(\mathcal{H}_{\mathrm{L}} \otimes \mathcal{H}_{\mathrm{R}})$. We start by defining a measurement on $\mathcal{H}_{\mathrm{L}}^{\vee n_{\mathrm{L}}} \otimes \mathcal{H}_{\mathrm{R}}^{\vee n_{\mathrm{R}}}$ comprised of left-right permutation symmetric pure product states. First, we fix a normalized element, $|\phi_0\rangle$, on our one-particle Hilbert spaces. The pure states we measure in are of the form $|\phi(U_{\mathrm{L}}, U_{\mathrm{R}})\rangle = (U_{\mathrm{L}}|\phi_0\rangle)^{\otimes n_{\mathrm{L}}} \otimes (U_{\mathrm{R}}|\phi_0\rangle)^{\otimes n_{\mathrm{R}}}$, where $U_{\mathrm{L}}, U_{\mathrm{R}} \in \mathrm{U}(d)$, and the PVM is constructed by looping over all unitaries U_{L} and U_{R}. We must confirm that this really defines a PVM, and find an appropriate normalizing constant. For this reason, consider the integral over the Haar measure of $\mathrm{U}(d)$:

$$\begin{aligned}\int \mathrm{d}U_{\mathrm{L}} dU_{\mathrm{R}} \left(U_{\mathrm{L}}|\phi_0\rangle\langle\phi_0|U_{\mathrm{L}}^\dagger\right)^{\otimes n_{\mathrm{L}}} \otimes \left(U_{\mathrm{R}}|\phi_0\rangle\langle\phi_0|U_{\mathrm{R}}^\dagger\right)^{\otimes n_{\mathrm{R}}} = \\ \frac{1}{a(n_{\mathrm{L}}, n_{\mathrm{R}})} \Pi_{n_{\mathrm{L}}}^{+(\mathrm{L})} \otimes \Pi_{n_{\mathrm{R}}}^{+(\mathrm{R})},\end{aligned} \tag{B.2}$$

where $\Pi_{n_{\mathrm{L}}}^{+(\mathrm{L})}$ and $\Pi_{n_{\mathrm{R}}}^{+(\mathrm{R})}$ denote the projections to the symmetric subspaces $\mathcal{H}_L^{\vee n_{\mathrm{L}}}$ and $\mathcal{H}_R^{\vee n_{\mathrm{R}}}$. The equality follows from Schur's lemma, and the fact that $\Pi_{n_{\mathrm{L}}}^{+(\mathrm{L})}$ and $\Pi_{n_{\mathrm{R}}}^{+(\mathrm{R})}$ project to irreducible subspaces of $D_{n_{\mathrm{L}}}^{\mathrm{U}(d)}$ and $D_{n_{\mathrm{R}}}^{\mathrm{U}(d)}$ respectively. The constant, $a(n_{\mathrm{L}}, n_{\mathrm{R}})$ can be determined by taking the trace of both sides of Eq. (B.2),

$$a(n_{\mathrm{L}}, n_{\mathrm{R}}) = \dim(\mathcal{H}_{\mathrm{L}}^{\vee n_{\mathrm{L}}})\dim(\mathcal{H}_{\mathrm{R}}^{\vee n_{\mathrm{R}}}) = \binom{d+n_{\mathrm{L}}-1}{n_{\mathrm{L}}}\binom{d+n_{\mathrm{R}}-1}{n_{\mathrm{R}}}. \tag{B.3}$$

We conclude that the measurements,

$$E(U_{\mathrm{L}}, U_{\mathrm{R}}) = a(n_{\mathrm{L}}, n_{\mathrm{R}})\left(U_{\mathrm{L}}|\phi_0\rangle\langle\phi_0|U_{\mathrm{L}}^{\dagger}\right)^{\otimes n_{\mathrm{L}}} \otimes \left(U_{\mathrm{R}}|\phi_0\rangle\langle\phi_0|U_{\mathrm{R}}^{\dagger}\right)^{\otimes n_{\mathrm{R}}}, \tag{B.4}$$

really form a PVM on $\mathcal{H}_{\mathrm{L}}^{\vee n_{\mathrm{L}}} \otimes \mathcal{H}_{\mathrm{R}}^{\vee n_{\mathrm{R}}}$.

Next, we prepare the uncorrelated state, $U_{\mathrm{L}}|\phi_0\rangle\langle\phi_0|U_{\mathrm{L}}^{\dagger} \otimes U_{\mathrm{R}}|\phi_0\rangle\langle\phi_0|U_{\mathrm{R}}^{\dagger}$ with probability $\mathrm{Tr}(\hat{\rho}E(U_{\mathrm{L}}, U_{\mathrm{R}}))$ for all unitaries U_{L} and U_{R}. This results in the separable state:

$$\begin{aligned}\sigma = a(n_{\mathrm{L}}, n_{\mathrm{R}})\mathrm{Tr}_{\mathrm{LR}} \int \mathrm{d}U_{\mathrm{L}}\mathrm{d}U_{\mathrm{R}} \left[\left(U_{\mathrm{L}}|\phi_0\rangle\langle\phi_0|U_{\mathrm{L}}^{\dagger}\right)^{\otimes n_{\mathrm{L}}+1} \otimes \left(U_{\mathrm{R}}|\phi_0\rangle\langle\phi_0|U_{\mathrm{R}}^{\dagger}\right)^{\otimes n_{\mathrm{R}}+1}\right] \cdot \\ \hat{\rho} \otimes \mathbb{1}^{(\mathrm{L})} \otimes \mathbb{1}^{(\mathrm{R})} = \\ \frac{a(n_{\mathrm{L}}, n_{\mathrm{R}})}{a(n_{\mathrm{L}}+1, n_{\mathrm{R}}+1)}\mathrm{Tr}_{\mathrm{LR}}\left((\Pi_{n_{\mathrm{L}}+1}^{+(\mathrm{L})} \otimes \Pi_{n_{\mathrm{R}}+1}^{+(\mathrm{R})})(\hat{\rho} \otimes \mathbb{1}^{(\mathrm{L})} \otimes \mathbb{1}^{(\mathrm{R})})\right),\end{aligned} \tag{B.5}$$

where Tr_{LR} denotes the partial trace over the original n_{L} left and n_{R} right Hilbert spaces.

We simplify Eq. (B.5), by making use of the permutation symmetry of $\hat{\rho}$. The projectors to the symmetric subspaces can be expressed with permutations in the form $\Pi_{n_{\mathrm{L}}}^{+} = \frac{1}{n_{\mathrm{L}}!}\sum_{\pi \in S_{n_{\mathrm{L}}}} D_{n_{\mathrm{L}}}^{S_{n_{\mathrm{L}}}}(\pi)$. Unfortunately, the projectors in Eq. (B.5) decompose to $S_{n_{\mathrm{L}}+1}$ and $S_{n_{\mathrm{R}}+1}$ permutations, while $\hat{\rho}$ is only invariant to $S_{n_{\mathrm{L}}}$ and $S_{n_{\mathrm{R}}}$ permutations. This problem can be dealt with by using the fact that, for every $\pi \in S_{n_{\mathrm{L}}+1}$, there is a unique decomposition, $D_{n_{\mathrm{L}}+1}^{S_{n_{\mathrm{L}}+1}}(\pi) = D_{n_{\mathrm{L}}}^{S_{n_{\mathrm{L}}}}(\pi')F_{i,n_{\mathrm{L}}+1}$, where $\pi' \in S_{n_{\mathrm{L}}}$, $i \in [1, n_{\mathrm{L}}+1]$ and $F_{i,n_{\mathrm{L}}+1}$ is the flip operator, that exchanges the i-th and $n_{\mathrm{L}}+1$-th elements of the tensor product. Accordingly, $\Pi_{n_{\mathrm{L}}+1}^{+} = \frac{1}{n_{\mathrm{L}}+1!}\sum_{\pi \in S_{n_{\mathrm{L}}}}\sum_{i=1}^{n_{\mathrm{L}}+1} D_{n_{\mathrm{L}}}^{S_{n_{\mathrm{L}}}}(\pi)F_{i,n_{\mathrm{L}}+1}$, and σ becomes,

$$\begin{aligned}\sigma = \frac{a(n_{\mathrm{L}}, n_{\mathrm{R}})}{a(n_{\mathrm{L}}+1, n_{\mathrm{R}}+1)}\frac{1}{(n_{\mathrm{L}}+1)(n_{\mathrm{R}}+1)} \cdot \\ \mathrm{Tr}_{\mathrm{LR}}\left(\left(\sum_{i=1}^{n_{\mathrm{L}}+1} F_{i,n_{\mathrm{L}}+1}^{(L)}\right) \otimes \left(\sum_{j=1}^{n_{\mathrm{R}}+1} F_{j,l+1}^{(\mathrm{R})}\right)(\hat{\rho} \otimes \mathbb{1}^{(\mathrm{L})} \otimes \mathbb{1}^{(\mathrm{R})})\right).\end{aligned} \tag{B.6}$$

In order to evaluate the product of the flip operators with $\hat{\rho}$, we have to separate the sums to different cases. If $i = n_{\mathrm{L}}+1$ or $j = n_{\mathrm{R}}+1$, then the corresponding flip operator is simply the identity. If either $i \neq n_{\mathrm{L}}+1$, $j \neq n_{\mathrm{R}}+1$, or both, we use that $\mathrm{Tr}_{\mathrm{LR}}\left(F_{i,n_{\mathrm{L}}+1}F_{j,n_{\mathrm{R}}+1}\hat{\rho} \otimes \mathbb{1}^{(\mathrm{L})} \otimes \mathbb{1}^{(\mathrm{R})}\right) = \rho$, and $\mathrm{Tr}_{\mathrm{LR}}\left(F_{i,n_{\mathrm{L}}+1}^{(\mathrm{L})}\hat{\rho} \otimes \mathbb{1} \otimes \mathbb{1}\right) = \mathrm{Tr}_{\mathrm{R}}\rho \otimes \mathbb{1}$ (similarly for the $F_{j,n_{\mathrm{R}}+1}^{(\mathrm{R})}$ case). Both of these identities can be confirmed simply,

e.g., by expanding everything in the basis of matrix units. After separating the cases and simplifying the coefficients, σ becomes:

$$\begin{aligned}\sigma =&\frac{1}{(d+n_{\mathrm{L}})(d+n_{\mathrm{R}})}\cdot \\ &\left(d^2\frac{\mathbb{1}^{(\mathrm{L})}\otimes\mathbb{1}^{(\mathrm{R})}}{d^2}+dn_{\mathrm{L}}\mathrm{Tr}_{\mathrm{R}}\rho\otimes\frac{\mathbb{1}^{(\mathrm{R})}}{d}+dn_{\mathrm{R}}\frac{\mathbb{1}^{(\mathrm{L})}}{d}\otimes\mathrm{Tr}_{\mathrm{L}}\rho+n_{\mathrm{L}}n_{\mathrm{R}}\rho\right).\end{aligned} \tag{B.7}$$

From here, the statement follows by applying the triangle inequality to $||\rho-\sigma||_1$. □

Appendix C

Expressing the BLBQ Hamiltonian with Casimir operators

In this section, we show the equivalence of the interaction Hamiltonian,

$$H_{12} = \sin(\theta) C_2^{\mathrm{SU}(3)} + \cos(\theta) C_2^{\mathrm{SU}(2)}, \tag{C.1}$$

with the traditional form of the bilinear-biquadratic Hamiltonian,

$$H_{12} = \cos(\gamma) \mathbf{S}_1 \mathbf{S}_2 + \sin(\gamma) (\mathbf{S}_1 \mathbf{S}_2)^2. \tag{C.2}$$

Instead of the generators $E^{\alpha\beta}$ defined in Eq. (3.54) of Section 3.8, we express the two-particle Casimir operator $C_2^{SU(2)}$, in the more conventional form of with spin operators S^α corresponding to the spin-1 representation of SU(2):

$$C_2^{\mathrm{SU}(2)} = \sum_{\mu=1}^{3} [S_1^\mu S_1^\mu + S_2^\mu S_2^\mu + 2 S_1^\mu S_2^\mu] = 4 \mathbb{1} + \sum_{\mu=1}^{3} 2 S_1^\mu S_2^\mu, \tag{C.3}$$

Here, we take into account, that the one-site Casimir operators are proportional to $\mathbb{1}$. The remaining task is expressing $C_2^{\mathrm{SU}(3)}$ with the "bilinear", $\mathbf{S}_1 \mathbf{S}_2$, and the "biquadratic", $(\mathbf{S}_1 \mathbf{S}_2)^2$, spin terms.

The two-particle Hilbert space, $\mathbb{C}^3 \otimes \mathbb{C}^3$, decomposes into spin 0, 1 and 2 irreducible subspaces under global SU(2) transformations. We denote the orthogonal projections to these subspaces by P_s, $s \in \{0, 1, 2\}$. These projections fulfill,

$$\mathbb{1} = P_0 + P_1 + P_2, \quad \text{and} \quad C_2^{\mathfrak{su}(2)} = 2 P_1 + 6 P_2. \tag{C.4}$$

Furthermore, with the help of Eq. (C.3), we can express the bilinear and biquadratic spin terms with the projections P_s as

$$\sum_{\mu=1}^{3} S_1^\mu S_2^\mu = -2P_0 - P_1 + P_2 \quad \text{and} \quad \left(\sum_{\mu=1}^{3} S_1^\mu S_2^\mu\right)^2 = 4P_0 + P_1 + P_2. \tag{C.5}$$

By inverting these relations, we obtain

$$P_0 = -\frac{1}{3}\mathbb{1} + \frac{1}{3}\left(\sum_{\mu=1}^{3} S_1^\mu S_2^\mu\right)^2, \tag{C.6a}$$

$$P_1 = \mathbb{1} - \frac{1}{2}\sum_{\mu=1}^{3} S_1^\mu S_2^\mu - \frac{1}{2}\left(\sum_{\mu=1}^{3} S_1^\mu S_2^\mu\right)^2, \tag{C.6b}$$

$$P_2 = \frac{1}{3}\mathbb{1} + \frac{1}{2}\sum_{\mu=1}^{3} S_1^\mu S_2^\mu + \frac{1}{6}\left(\sum_{\mu=1}^{3} S_1^\mu S_2^\mu\right)^2. \tag{C.6c}$$

Under global SU(3) transformations, the two-particle Hilbert space decomposes into irreducible subspaces labeled by $(2,0)$ and $(1,1)$; which are respectively the symmetric and antisymmetric subspaces of $\mathbb{C}^3 \otimes \mathbb{C}^3$. Since $\mathrm{SU}(2) \subset \mathrm{SU}(3)$, these irreducible subspaces must decompose into direct sums of the SU(2) irreducible subspaces. Indeed, according to Eq. (5.16), the symmetric subspace decomposes as

$$P_{(2,0)} = P_0 + P_2, \quad \text{which leaves,} \quad P_{(1,1)} = P_1. \tag{C.7}$$

After taking into account the eigenvalues of $C_2^{\mathrm{SU}(3)}$, that are given in Eq. (3.58), we can express $C_2^{\mathrm{SU}(3)}$ with the bilinear and biquadratic spin terms:

$$\begin{aligned} C_2^{\mathrm{SU}(3)} = \frac{20}{3}P_{(2,0)} + \frac{8}{3}P_{(1,1)} = \frac{20}{3}P_0 + \frac{8}{3}P_1 + \frac{20}{3}P_2 = \\ \frac{8}{3}\mathbb{1} + 2\sum_{\mu=1}^{3} S_1^\mu S_2^\mu + 2\Big(\sum_{\mu=1}^{3} S_1^\mu S_2^\mu\Big)^2. \end{aligned} \tag{C.8}$$

This concludes the proof. According to the Eqs. (C.8) and (C.3), the conversion between the angle parameters θ and γ used in Eqs. (C.1) and (C.2) is given by

$$1 + \mathrm{ctg}(\theta) = \mathrm{ctg}(\gamma). \tag{C.9}$$

Appendix D

The minimum Young diagram in the SU(3) tensor product

In this appendix, we prove Proposition 16, which we recount here:

Proposition 23. *The minimum diagram with respect to dominance order in the irrep decomposition of* $D^{\mathrm{SU}(3)}_{\lambda^{(\mathrm{A})}} \otimes D^{\mathrm{SU}(3)}_{\lambda^{(\mathrm{B})}}$*, is the last diagram that the direct sum in the closed formula, Eq. (3.53), for the irrep decomposition loops through. That is, the diagram*

$$\begin{aligned}\lambda(k_{2,1}, k_{2,2}, k_{1,1}) = \\ (\lambda_1^{(\mathrm{A})} + \lambda_1^{(\mathrm{B})} - k_{2,1} - k_{2,2}, \lambda_2^{(\mathrm{A})} + \lambda_2^{(\mathrm{B})} - k_{1,1} + k_{2,2}, k_{2,1} + k_{1,1}),\end{aligned} \tag{D.1}$$

for which all three running indices take their maximum values:

$$\begin{aligned} k_{2,1} &= u(1,1) = min\{\mu_1 - \mu_2, \lambda_2^{(\mathrm{A})}\} \\ k_{2,2} &= u(1,2)|_{u(1,1)} = min\{\lambda_1^{(\mathrm{A})} - \lambda_2^{(\mathrm{A})}, \lambda_1^{(\mathrm{B})} - u(1,1)\}, \\ k_{1,1} &= u(2,1)|_{u(1,1),u(1,2)} = min\{\lambda_2^{(\mathrm{A})} + u(1,2) - u(1,1), \lambda_2^{(\mathrm{B})}\}. \end{aligned} \tag{D.2}$$

Proof. For every diagram in the product, labeled by the indices $(k'_{2,1}, k'_{2,2}, k'_{1,1})$, we construct a sequence of diagrams starting from our proposed minimum diagram, and ending with $\lambda(k'_{2,1}, k'_{2,2}, k'_{1,1})$, then show that every diagram in the sequence dominates the previous one. The sequence in question is:

$$\begin{aligned} &\lambda(u(1,1), u(1,2), u(2,1)), \lambda(u(1,1)-1, u(1,2), u(2,1)), \\ &\lambda(u(1,1)-2, u(1,2), u(2,1)), \ldots, \lambda(k'_{2,1}, u(1,2), u(2,1)), \\ &\lambda(k'_{2,1}, u(1,2)-1, u(2,1)), \lambda(k'_{2,1}, u(1,2)-2, u(2,1)), \ldots, \lambda(k'_{2,1}, k'_{2,2}, u(2,1)), \\ &\lambda(k'_{2,1}, k'_{2,2}, u(2,1)-1), \lambda(k'_{2,1}, k'_{2,2}, u(2,1)-2), \ldots, \lambda(k'_{2,1}, k'_{2,2}, k'_{1,1}). \end{aligned} \tag{D.3}$$

Although, we used a shortened notation for the shake of convenience, it is implied that the values of $u(j,h)$ may depend on the values of the other running indices;

e.g.: $\lambda(k'_{2,1}, k'_{2,2}, u(2,1))$ should actually be $\lambda(k'_{2,1}, k'_{2,2}, u(2,1)|_{k'_{2,1},k'_{2,2}})$. Since in the sequence we change the indices $k_{d-j,h}$ in the order that they appear in the nested direct sums of Eq. (3.53), all diagrams of the sequence correspond to a valid product diagram. We also note that the same diagram may appear in the sequence for multiple sets of the $k_{d-j,h}$ indices.

We divide the sequence in Eq. (D.3) into three subsequences, each of which consists of elements that differ in only one of the $k_{d-j,h}$ indices. We show that each subsequence is increasing in dominance order, starting with the most simple case of the last one. For this, we need to show that $\lambda(k_{2,1}, k_{2,2}, k_{1,1}) \trianglelefteq \lambda(k_{2,1}, k_{2,2}, k_{1,1}-1)$ for all valid distributions of $k_{d-j,h}$ indices. Let us define

$$\Delta_j^{(3)} = \sum_{i=1}^{j} \left[\lambda_i(k_{2,1}, k_{2,2}, k_{1,1}-1) - \lambda_i(k_{2,1}, k_{2,2}, k_{1,1})\right]. \tag{D.4}$$

According to Definition 2, $\lambda(k_{2,1}, k_{2,2}, k_{1,1}) \trianglelefteq \lambda(k_{2,1}, k_{2,2}, k_{1,1}-1)$ iff $\Delta_j^{(3)} \geq 0$ for $j = 1, 2, 3$. Since we have $\sum_{i=1}^{3} \lambda_i(k_{2,1}, k_{2,2}, k_{1,1}) = 2N$ for all diagrams in the product, $\Delta_3 = 0$ in all cases. Moreover, simple substitution into Eq. (D.1) gives us $\Delta_1 = 0$ and $\Delta_2 = 1$.

We continue with the second subsequence. Similarly to the last case, we need to show that $\Delta_j^{(2)} \geq 0$ for $j = 1, 2, 3$ and all valid distributions of the $k_{d-j,h}$ indices, where $\Delta_j^{(2)}$ is defined as:

$$\Delta_j^{(2)} = \sum_{i=1}^{j} \left[\lambda_i(k_{2,1}, k_{2,2}-1, u(2,1)|_{k_{2,1},k_{2,2}-1}) - \lambda_i(k_{2,1}, k_{2,2}, u(2,1)|_{k_{2,1},k_{2,2}})\right]. \tag{D.5}$$

Again, we have $\Delta_3^{(2)} = 0$, and substitution into Eq. (D.1) gives $\Delta_1^{(2)} = 1$. For $\Delta_2^{(2)}$, the min function in the definition of $u(2,1)$ gives us multiple cases:

$$\Delta_2 = \min(\lambda_2^{(\mathrm{A})} + k_{2,2} - k_{2,1}, \lambda_2^{(\mathrm{B})}) - \min(\lambda_2^{(\mathrm{A})} + k_{2,2} - k_{2,1} - 1) = \begin{cases} 0 & \text{if} \quad \mu_2 \leq \lambda_2^{(\mathrm{A})} + k_{2,2} - k_{2,1} - 1 \\ 1 & \text{if} \quad \mu_2 > \lambda_2^{(\mathrm{A})} + k_{2,2} - k_{2,1} - 1 \end{cases}. \tag{D.6}$$

For the first subsequence we define

$$\Delta_j^{(1)} = \sum_{i=1}^{j} \Big[\lambda_i(k_{2,1}-1, u(1,2)|_{k_{2,1}-1}, u(2,1)|_{k_{2,1}-1,u(1,2)|_{k_{2,1}-1}}) - \lambda_i(k_{2,1}, u(1,2)|_{k_{2,1}}, u(2,1)|_{k_{2,1},u(1,2)|_{k_{2,1}}})\Big], \tag{D.7}$$

and show that independently of the distribution of $k_{d-j,h}$, $\Delta_j^{(1)} \geq 0$ for $j = 1, 2, 3$. Similarly to the previous cases, $\Delta_3^{(1)} = 0$. Taking only the first row of λ into account gives us,

$$\Delta_1^{(1)} = \min(\lambda_1^{(\mathrm{A})} - \lambda_2^{(\mathrm{A})}, \lambda_1^{(\mathrm{B})} - k_{2,1}) - \min(\lambda_1^{(\mathrm{A})} - \lambda_2^{(\mathrm{A})}, \lambda_1^{(\mathrm{B})} - k_{2,1} + 1) + 1 = \begin{cases} 1 & \text{if} \quad \lambda_1^{(\mathrm{A})} - \lambda_2^{(\mathrm{A})} \leq \lambda_1^{(\mathrm{B})} - k_{2,1} \\ 0 & \text{if} \quad \lambda_1^{(\mathrm{A})} - \lambda_2^{(\mathrm{A})} > \lambda_1^{(\mathrm{B})} - k_{2,1} \end{cases} . \tag{D.8}$$

The contributions of the second row contain min functions embedded into each other, this gives us a multitude of cases in $\Delta_2^{(1)}$,

$$\begin{aligned} \Delta_2^{(1)} = &\min\left(\lambda_2^{(\mathrm{A})} - k_{2,1} + \min(\lambda_1^{(\mathrm{A})} - \lambda_2^{(\mathrm{A})}, \lambda_1^{(\mathrm{B})} - k_{2,1}), \lambda_2^{(\mathrm{B})}\right) - \\ &\min\left(\lambda_2^{(\mathrm{A})} - k_{2,1} + \min(\lambda_1^{(\mathrm{A})} - \lambda_2^{(\mathrm{A})}, \lambda_1^{(\mathrm{B})} - k_{2,1} + 1) + 1, \lambda_2^{(\mathrm{B})}\right) + 1 = \\ &\begin{cases} 1 & \text{if} \quad \lambda_1^{(\mathrm{A})} - \lambda_2^{(\mathrm{A})} \leq \lambda_1^{(\mathrm{B})} - k_{2,1} \quad \text{and} \quad \lambda_2^{(\mathrm{B})} \leq \lambda_1^{(\mathrm{A})} - k_{2,1} \\ 0 & \text{if} \quad \lambda_1^{(\mathrm{A})} - \lambda_2^{(\mathrm{A})} \leq \lambda_1^{(\mathrm{B})} - k_{2,1} \quad \text{and} \quad \lambda_2^{(\mathrm{B})} > \lambda_1^{(\mathrm{A})} - k_{2,1} \\ 1 & \text{if} \quad \lambda_1^{(\mathrm{A})} - \lambda_2^{(\mathrm{A})} > \lambda_1^{(\mathrm{B})} - k_{2,1} \quad \text{and} \quad \lambda_2^{(\mathrm{B})} \leq \lambda_2^{(\mathrm{A})} + \lambda_1^{(\mathrm{B})} - 2k_{2,1} \\ 0 & \text{if} \quad \lambda_1^{(\mathrm{A})} - \lambda_2^{(\mathrm{A})} > \lambda_1^{(\mathrm{B})} - k_{2,1} \quad \text{and} \quad \lambda_2^{(\mathrm{B})} - 1 = \lambda_2^{(\mathrm{A})} + \lambda_1^{(\mathrm{B})} - 2k_{2,1} \\ -1 & \text{if} \quad \lambda_1^{(\mathrm{A})} - \lambda_2^{(\mathrm{A})} > \lambda_1^{(\mathrm{B})} - k_{2,1} \quad \text{and} \quad \lambda_2^{(\mathrm{B})} - 1 > \lambda_2^{(\mathrm{A})} + \lambda_1^{(\mathrm{B})} - 2k_{2,1} \end{cases} . \end{aligned} \tag{D.9}$$

The last case of Eq. (D.9) poses a problem. If a $\lambda(k_{2,1}, k_{2,2}, k_{1,1})$ product diagram with a $k_{2,1}$ index that satisfies the conditions of the last case exists, then the first subsequence of Eq. (D.3) is not necessarily increasing. Let us take a further look at these conditions. Since $k_{2,1} \geq 0$ the first condition, $\lambda_1^{(\mathrm{A})} - \lambda_2^{(\mathrm{A})} > \lambda_1^{(\mathrm{B})} - k_{2,1}$, can possibly be satisfied depending on $\lambda^{(\mathrm{A})}$ and $\lambda^{(\mathrm{B})}$. We can still compare the second condition, $\lambda_2^{(\mathrm{B})} - 1 > \lambda_2^{(\mathrm{A})} + \lambda_1^{(\mathrm{B})} - 2k_{2,1}$, with the upper bound $k_{2,1} \leq u(1,1) = \min(\lambda_1^{(\mathrm{B})} - \lambda_2^{(\mathrm{B})}, \lambda_2^{(\mathrm{A})})$. This yields a necessary condition:

$$\begin{aligned} &\lambda_2^{(\mathrm{A})} + \lambda_1^{(\mathrm{B})} - 2\min(\lambda_1^{(\mathrm{B})} - \lambda_2^{(\mathrm{B})}, \lambda_2^{(\mathrm{A})}) < \lambda_2^{(\mathrm{B})} - 1 \iff \\ &(\lambda_1^{(\mathrm{B})} - \lambda_2^{(\mathrm{B})} \leq \lambda_2^{(\mathrm{A})} \text{ and } \lambda_1^{(\mathrm{B})} - \lambda_2^{(\mathrm{B})} > \lambda_2^{(\mathrm{A})} + 1) \text{ or} \\ &(\lambda_1^{(\mathrm{B})} - \lambda_2^{(\mathrm{B})} \geq \lambda_2^{(\mathrm{A})} \text{ and } \lambda_1^{(\mathrm{B})} - \lambda_2^{(\mathrm{B})} < \lambda_2^{(\mathrm{A})} - 1), \end{aligned} \tag{D.10}$$

which is a contradiction. Thus, we conclude that the sequence in Eq. (D.3) is increasing in dominance order, and consequently, the product diagram described by the indices in Eq. (D.2) is the minimum in the irrep decomposition of $D^{\mathrm{SU}(3)}_{\lambda^{(\mathrm{A})}} \otimes D^{\mathrm{SU}(3)}_{\lambda^{(\mathrm{B})}}$ with respect to dominance order. □

The author's publications

[1] D. Jakab, G. Szirmai, and Z. Zimborás, Journal of Physics A: Mathematical and Theoretical **51**, 105201 (2018).

[2] D. Jakab and Z. Zimborás, Physical Review B **103**, 214448 (2021).

[3] D. Jakab, A. Solymos, and Z. Zimborás, Extendibility of Werner States (2022), arXiv:2208.13743 [quant-ph] .

[4] D. Jakab, E. Szirmai, M. Lewenstein, and G. Szirmai, Physical Review B **93**, 064434 (2016)

Bibliography

[5] A. I. Akhiezer, S. Peletminskii, and V. G. Baryakhtar, *Spin waves* (North-Holland, 1968).

[6] J. Van Vleck, The Journal of Chemical Physics **9**, 85 (1941).

[7] D. C. Mattis, *The Theory of Magnetism I*, Springer Series in Solid-State Sciences (Springer Berlin Heidelberg, 1981) p. nil.

[8] W. Marshall, Proc. R. Soc. **232**, 48 (1955).

[9] E. Lieb and D. Mattis, Journal of Mathematical Physics **3**, 749 (1962).

[10] N. D. Mermin and H. Wagner, Physical Review Letters **17**, 1307–1307 (1966).

[11] A. Auerbach, Graduate Texts in Contemporary Physics 10.1007/978-1-4612-0869-3 (1994).

[12] H. Bethe, Zeitschrift für Physik **71**, 205–226 (1931).

[13] J. T. Chalker, P. C. W. Holdsworth, and E. F. Shender, Phys. Rev. Lett. **68**, 855 (1992).

[14] R. Moessner and J. T. Chalker, Physical Review B **58**, 12049–12062 (1998).

[15] R. Moessner and J. T. Chalker, Physical Review Letters **80**, 2929–2932 (1998).

[16] X.-G. Wen, Physical Review B **65**, 165113 (2002).

[17] P. Anderson, Materials Research Bulletin **8**, 153–160 (1973).

[18] P. Fazekas and P. W. Anderson, Philosophical Magazine **30**, 423 (1974).

[19] P. W. Anderson, science **235**, 1196 (1987).

[20] G. Baskaran, Z. Zou, and P. W. Anderson, Solid state communications **63**, 973 (1987).

[21] I. Affleck, T. Kennedy, E. H. Lieb, and H. Tasaki, Communications in Mathematical Physics **115**, 477528 (1988).

[22] I. Affleck, T. Kennedy, E. H. Lieb, and H. Tasaki, Phys. Rev. Lett. **59**, 799 (1987).

[23] P. Nataf and F. Mila, Phys. Rev. B **93**, 155134 (2016).

[24] K. Wan, P. Nataf, and F. Mila, Phys. Rev. B **96**, 115159 (2017).

[25] M. P. Nightingale and H. W. J. Blöte, Phys. Rev. B **33**, 659 (1986).

[26] K. Harada and N. Kawashima, J. Phys. Soc. Jpn. **70**, 13 (2001).

[27] K. Harada and N. Kawashima, Phys. Rev. B **65**, 052403 (2002).

[28] D. Porras, F. Verstraete, and J. I. Cirac, Phys. Rev. B **73**, 014410 (2006).

[29] K. Buchta, G. Fáth, O. Legeza, and J. Sólyom, Phys. Rev. B **72**, 054433 (2005).

[30] M. Rizzi, D. Rossini, G. De Chiara, S. Montangero, and R. Fazio, Phys. Rev. Lett. **95**, 240404 (2005).

[31] F. Verstraete, V. Murg, and J. I. Cirac, Advances in Physics **57**, 143 (2008).

[32] V. Murg, F. Verstraete, and J. I. Cirac, Physical Review A **75**, 033605 (2007).

[33] F. Verstraete and J. I. Cirac, arXiv preprint cond-mat/0407066 (2004).

[34] R. P. Feynman, Int. J. Theor. Phys **21** (1982).

[35] S. Lloyd, Science , 1073 (1996).

[36] A. Trabesinger, Nature Physics **8**, 263 (2012).

[37] R. Grimm, M. Weidemüller, and Y. B. Ovchinnikov, in *Advances in atomic, molecular, and optical physics*, Vol. 42 (Elsevier, 2000) pp. 95–170.

[38] N. Goldman, J. C. Budich, and P. Zoller, Nature Physics **12**, 639 (2016).

[39] L. W. Cheuk, M. A. Nichols, M. Okan, T. Gersdorf, V. V. Ramasesh, W. S. Bakr, T. Lompe, and M. W. Zwierlein, Physical review letters **114**, 193001 (2015).

[40] W. S. Bakr, J. I. Gillen, A. Peng, S. Fölling, and M. Greiner, Nature **462**, 74 (2009).

[41] J. F. Sherson, C. Weitenberg, M. Endres, M. Cheneau, I. Bloch, and S. Kuhr, Nature **467**, 68 (2010).

[42] J. Simon, W. S. Bakr, R. Ma, M. E. Tai, P. M. Preiss, and M. Greiner, Nature **472**, 307 (2011).

[43] A. V. Gorshkov, M. Hermele, V. Gurarie, C. Xu, P. S. Julienne, J. Ye, P. Zoller, E. Demler, M. D. Lukin, and A. M. Rey, Nature Physics **6**, 289 (2010).

[44] M. Saffman, T. G. Walker, and K. Mølmer, Rev. Mod. Phys. **82**, 2313 (2010).

[45] D. Porras and J. I. Cirac, Phys. Rev. Lett. **92**, 207901 (2004).

[46] M. E. Beverland, G. Alagic, M. J. Martin, A. P. Koller, A. M. Rey, and A. V. Gorshkov, Physical Review A **93**, 10.1103/physreva.93.051601 (2016).

[47] J. I. Cirac, M. Lewenstein, K. Mølmer, and P. Zoller, Phys. Rev. A **57**, 1208 (1998).

[48] S. Morrison and A. S. Parkins, Phys. Rev. Lett. **100**, 040403 (2008).

[49] G. Chen, J. Q. Liang, and S. Jia, Opt. Express **17**, 19682 (2009).

[50] T. Zibold, E. Nicklas, C. Gross, and M. K. Oberthaler, Phys. Rev. Lett. **105**, 204101 (2010).

[51] C.-L. Hung, A. González-Tudela, J. I. Cirac, and H. J. Kimble, Proc. Natl. Acad. Sci. U.S.A. **113**, E4946 (2016).

[52] T. Graß and M. Lewenstein, EPJ Quantum Technology **1**, 8 (2014).

[53] F. Trimborn, R. F. Werner, and D. Witthaut, J. Phys. A **49**, 135302 (2016).

[54] M. Christandl, R. König, G. Mitchison, and R. Renner, Commun. Mat. Phys. **273**, 473 (2007).

[55] Z. Ammari and F. Nier, Annales Henri Poincaré **9**, 1503 (2008).

[56] C. Krumnow, Z. Zimborás, and J. Eisert, J. Math. Phys. **58**, 122204 (2017).

[57] C. S. Jürgen Fuchs, *Symmetries, lie algebras and representations: a graduate course for physicists*, Cambridge monographs on mathematical physics (Cambridge University Press, 1997).

[58] W. Fulton and J. Harris, *Representation theory: a first course*, Vol. 129 (Springer Science & Business Media, 2013).

[59] B. E. Sagan, *The symmetric group: representations, combinatorial algorithms, and symmetric functions*, Vol. 203 (Springer Science & Business Media, 2013).

[60] A. Albert, Bulletin of the American Mathematical Society **47**, 357 (1941).

[61] F. D. Murnaghan, Bull. Amer. Math. Soc **47**, 359 (1941).

[62] G. de Beauregard Robinson, *Representation theory of the symmetric group*, 12 (Edinburgh: University Press, 1961).

[63] F. Iachello, *Lie algebras and applications*, Vol. 12 (Springer Berlin Heidelberg, 2006).

[64] D. L.-A. Richardson, Trans. Royal Soc. London , 99 (1934).

[65] G. P. Thomas, Advances in Mathematics **30**, 8 (1978).

[66] H. Schlosser, Mathematische Nachrichten **134**, 237 (1987).

[67] A. Perelomov and V. Popov, SOVIET JOURNAL OF NUCLEAR PHYSICS-USSR **3**, 676 (1966).

[68] R. F. Werner, Physical Review A **40**, 4277–4281 (1989).

[69] M. Horodecki and P. Horodecki, Physical Review A **59**, 4206 (1999).

[70] M. A. Nielsen and I. L. Chuang, *Quantum Computation and Quantum Information* (Cambridge University Press, 2009).

[71] V. Coffman, J. Kundu, and W. K. Wootters, Phys. Rev. A **61**, 052306 (2000).

[72] B. M. Terhal, IBM Journal of Research and Development **48**, 71 (2004).

[73] T. J. Osborne and F. Verstraete, Phys. Rev. Lett. **96**, 220503 (2006).

[74] J. S. Kim, G. Gour, and B. C. Sanders, Contemporary Physics **53**, 417 (2012), https://doi.org/10.1080/00107514.2012.725560 .

[75] C. H. Bennett, D. P. DiVincenzo, J. A. Smolin, and W. K. Wootters, Phys. Rev. A **54**, 3824 (1996).

[76] R. F. Werner, Letters in Mathematical Physics **17**, 359 (1989).

[77] R. F. Werner, letters in mathematical physics **19**, 319 (1990).

[78] P. D. Johnson and L. Viola, Physical Review A **88**, 032323 (2013).

[79] A. C. Doherty, Journal of Physics A: Mathematical and Theoretical **47**, 424004 (2014).

[80] A. A. Klyachko, Journal of Physics: Conference Series **36**, 72 (2006).

[81] M. Christandl, B. Doran, S. Kousidis, and M. Walter, Communications in mathematical physics **332**, 1 (2014).

[82] S. A. Ocko, X. Chen, B. Zeng, B. Yoshida, Z. Ji, M. B. Ruskai, and I. L. Chuang, Phys. Rev. Lett. **106**, 110501 (2011).

[83] D. A. Mazziotti, Chemical Reviews **112**, 244 (2012), pMID: 21863900, https://doi.org/10.1021/cr2000493 .

[84] M. Fannes, J. T. Lewis, and A. Verbeure, Letters in mathematical physics **15**, 255 (1988).

[85] R. Horodecki, P. Horodecki, M. Horodecki, and K. Horodecki, Reviews of modern physics **81**, 865 (2009).

[86] M. L. Nowakowski, Journal of Physics A: Mathematical and Theoretical **49**, 385301 (2016).

[87] S. Boyd, S. P. Boyd, and L. Vandenberghe, *Convex optimization* (Cambridge university press, 2004).

[88] A. C. Doherty, P. A. Parrilo, and F. M. Spedalieri, Phys. Rev. Lett. **88**, 187904 (2002).

[89] A. C. Doherty, P. A. Parrilo, and F. M. Spedalieri, Phys. Rev. A **69**, 022308 (2004).

[90] S. J. Benson, Y. Ye, and X. Zhang, SIAM Journal on Optimization **10**, 443 (2000).

[91] J. Lee and M. Kim, Physical review letters **84**, 4236 (2000).

[92] A. J. Short, Physical review letters **102**, 180502 (2009).

[93] N. A. Peters, J. B. Altepeter, D. Branning, E. R. Jeffrey, T.-C. Wei, and P. G. Kwiat, Phys. Rev. Lett. **92**, 133601 (2004).

[94] P. Zanardi and M. Rasetti, Physical Review Letters **79**, 3306 (1997).

[95] D. A. Lidar, I. L. Chuang, and K. B. Whaley, Physical Review Letters **81**, 2594 (1998).

[96] G. S. Agarwal and K. T. Kapale, Phys. Rev. A **73**, 022315 (2006).

[97] K. G. H. Vollbrecht and R. F. Werner, Physical Review A **64**, 062307 (2001).

[98] K. Chen, S. Albeverio, and S.-M. Fei, Reports on Mathematical Physics **58**, 325 (2006).

[99] M. Horodecki, P. Horodecki, and R. Horodecki, Physical Review A **60**, 1888 (1999).

[100] P. Rungta and C. M. Caves, Physical Review A **67**, 012307 (2003).

[101] M. Kochmański, T. Paszkiewicz, and S. Wolski, Eur. J. Phys. **34**, 1555 (2013).

[102] D. Sherrington and S. Kirkpatrick, Phys. Rev. Lett. **35**, 1792 (1975).

[103] J. Vidal, G. Palacios, and R. Mosseri, Phys. Rev. A **69**, 022107 (2004).

[104] T. J. Osborne, Phys. Rev. B **74**, 094411 (2006).

[105] L. Chayes, N. Crawford, D. Ioffe, and A. Levit, J. Stat. Phys. **133**, 131 (2008).

[106] P. R. Weiss, Phys. Rev. **74**, 1493 (1948).

[107] B. Sutherland, Phys. Rev. B **12**, 3795 (1975).

[108] N. Read and S. Sachdev, Phys. Rev. Lett. **62**, 1694 (1989).

[109] J. B. Marston and I. Affleck, Phys. Rev. B **39**, 11538 (1989).

[110] K. I. Kugel' and D. I. Khomskiĭ, Soviet Journal of Experimental and Theoretical Physics **37**, 725 (1973).

[111] D. P. Arovas and A. Auerbach, Phys. Rev. B **52**, 10114 (1995).

[112] S. K. Pati, R. R. P. Singh, and D. I. Khomskii, Phys. Rev. Lett. **81**, 5406 (1998).

[113] Y. Q. Li, M. Ma, D. N. Shi, and F. C. Zhang, Phys. Rev. Lett. **81**, 3527 (1998).

[114] K. Penc, M. Mambrini, P. Fazekas, and F. Mila, Phys. Rev. B **68**, 012408 (2003).

[115] Y. Tokura and N. Nagaosa, Science **288**, 462 (2000).

[116] K. Harada, N. Kawashima, and M. Troyer, Phys. Rev. Lett. **90**, 117203 (2003).

[117] F. F. Assaad, Phys. Rev. B **71**, 075103 (2005).

[118] M. Greiter and S. Rachel, Phys. Rev. B **75**, 184441 (2007).

[119] A. Rapp, W. Hofstetter, and G. Zaránd, Phys. Rev. B **77**, 144520 (2008).

[120] C. Xu and C. Wu, Phys. Rev. B **77**, 134449 (2008).

[121] F. D. M. Haldane, Phys. Lett. A **93**, 464 (1983).

[122] F. D. M. Haldane, Phys. Rev. Lett. **50**, 1153 (1983).

[123] L. Takhtajan, Phys. Lett. A **87**, 479 (1982).

[124] H. Babujian, Phys. Lett. A **90**, 479 (1982).

[125] H. Babujian, Nucl. Phys. B **215**, 317 (1983).

[126] G. Uimin, Pis' ma Zh. Eksp. Teor. Fiz **12**, 332 (1970).

[127] C. K. Lai, J. Mat. Phys. **15**, 1675 (1974).

[128] F. Pollmann, E. Berg, A. M. Turner, and M. Oshikawa, Phys. Rev. B **85**, 075125 (2012).

[129] A. V. Chubukov, J. Phys. Condens. Matter **2**, 1593 (1990).

[130] A. V. Chubukov, Phys. Rev. B **43**, 3337 (1991).

[131] A. Läuchli, G. Schmid, and S. Trebst, Phys. Rev. B **74**, 144426 (2006).

[132] S. Hu, A. M. Turner, K. Penc, and F. Pollmann, Phys. Rev. Lett. **113**, 027202 (2014).

[133] N. Papanicolaou, Nucl. Phys. B **305**, 367 (1988).

[134] K. Penc and A. M. Läuchli, in *Introduction to Frustrated Magnetism* (Springer Berlin Heidelberg, 2011) pp. 331–362.

[135] I. Urizar-Lanz, P. Hyllus, I. L. Egusquiza, M. W. Mitchell, and G. Tóth, Phys. Rev. A **88**, 013626 (2013).

[136] I. Apellaniz, I. Urizar-Lanz, Z. Zimboras, P. Hyllus, and G. Toth, preprint arXiv:1703.09056 (2017).

[137] M. Xu, D. A. Tieri, E. C. Fine, J. K. Thompson, and M. J. Holland, Phys. Rev. Lett. **113**, 154101 (2014).

[138] A. Roth and K. Hammerer, Phys. Rev. A **94**, 043841 (2016).

[139] J. M. Weiner, K. C. Cox, J. G. Bohnet, and J. K. Thompson, Phys. Rev. A **95**, 033808 (2017).

[140] T. Brylawski, Discrete mathematics **6**, 201 (1973).

[141] S. Friedli and Y. Velenik, *Statistical Mechanics of Lattice Systems: A Concrete Mathematical Introduction* (Cambridge University Press, 2017).

[142] I. Apellaniz, I. n. Urizar-Lanz, Z. Zimborás, P. Hyllus, and G. Tóth, Phys. Rev. A **97**, 053603 (2018).

[143] K. Lange, J. Peise, B. Lücke, I. Kruse, G. Vitagliano, I. Apellaniz, M. Kleinmann, G. Tóth, and C. Klempt, Science **360**, 416 (2018).

[144] T. Y. Lam, Journal of Pure and Applied Algebra **10**, 81 (1977).

[145] O. Azenhas, Linear and Multilinear Algebra **46**, 51 (1999).

[146] S. Doplicher and J. E. Roberts, Journal of Operator Theory , 283 (1988).

[147] Z. Zimboras, arXiv preprint math/0512107 (2005)